From the Department of Cardiothoracic Surgery, University of Cape Town

Investigation of synthetic hydrogels as therapy for myocardial infarction

Dr. med. Karen Kadner

Thesis presented for the degree of
Doctor of Philosophy (PhD)

Submitted to

Faculty of Health Sciences
UNIVERSITY OF CAPE TOWN

September 2011

Table of contents

Declaration 7

Acknowledgements 8

List of Figures 9

List of Tables and equations 11

Abbreviations 12

Summary 17

1 Investigation of degradable PEG hydrogels as treatment after myocardial infarction 19

1.1 Introduction 19

1.1.1 Myocardial infarction 19

1.1.1.1 Incidence and economic burden of cardiovascular diseases 19

1.1.1.2 Risk factors 20

1.1.1.3 Atherosclerosis leading to myocardial infarction 21

1.1.1.4 Diagnosis of myocardial infarction 22

1.1.1.5 Post-MI remodeling 23

1.1.1.6 Management and prognosis of myocardial infarction 28

1.1.2 Biomaterials for the treatment of myocardial infarcts 32

1.1.2.1 Natural polymer matrices 34

1.1.2.2 Synthetic polymer matrices 37

1.1.2.3 Host responses to biomaterials 41

1.1.2.4 Timing 42

1.2 Project aims 47

1.3 Results and discussion 48

1.3.1 Preliminary *in vitro* characterization of PEG hydrogels 48

1.3.1.1 Gelling time 49

1.3.1.2 Swelling 50

1.3.1.3 Degradation 51
1.3.2 Subcutaneous assessment of biocompatibility 52
1.3.3 Intramyocardial evaluation of biocompatibility and time to degradation 54
1.3.4 Effect of MMP-1s crosslinked 20PEG-8VS on the function of healthy hearts 58
1.3.5 Investigation of MMP-1 degradable PEG hydrogel for treatment of myocardial infarction 60
1.3.5.1 Functional assessment 61
1.3.5.2 Infarct size and scar thickness 64
1.3.5.3 Assessment of hydrogel distribution using Alexa Fluor® 66
1.3.5.4 Corrosion casting 68
1.3.5.5 Assessment of retention of gel within the heart after injection 69
1.3.5.6 Inflammation 70
1.3.6 Summary 73

2 Utilization of MMP-1 degradable PEG hydrogels for controlled local drug release 78
2.1 Introduction 78
2.1.1 Corticosteroid administration after myocardial infarction 78
2.1.2 Controlled release of dexamethasone utilizing PEG hydrogels 80
2.2 Project aims 82
2.3 Results and discussion 83
2.3.1 Assessment of *in vitro* dexamethasone elution 83
2.3.2 Activity of dexamethasone eluted from PEG hydrogels 87
2.3.3 *In vivo* evaluation of dexamethasone release from PEG hydrogels 88
2.3.3.1 *In vivo* elution of dexamethasone 89
2.3.3.2 Cardiac function 91
2.3.3.3 Histological findings 92
2.3.4 Summary 93

3 Determining the ability of PEG hydrogels with tethered dexamethasone to prolong transduced cardiac gene expression when delivered in conjunction with an adenovirus 95
3.1 Introduction 95

3.1.1 Adenoviral vectors for gene therapy 95
3.1.2 Modulation of immune response through combined delivery with dexamethasone 96
3.2 Project aims 97
3.3 Results and discussion 98
3.3.1 Quantification of GFP expressing cells and tissue damage 98
3.3.2 Inflammatory and immune response 101
3.3.3 Summary 103

4 Conclusions 104

5 Material and methods 106
5.1 *In vitro* preparation and preliminary experiments 106
5.1.1 Polyethylene glycol derivatisation 106
5.1.2 Preliminary *in vitro* characterization of PEG hydrogels 107
5.2 *In vivo* evaluation of degradable PEG hydrogels 107
5.2.1 Animals 107
5.2.2 Surgical procedures 108
5.2.2.1 Pre-surgical preparation 108
5.2.2.2 Subcutaneous implantation 108
5.2.2.3 Myocardial infarct model 109
5.2.2.4 Postoperative care 111
5.2.3 Echocardiography 111
5.2.3.1 Sedation 111
5.2.3.2 2D and M-mode 112
5.2.4 Termination of *in vivo* experiments 112
5.2.4.1 Preparation 113
5.2.4.2 Explantation of subcutaneously positioned PEG discs 113
5.2.4.3 Harvesting the heart (myocardial infarct model) 113
5.3 Post-mortem analysis 113
5.3.1 Histology and image processing 113
5.3.1.1 Embedding of subcutaneously positioned PEG discs 113

5.3.1.2 Embedding of hearts (myocardial infarct model) 114
5.3.1.3 Haematoxylin & Eosin staining 114
5.3.1.4 Modified Masson's Trichrome staining 116
5.3.1.5 ED1 & Neutrophil Elastase Double Fluorescent staining 117
5.3.1.6 DAPI staining 117
5.3.1.7 Image acquisition 118
5.3.1.8 Measurements of infarct size and scar thickness 118
5.3.2 Quantification of lead 119
5.3.2.1 Attachment of lead to PEG hydrogels 119
5.3.2.2 Analysis of lead extraction from the hearts 119
5.3.3 Visualization of corrosion cast 119
5.4 Utilization of MMP-1 degradable PEG hydrogels for controlled local drug release 119
5.4.1 Incorporation of dexamethasone into PEG hydrogels 119
5.4.2 Dexamethasone elution 120
5.4.3 Activity of dexamethasone eluted from PEG hydrogels 121
5.4.4 *In vivo* assessment 122
5.4.5 Dexamethasone quantification 122
5.5 Determining the ability of PEG hydrogels with tethered dexamethasone to prolong cardiac gene expression when delivered in conjunction with adenovirus 123
5.5.1 *In vitro* preparation 123
5.5.2 *In vivo* procedure 123
5.5.3 Analysis 123
5.6 Statistical analyses 124
5.7 Reagents and equipment 125

6 References 135

Declaration

I, Dr. Karen Kadner, hereby declare that the work, on which this thesis is based, is my original work (except where acknowledgements indicate otherwise) and that neither the whole work nor any part of it has been, is being or is to be submitted for another degree in this or any other university.

I grant the University of Cape Town free license to reproduce this thesis in whole or in part for the purpose of research.

Signature

Date

Acknowledgements

If I had to single out one person that needs to be acknowledged and thanked, then surely that would be my supervisor Dr Neil Davies. Having been thrown by him into the deep end certainly was uncomfortable initially, but looking back, I now understand that this has made me grow immensely and that he has done me a world of good with the kind of support he gave.

I would like to thank Prof Peter Zilla, Head of Cardiothoracic Surgery, for giving me the opportunity to undertake my PhD studies in his department. Dr Deon Bezuidenhout, Lage Ahrenstedt and Anel Ooshuysen (Polymer Science Laboratory, Cardiovascular Research Unit) need to be acknowledged for the manufacturing of PEG hydrogels, the attachment of dexamethasone, the *in vitro* evaluation thereof, as well as having taught me everything I know about polymers. Dr. Paul Human, Deputy Director of the Cardiovascular Research Unit, has always been extremely helpful with regards to statistical analyses as well as poster and PowerPoint presentations. Working with Rodney Lucas and Noël Markgraf, who were the best possible teachers for all animal-involving experiments, as well as Subash Govender and Melanie Black, who need to be thanked for the histological processing of tissue samples, was nothing but an absolute pleasure. Moreover, I am very appreciative of Dr. Christel Tinguely (Dept. of Geological Sciences, UCT) and Dr. Lubbe Wiesner (Division of Clinical Pharmacology, UCT), both being particularly helpful with the quantifications of lead and dexamethasone, as well as Jörg Müller from the Charité Berlin in Germany, who was unsurpassable when it came to getting hold of the most inaccessible journal articles in absolutely no time. Carrying out my studies would not have been possible without the financial support of Medtronic Inc., the German Academic Exchange Service (DAAD) as well as scholarship from the Centre for High Performance Computing (CHPC) through the 2010-2013 CHPC flagship project “Computational Mechanics and Electro-elasticity Towards Improved Understanding of the Biomechanics of Myocardial Infarction and the Development of Novel Therapies”. It would, however, also not have been possible without the friendship, generosity, advice and moral support of Hamman de Vaal, Jordi Reddy, Mona Bracher, Sarah-Kate Sharp, Letatia Kiewietz, Katrin Rahmfeld, Dr. Thomas Franz, Dr. Cobus Stofberg and Heber van Zyl as well as, of course, Dr. Tumi Taunyane – the man by my side. All of the above contributed in different ways to Cape Town truly becoming a “home away from home”.

List of figures

Figure 1:	Ventricular dilatation associated with progressive heart failure	27
Figure 2a:	Chemistry of Michael-type addition reaction	39
Figure 2b:	Polymerization of multiarm PEG hydrogels	40
Figure 3:	Gelling time	49
Figure 4:	Amount of swelling and time to degradation, comparing various degradable PEG gels	50
Figure 5:	Stitched microscopic images of ED1 stained PEG hydrogel discs	53
Figure 6:	ED1-based intramyocardial evaluation of biocompatibility and time to degradation	55
Figure 7:	Masson's Trichrome-based intramyocardial evaluation of biocompatibility and time to Degradation	56
Figure 8:	Effect of intramyocardial hydrogel injection on the function of uninfarcted hearts, 14 days after the injection	59
Figure 9:	Effect of intramyocardial hydrogel injection on the function of uninfarcted hearts, 28 days after the injection	59
Figure 10:	Effect of intramyocardial hydrogel injection on fractional shortening (FS), 14 days post-MI	61
Figure 11:	Effect of intramyocardial hydrogel injection on fractional shortening (FS), 28 days post-MI	62
Figure 12:	Effect of intramyocardial hydrogel injection on end-systolic diameter (ESD), 14 days post-MI	62
Figure 13:	Effect of intramyocardial hydrogel injection on end-systolic diameter (ESD), 28 days post-MI	63
Figure 14:	Scar thickness	65
Figure 15:	Distribution pattern of Alexa Fluor®-labelled MMP-1 degradable hydrogel	66
Figure 16:	Degradation of MMP-1 cleavable hydrogel, labelled with Alexa Fluor®	67
Figure 17:	SEM picture of corrosion cast, injected immediately post-MI	69
Figure 18:	Inflammatory reaction after immediate and delayed hydrogel injection	72
Figure 19:	Incorporation of drugs	81
Figure 20:	Dexamethasone elution from 20PEG-8Ac	84
Figure 21:	Dexamethasone elution from 20PEG-8VS	84
Figure 22:	Elution of entrapped dexamethasone, directly comparing degradable and non-degradable PEG hydrogels	85
Figure 23:	Dexamethasone elution, comparing different dosages and shapes	86
Figure 24:	Activity of dexamethasone eluted from degradable 20PEG-8Ac	87
Figure 25:	Activity of dexamethasone eluted from non-degradable 20PEG-8VS	88
Figure 26:	Postoperative weight development of rats with MI	90
Figure 27:	Average scar thickness of infarcted rat hearts	93
Figure 28:	Area of cells expressing GFP	99
Figure 29:	Tissue damage	100

Figure 30: Macrophage response 101
Figure 31: T-lymphocyte response 102

List of tables and equations

Table 1:	Examples of hydrogels from natural and synthetic materials	34
Table 2a:	Examples of studies with intramyocardial biomaterial injection immediately post-MI	44
Table 2b:	Examples of MI studies with delayed intramyocardial biomaterial injection	45
Table 3:	Gelling times	49
Table 4:	Echocardiographic assessment of myocardial function at two and four weeks post-MI	61
Table 5:	Content iso-osmotic PBS solution	106
Table 6:	Protocol Mayer's Haematoxylin	115
Table 7:	Protocol alcoholic EosinY/Phloxine B solution	115
Table 8:	Content Bouin's Fluid	116
Table 9:	Content Acid Fuchsin	116
Table 10:	Content TBS	117
Table 11:	Reagents	125
Table 12:	Equipment	130

Equation 1:	Law of Laplace	27
Equation 2:	Calculation of fractional shortening (FS)	112
Equation 3:	Calculation of released dexamethasone	120

Abbreviations

AAV	Adeno-associated virus
ACE	Angiotensin-converting enzyme
ACS	Acute coronary syndrome
Adv	Adenovirus
$AlK(SO_4)_2$	Aluminium potassium sulfate
AR	Androgen receptor
ATCC	American Type Culture Collection
bFGF	Basic fibroblast growth factor
BSA	Bovine serum albumin
BSL	Biosafety level
^{14}C	Carbon
Ca^{2+}	Calcium
CH_3COOH	Acetic acid
$C_2H_3Cl_3O_2$	Chloral hydrate
C_2H_5OH	Ethyl alcohol
C_3H_3ClO	Acryloyl chloride
$C_4H_6O_2S$	Divinylsulfone
$C_6H_8O_7$	Citric acid
cm	Centimeter
CPK	Creatine phosphokinase
CSC	Cardiac stem cell
CVD	Cardiovascular disease
DAPI	4',6-diamidino-2-phenylindole
DCM	Dichloromethane
dl	Deciliter
DM	Diabetes mellitus
DMSO	Dimethyl sulfoxide
DNA	Deoxyribonucleic acid
DTT	Dithiothreitol

ECG	Electrocardiogram
ECM	Extracellular matrix
ED1	Cellular marker specific for macrophages
EDD	End-diastolic diameter
EF	Ejection fraction
eNOS	Endothelial nitric oxide synthase
EPO	Erythropoietin
ESC	Embryonic stem cell
ESD	End-systolic diameter
FBGC	Foreign body giant cell
Fig.	Figure
FS	Fractional shortening
g	Gram
GFP	Green fluorescent protein
GR	Glucocorticoid receptor
GRE	Glucocorticoid response elements
h	Hour
h	Wall thickness
HA	Hyaluronic acid
HCl	Hydrochloric acid
HDL	High-density lipoprotein
H&E	Haematoxylin & Eosin
HEMAPTMC	Hydroxyl ethyl methacrylate-poly(trimethylene carbonate
HF	Heart failure
HNO_3	Nitric acid
H_2O_2	Hydrogen peroxide
HPLC	High-performance liquid chromatography
HSC	Hematopoetic stem cell
HSP	Heat shock protein
ICP-MS	Inductively coupled plasma mass spectroscopy
IGF	Insulin-like growth factor
IgG	Immunoglobulin G
iPBS	Iso-osmotic phosphate buffered saline
iPS	Induced pluripotent stem cell

KCl	Potassium chloride
kDa	Kilo Dalton
kg	Kilogram
KOH	Potassium hydroxide
l	Liter
LAD	Left anterior descending coronary artery
LC-MS/MS	Liquid chromatographic tandem mass spectrometric assay
LDL	Low-density lipoprotein
L-NAME	N(ω)-nitro-L-arginine methyl ester
LV	Left ventricle
MAPK	Mitogen-activated protein kinase
MI	Myocardial infarction
min	Minutes
MeHA	Methacrylated Hyaluronic acid
mg	Milligram
ml	Milliliter
mm	Millimeter
mM	Millimolar
mmHg	Millimeters of mercury
mmol	Millimole
MMP	Matrix metalloproteinase
MMP-1s	MMP-1 cleavable peptide (MMP-1 substrate)
MMTV	Mouse mammary tumor virus
MSC	Mesenchymal stem cell
MT	Masson's Trichrome
m/v	mass /volume
m/z	Mass-to-charge ratio
n	Number
NaH	Sodium hydride
$NaH_2PO_4.1H_2O$	Sodium phosphate monobasic monohydrate
$Na_2HPO_4.12H_2O$	Sodium phosphate dibasic dodecahydrate
NaCl	Sodium chloride
NaH	Sodium hydride
$NaIO_3$	Sodium iodate

NaOH	Sodium hydroxide
NF-κB	Nuclear factor kappa B
ng	Nanogram
NIPAAm	*N*-isopropyl acrylamide
nm	Nanometer
NO	Nitric oxide
NRMI	National registry of myocardial infarction
NSTEMI	non-ST segment elevation myocardial infarction
NYHA	New York Heart Association
p	Pressure
p	Statistical significance
PCI	Percutaneous coronary intervention
PCL	Poly(ε-caprolactone)
PDGF	Platelet-derived growth factor
PEG	Poly(ethylene glycol)
pfu	Plaque-forming unit
PI3-kinase	Phosphatidylinositol 3-kinase
PLSD	Protected least significant difference
ppb	Parts per billion
r	Radius
RGD	Arginin-Glycine-Aspartat amino-acid sequence
rpm	Rounds per minute
SAP	Self-assembling peptide
SDF	Stromal cell-derived factor
SEM	Scanning electron microscope
SEM	Standard error of the mean
sGC	Soluble guanylate cyclase
STEMI	ST segment elevation myocardial infarction
T	Wall stress of a round chamber
Tab.	Table
TBS	Tris-buffered saline
TEA	Triethylamine
THF	Tetrahydrofurane
TIMI	Thrombolysis in myocardial infarction trial

TLR	Toll-like receptor
UA	Unstable angina
VEGF	Vascular endothelial growth factor
VFWR	Ventricular free wall rupture
VIS	Visiopharm Integrator Systems
WHO	World Health Organization
µg	Microgram
µl	Microliter
µm	Micrometer
20PEG-8VS	20kDa, 8arm PEG-Vinylsulphone
20PEG-8Ac	20kDa, 8arm PEG-Acrylate
2nPEG-2SH	2kDa dithiolated PEG
10nPEG-4SH	10kDa tetrathiolated PEG

Investigation of synthetic hydrogels as therapy for myocardial infarction

This thesis investigated the potential of synthetic polyethylene glycol (PEG) hydrogels for restoration of biomechanical integrity and for controlled cardiac release of drugs.

Post-myocardial infarct (MI) remodelling has been shown to cause a progressive decline in left ventricular performance due to a series of histopathological and structural changes that lead to heart failure in one third of the patients. The delivery of hydrogels is a promising approach, as first results indicate a reduction in post-MI remodeling by limiting increased wall stresses. However, there is no consensus in the present literature on the influence of timing of delivery of treatment. The aim of this study was to directly compare the effect of injecting an enzymatically degradable polyethylene glycol (PEG) hydrogel into the myocardium immediately or seven days after permanent ligation of the left anterior descending artery in rats on pathological remodeling. Rats that received their treatment delayed by one week had significantly higher fractional shortening values ($p<0.05$) and significantly thicker scars ($p<0.05$) than those after immediate treatment or those of the saline control group. Thus, the timing of post-MI biomaterial application did determine the extent to which pathological remodeling could be ameliorated, with hydrogel injections into one-week-old myocardial infarcts being superior to immediate treatment. The inflammatory responses to the hydrogels and their physical distribution in the heart were investigated further within the cardiac tissue. It seems likely that the timing of biomaterial injection influences the distribution pattern of the PEG, resulting in favorable outcome after delayed hydrogel delivery.

The enzymatically degradable PEG hydrogels were also investigated as a means of delivering dexamethasone in a localized and controlled manner. Dexamethasone has been the subject of some controversy as post-MI treatment. Although slow release of the agent could be demonstrated *in vitro*, *in vivo* experiments showed no dexamethasone-induced improvement of post-MI cardiac performance, instead they indicated the additional thinning of infarcted tissue.

Gene therapy is an area of enormous promise for many pathologies, MI included. Adenovirus is a widely used vector but its efficacy is limited by an inflammatory response towards infected cells. In this study, the ability of PEG hydrogels with tethered dexamethasone to prolong cardiac gene expression when delivered in conjunction with adenovirus was explored. The results indicate that this approach has promise.

1 Investigation of degradable PEG hydrogels as treatment after myocardial infarction

1.1 Introduction

1.1.1 Myocardial infarction

1.1.1.1 Incidence and economic burden of cardiovascular diseases

In the United States about 81 million adults (and thus more than one in three) suffer from one or more types of cardiovascular diseases (CVDs), of which high blood pressure, coronary heart diseases and stroke have the highest incidence [1]. In 2007 cardiovascular diseases resulted in more than 79 million physician office visits as well as more than four million visits to emergency departments [2, 3]. Coronary heart diseases account for more than half of all cardiovascular events of people younger than 75 years of age [4]. During the course of this year, an estimated 785000 Americans will suffer a new and about 470000 a recurrent heart attack [5], thus on average every 34 seconds an American will experience a myocardial infarction [6].

According to the World Health Organization (WHO), in 2004 about 17.1 million people passed away due to a cardiovascular disease, which corresponds to 29% of all mortalities and thus makes it the number one cause of death worldwide [7, 8]. Approximately every minute, someone will die of a coronary event [5].

Obviously the value of human life is beyond analysis, however, estimated direct and indirect healthcare costs for 2010 amounted to $503.2 billion [1]. Interestingly, a shift from developed to developing countries is being noted [9]: more then 80% of all deaths due to cardiovascular diseases occur in low- and middle-income countries, as people there have less access to prevention efforts and effective health care services, while being as much exposed to relevant risk factors as people living in the “first world” [7].

1.1.1.2 Risk factors

Established risk factors have to meet three conditions: 1) a high prevalence in several populations; 2) a significant independent impact on the risk of the respective disease and 3) their control and treatment must result in risk reduction [10].

About 80 to 90% of people dying from ischemic cardiomyopathy had one or more of the following major risk factors that were influenced by their lifestyle and thus the disease could have been prevented [11]: hypertension, diabetes mellitus (DM), high levels of LDL, smoking, physical inactivity and obesity.

Hypertension is defined as systolic blood pressure higher than 140mmHg and diastolic blood pressure above 90mmHg. Every ten-point increase in diastolic blood pressure or twenty-point increase in systolic blood pressure doubles the risk of cardiovascular diseases [10].

Cardiovascular disease death rates among adults with DM are two to four times higher than the rates of those, who do not suffer from the disease [1]. The worldwide prevalence of DM for all age groups is increasing, with the total number rising from 171 million (2000) to projected 366 million (2030) [12].

Cholesterol is transported around the body with low-density lipoprotein (LDL) or high-density lipoprotein (HDL); high levels of LDL promoting cardiovascular diseases, while HDL lowers the risk thereof. As high cholesterol is estimated to cause around a third of cardiovascular diseases worldwide, LDL levels of less than 100mg/dL are considered ideal [13]. Yet, elevated cholesterol levels are quite common, such as in Canada, where about 40% of the people are affected [14].

Smoking injures the endothelial lining of blood vessels, promotes coronary artery spasm as well as the formation of cholesterol plaques and blood clots and elevates blood pressure while simultaneously increasing LDL cholesterol levels [10]. Presently cigarette smoking is a potent independent predictor of cardiac arrest in patients with coronary heart disease [15]. Hence, according to a cohort study conducted in the United Kingdom, the mortality was 60% higher in smokers (and 80% higher in heavy smokers) relative to nonsmokers [14].

Physical inactivity doubles the relative risk of coronary heart disease, an increase in risk comparable to that observed for high blood cholesterol, hypertension or cigarette smoking [16]. Regular exercise results in a significant decrease of diastolic blood pressure (-2mmHg), triglycerides (-0.2mmol/l) and fasting glucose (-0.2mmol/l) [17].

Overweight children and adolescents typically have a higher prevalence of established risk factors for cardiovascular diseases such as hypertension, hyperlipidemia and diabetes later in their lives [18].

In industrialized countries, lower socioeconomic groups have a higher incidence of cardiovascular diseases along with an increased mortality, as the prevalence of risk factors is higher, while the use of medication and access to treatment is lower [10]. In developing countries, coronary heart diseases have traditionally been more frequent in people with a higher education and more income, but this is beginning to change: as the cardiovascular disease epidemic matures, also there the burden shifts towards groups of lower socio-economic status [14].

Apart from the above-mentioned behavioral risk factors, several studies provide consistent evidence of a significant connection between a positive family history and the incidence of cardiovascular diseases [19, 20], heart failure [21], sudden cardiac death [22] as well as underlying causes such as atherosclerosis [23, 24].

1.1.1.3 Atherosclerosis leading to myocardial infarction

The underlying cause of the majority of coronary heart disease and stroke is atherosclerosis, a progressive subendothelial accumulation of lipids and fibrous elements, typically protected by a fibrous cap [25].

Numerous pathophysiological observations led to the formulation of the response-to-injury hypothesis of atherosclerosis, which proposes endothelial dysfunction as the first step in the development of the syndrome [26]. Some of the causes leading to endothelial dysfunction include hyperlipidemia, high blood pressure, diabetes mellitus and free radicals caused by cigarette smoking [27, 28]. In fact, it has been shown that those risk factors increase the likelihood of atherosclerosis by as much as seven times [29]. The injury augments the permeability as well as the adhesiveness of the endothelium, leading to the aggregation of lipid-rich macrophages and T-lymphocytes within the innermost layer of the arterial wall, the intima [30]. This aggregation is called a “fatty streak” and is considered the earliest recognizable lesion of atherosclerosis [30]. Eventually, this chronic inflammatory response stimulates the migration and proliferation of smooth muscle cells and precedes the development of an “intermediate lesion” [31-36]. The consequential thickening of the arterial wall can be compensated by gradual dilation, so that up to a certain point, the lumen remains unaltered [37].

Sustained inflammation, however, results in rising numbers of lymphocytes, which release hydrolytic enzymes, cytokines, chemokines as well as growth factors [38, 39] and provoke further damage as well as focal necrosis [40]. Accumulation of mononuclear cells, migration and proliferation of smooth muscle cells as well as the development of fibrous tissue lead to the further extension of the lesion, which gets protected by a dense fibrous cap that covers a core of lipid and necrotic debris and this stage is termed “advanced” [41].

At some point, it is impossible to compensate the narrowing of the lumen by dilation, so that the lesion starts altering the blood flow in the artery [41]. That may result in an imbalance between oxygen demand and supply, especially if there is an increased need for oxygen, such as during exertion. The resulting predictable chest discomfort therefore typically occurs during exercise and resolves at rest or sublingual administration of nitroglycerin [42].

The most dangerous complication of advanced lesions, however, is a sudden rupture of the fibrous cap, exposing thrombogenetic material to the blood stream, resulting in platelet aggregation, thrombus formation and consequently, a rapid occlusion of the artery [43]. As this leads to reduced myocardial oxygen supply, rather than being a consequence of increased oxygen demand, such as during exercise-induced angina, the subsequent chest pain can even occur at rest, which is one cardinal sign of a possible MI [44]. In addition, the patient may experience unspecific symptoms such as diaphoresis, light-headedness, nausea and breathlessness and may present with cool and pale skin, low-grade fever, irregular pulse, decreased or elevated blood pressure as well as neck vein distension [45, 46]. Yet, studies have shown that an estimated 20% to 40% of first and recurrent myocardial infarcts, especially in elderly patients, women and those suffering from diabetes mellitus, are silent and are therefore difficult to diagnose, which carries an increased likelihood for delays in seeking medical attention [47-49]. In fact, 50% of men and 64% of women, who die suddenly of acute coronary syndrome, had no symptoms prior to the event [1].

1.1.1.4 Diagnosis of myocardial infarction

The term acute coronary syndrome (ACS) covers a spectrum of acute myocardial ischemic states, encompassing the following three types: unstable angina (UA), acute non-ST segment elevation myocardial infarction (NSTEMI) and acute ST segment elevation myocardial infarction (STEMI), denoted on the electrocardiogram (ECG) [50].

In a STEMI the coronary artery is completely blocked and as a result virtually all cardiac tissue previously supplied by the affected artery starts to die; ST segment elevation seen on the ECG therefore reflects active and ongoing transmural myocardial injury. In the less severe NSTEMI the clot only partially occludes the artery and as a result only a fraction of the heart muscle supplied by it dies, consequently no ST segment elevation is seen in the ECG.

To further distinguish whether the patient suffers from a NSTEMI or an UA, the measurement of cardiac enzymes, which get released into the circulation should there be any heart muscle damage, are a sensitive and helpful tool [46]. If the enzymes are elevated, an evidence for myocardial necrosis, the patient suffers from a NSTEMI, if they are within normal range the patient has an UA.

Patients presenting with chest pain are initially treated as if an MI has occurred and are then carefully investigated to establish a more precise diagnosis, as this determines their further treatment [51, 52]. Thus, in order to classify the patient into one of the above groups, it is essential to obtain an ECG, to quantify serum cardiac biomarkers and to look for imaging evidence of new loss of viable myocardium or new regional wall motion abnormalities [53].

According to the WHO guidelines, which were refined in 2000, diagnostic of an MI is a combination of two out of three characteristics: typical symptoms, cardiac Troponin elevation or ECG changes indicative of ischemia, such as pathological Q-waves or ST-elevation/depression [54].

1.1.1.5 Post-MI remodeling

The mechanism, with which the myocardium responds to the ischemic injury, is a complex multifactorial process known as left ventricular (LV) remodeling [55].

Briefly, the occlusion of a coronary artery leads to irreversible death of cardiomyocytes in the area previously supplied by it, and, depending on the infarct size, an initial thinning and distension of the infarcted myocardium [56]. This is followed by the initiation of a neurohormonal cascade that aims to compensate for the lack of contractile function and subsequent hypertrophy of the non-infarcted myocardium, activated by biomechanical stresses in response to hemodynamic load increase [55, 56].

Cardiac output can be maintained initially and may even result in hyperfunction of the left ventricle, but over time, these compensatory mechanisms fail, resulting in a progressive deterioration of cardiac performance [55, 56]. The end result is a dilated, underperforming ventricle, causing the clinical symptoms of heart failure (HF) [57].

The structural and mechanical changes of a healing myocardial infarct have been divided into four phases: 1) acute ischemia; 2) necrotic phase; 3) fibrotic phase and 4) the remodeling phase [58]:

1) Acute ischemia phase

The first phase refers to the initial six hours after permanent coronary artery occlusion, during which the infarcted myocardium undergoes a transition from an active, force-generating material to a passive, viscoelastic one [58].

Generally, hypoxia causes a change from oxidative to glycolytic energy production with increased glucose consumption, lactic acid production and consequently a decreasing intracellular pH [59, 60]. The latter is an important regulator of cardiac performance and has its steady state at around 7.1-7.3 [61]. It declines moderately with an increase in heart rate [62, 63] but more severely if the myocardium is in an ischemic state [64]. The resulting acidosis is partly responsible for arrhythmia and failure of contraction [65-67].

Simultaneously matrix-associated glycoproteins start to break down as early as 40 minutes after infarction, while collagen and elastin fibers get damaged in the first two hours, possibly due to early activation of matrix metalloproteinases (MMP) [68-70]. Within 30 seconds after experimental infarct induction, no effective work is performed by the ischemic myocardium; instead, work is being done *on* rather than *by* the segment [71]. Thus the left ventricle appears to be more compliant than usual shortly after coronary artery ligation [72], but becomes less compliant than normal a few hours afterwards [73]. Apart from the disruption of structural proteins such as collagen or titin, the initially increased LV compliance could be explained with a loss of coronary perfusion pressure in the occluded vessel, while the subsequent stiffening of the infarcted myocardium is likely due to edema [74-76].

With non-contractile, dying tissue forms the ischemic area, infarct expansion induces an increase of the volume load, which, in turn, leads to an augmentation of the pressure load [77], resulting in a mixed pressure and especially volume overload [78].

The consequential decline of ejection fraction (EF) has been shown to be in direct proportion to the size of the infarct [79]. However, due to the Frank-Starling mechanism, the increasing LV volume augments the contractility of the remaining healthy myocardium and therefore the stroke volume, so that cardiac output initially remains relatively normal [80]. Thus, initial post-MI remodeling could be beneficial and could even promote survival, however, it holds deleterious long-term hemodynamic consequences [77].

2) Necrotic phase

This period is characterized by inflammation and necrosis, starting with infarct stiffening six hours post-MI and ending after about one week [58].

Removal of dead muscle occurs [81], while collagenase and gelatinase activity of MMP-1, MMP-2 and MMP-9 is elevated, continuing with the disruption of the collagen network of the myocardium [68, 70, 82-89]. Newly formed collagen is not yet properly crosslinked [90, 91], which could be an explanation for the side-to-side slippage of cardiomyocytes that hypothetically contributes to their elongation with subsequent thinning of the left-ventricular wall [77, 92]. Thus, it is not surprising that infarct rupture is most likely to occur during this period [93-96]. Although overall rare in its occurrence (incidence ranging from 0.8%-6.2%), ventricular free wall rupture (VFWR) remains a dreaded complication of MI as it accounts for as much as 15% of the in-hospital mortality and is the second most common cause of death after cardiogenic shock secondary to an acute myocardial infarction [97, 98]. Interestingly, according to the National Registry of Myocardial Infarction (NRMI), cardiac rupture is seen more often in patients undergoing thrombolysis (12.1%) than in patients who don't (6.1%, $p<0.001$), typically within the first 24 to 48 hours after the infarct has occurred [99, 100]. Similarly, in the *Thrombolysis in Myocardial Infarction II* trial (TIMI-II), cardiac rupture was the cause of death in 16% of patients dying within 18 hours of thrombolytic therapy [101]. The explanation seems to be an increased incidence of intramyocardial hemorrhage caused by the thrombolytic therapy, which generates plasmin, a non-specific proteolytic enzyme that boosts collagen breakdown [102-104].

The activation of the immune system during the necrotic phase follows the same pattern as after any infection: most microorganisms encountered by a healthy individual are identified and eliminated within hours by defense mechanisms that are not antigen-specific: the so-called innate immune system [105].

The heart itself possesses all components of the innate immune system, including pattern recognition receptors and effector proteins [105, 106]. Although it is commonly accepted that the innate immune system is activated by microbial patterns, Matzinger and co-workers assumed that cell damage rather than foreignness is what triggers an immune response [107]. In support of this hypothesis, they have proven that, in the absence of any foreign pathogens, resting dendritic cells can be activated by necrotic cells [107], such as cardiomyocytes that have been damaged by ischemia [105, 108-110]. That results in the release of intracellular proteins and triggers the launching of pattern recognition receptors such as Toll-like receptors (TLRs), the transcription nuclear factor kappa B (NF-κB) and complement [105, 108, 109]. NF-κB, in turn, activates genes involved in inflammation, cardiomyocyte growth, contractile function and death as well as extracellular matrix remodeling [111]. Adhesive proteins such as fibronectin [112, 113], laminin and collagen type IV [114] emerge at about three to four days post-MI in animal models.

3) Fibrotic phase

The fibrotic phase is the period of healing, which is dominated by new collagen deposition, starting one week post-MI with rapidly increasing collagen content and ending as soon as the collagen accumulation slows down, roughly after three weeks [58]. During this phase infarct stiffness peaks, with segment lengths changing not more than 2% over the cardiac cycle, which results in impaired filling and thus in diastolic dysfunction [115].

4) Remodeling phase

Only the onset of this final period can be defined, since a healing scar is dynamic, living tissue that, because of its ongoing activity, may never reach a steady, mature configuration [116]. Due to increased crosslinking of collagen, the dominant effect during the remodeling phase is the shrinkage of the scar [117-119]. Scar shrinkage appears to reverse infarct expansion: by reducing scar size and consequential cavity dilation, wall motion abnormalities can partially improve [119-121]. However, patients suffering from a large infarct may still experience functional impairment, as scar shrinkage will be dominated by cavity dilation (illustrated in Figure 1) [122, 123].

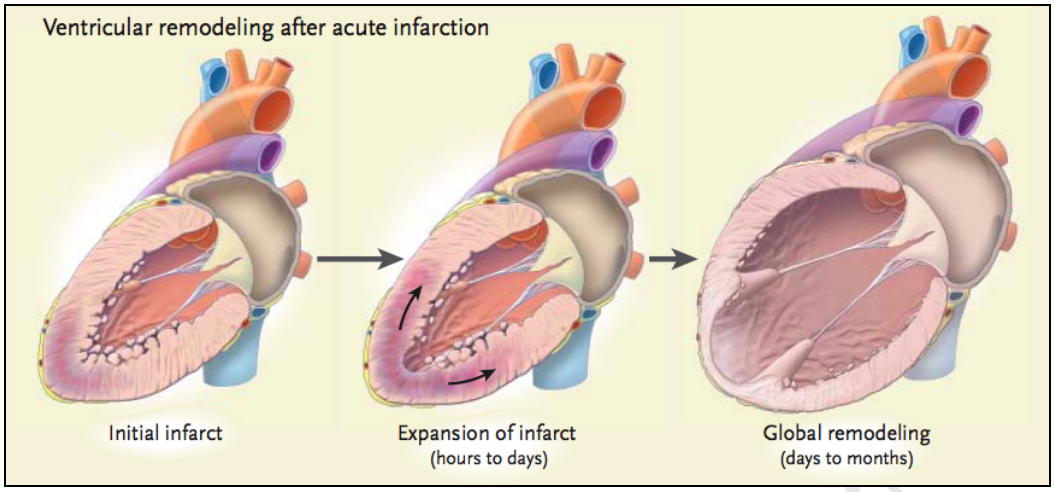

***Fig. 1: Ventricular dilatation associated with progressive heart failure**. Figure adapted from Jessup and Bronzena [124]*

In contrast to early infarct expansion, late ventricular enlargement after myocardial infarction, is caused by an increase in the segment length of the remaining non-infarcted tissue [125]. That places the non-infarcted myocardium at a mechanical disadvantage, with higher systolic stresses required to eject against a given pressure [58]. The rising systolic and diastolic volumes, which lead to global ventricular dilation and increased wall stresses, result in the cardiomyocytes losing the capacity to shorten effectively, leading to further stretching and continuing decrease in cardiac performance [126].

The physics behind this mechanism can be explained by the Law of Laplace (Equation 1), where the stress in the wall of a round chamber (T) is directly related to the pressure in the chamber (P), the radius of the curvature (R) and the thickness of the wall (h) [126]:

$$T = \frac{PR}{h}$$

***Eq. 1: Law of Laplace**. As pressure and radius increase, the LV free wall thins, which augments cardiac wall stress and ultimately leads to even more dilation, thinning and stress [126].*

The resulting HF describes a state in which cardiac output is insufficient in meeting the body's requirements for oxygen and nutrients. The failing heart is characterized by reduced rates of shortening and relengthening (decreased force production) and diminished responsiveness to β-adrenergic stimulation [127-131].

One of the first symptoms resulting from an inadequate performance of the heart might be shortness of breath, which has been used as basis to classify the severity of HF by the New York Heart Association in 1964 (NYHA 1: no breathlessness, NYHA 2: breathlessness on severe exertion, NYHA 3: breathlessness on mild exertion and NYHA 4: breathlessness at rest) [132]. Apart from that, poor cardiac output can cause edema, skeletal muscle fatigue and generalized tiredness, resulting in HF being disabling and possibly severely reducing a patient's quality of life [124, 133, 134]. The staging criteria for HF has been updated by the American College of Cardiology/American Heart Association in 2001: Stage A: patient at high risk for developing HF, but who does not yet demonstrate impaired LV function, Stage B: asymptomatic patient with structural heart disorder, Stage C: patient with current or past symptoms of HF, which are manageable with medical treatment, Stage D: patient that suffers from severe HF and requires advanced treatment strategies such as continuous inotropic infusions or heart transplant [135].

1.1.1.6 Management and prognosis of myocardial infarction

Management

An acute MI is a medical emergency that requires prompt recognition, since the beneficial effects of reperfusion therapy are substantially higher within the first two hours after the onset of symptoms [136-138]. A sudden cardiac arrest victim's chances of survival fall rapidly for every minute that defibrillation was delayed to 5% at 15 minutes [139-142]. Overall survival rates improve by up to 50% if treatment begins within one hour, however, most patients are admitted to the hospital 2.5 to three hours after onset of symptoms [143].

Every patient presenting with chest pain should be managed as if the pain was ischemic in origin until clear evidence of the contrary is established [46]. Thus, the simultaneous accomplishment of the following goals is fundamental: relief of ischemic chest pain, assessment and optimization of the hemodynamic status and confirmation of the diagnosis, as well as timely initiation of antithrombotic and reperfusion therapy [53]. Patients are supposed to be started on aspirin [144, 145], nitroglycerin, morphine sulphate, betablockers, calcium channel blockers and heparin [46, 53], while the right reperfusion strategy needs to be selected for each individual case [146].

Patients presenting with ST-segment elevation benefit from reperfusion through thrombolysis [138, 147] or percutaneous coronary intervention (PCI) [148], which results in a statistically significant decrease in death rates, cardiogenic shock, heart failure and pulmonary edema [149]. Fibrinolytic therapy, however, does not improve the clinical outcome of patients presenting with NSTEMI and is therefore contraindicated [46, 150]. Twenty-eight studies conducted between 1977 and 2007 found that revascularization by PCI in conjunction with medical therapy or coronary bypass surgery in patients with non-acute coronary artery disease significantly improves survival compared to medical treatment alone [151]. It can be concluded that primary PCI is the superior alternative to fibrinolysis within 90 minutes after symptom onset, while the latter is appropriate for up to 12 hours if PCI was unavailable in the first two hours [148, 152, 153].

Post-MI, patients are treated with several long-term medications to improve function and to prevent secondary cardiovascular events. The main goal is to reduce the load in order to lessen distending or deforming forces [77]. ACE-inhibitor therapy can be seen as a means to moderate the increase in apical wall stress and to normalize the dilation of the left ventricle [154-156]. It acts, in part, by reducing the preload and therefore the LV operating volume [157]. If LV dilation is avoided, then the pure hypertrophic response of surviving myocytes gives hemodynamic benefit [158]. Betablockers act by reducing the afterload and thus the intracavity systolic pressure [77]. Further benefits are obtained when antiplatelet drug therapy [159], statins [160, 161] as well as aldosterone antagonists [162] are added to the long-term medication.

Prognosis and the search for therapeutic alternatives

Long-term progressive remodeling of the LV can still occur up to two years after myocardial infarction [163] and is the leading cause of systolic dysfunction and HF - in fact, according to 13 multicenter HF treatment trials involving more than 20000 patients, coronary artery disease was the underlying cause in almost 70% of the cases [164]. Unfortunately, there are only a limited number of options available to prevent progression to HF, such as medicamentous treatment, which is supposed to improve systolic function and decrease the workload [165, 166], biventricular pacing [167, 168] or mechanical approaches including CorCap (Acorn Cardiovacular Inc.) and HeartNet (Paracor Medical Inc.), employing Dacron and nitinol wraps to provide physical support [169, 170].

Alternatively, surgical approaches such as the endoventricular patch plasty (Dor procedure) and partial left ventriculectomy (Batista procedure) aim to improve performance by giving a spherical dilated ventricle a more elongated shape [171, 172].

Although all those therapy options are able to delay remodeling or HF, none is able to reverse it. Consequently, more than 50% of patients that were given the diagnosis of HF are dead within five years [173]. Organ transplantation remains the treatment option with the most favorable outcome, offering a five-year survival rate of around 65%, but is limited by a general shortage of donor hearts [174]. As a result, most of those patients are left with ventricular assist devices used as bridge to transplant or for destination therapy [127, 175, 176] or ultimately hospice care.

The poor long-term prognosis of heart failure patients and immense public health implications have fuelled interest in trying to establish therapeutic alternatives to those detailed above.

Research has shown that there is extensive proliferation of human cardiomyocytes during human fetal life, but that it slows down dramatically around the time of birth [177]. In a groundbreaking approach to substantiate this hypothesis, Bergman *et al.* took advantage of the integration of ^{14}C into DNA, generated by nuclear bomb testing during the Cold War [178]. Based on the post-mortem ^{14}C content in human cardiomyocyte DNA, they were able to conclude that at the age of 25, indeed only 1% of cardiomyocytes are replaced annually while the rate declines to 0.45% in aging hearts and that less than half of cardiomyocytes are exchanged during a normal life span [178]. Thus, in contrast to zebra fish, which are able to fully regenerate hearts within eight weeks even after 20% ventricular resection, cardiac regeneration in mammals is hindered by the fact that renewal of heart muscle is virtually absent [179, 180]. In view of that, Anversa *et al*. managed to identify a lineage of cardiac stem cells (CSCs) residing in the heart [181], but in the circumstance of acute muscle cell death from MI, their regenerative capacity is grossly inadequate to compensate for the loss of up to one billion cardiomyocytes [182-184]. Consequently, tremendous scientific as well as public interest and excitement have been generated by the possibility of stem cell based myocardial repopulation and the idea of rebuilding the injured heart from its component parts [182, 184, 185]. Ideally, transplanted cells would imitate the lost myocytes morphologically and functionally and establish electrical connectivity with the native myocardial cells [182].

A wide variety of cells have been considered for cardiac therapy [183]:
Skeletal myoblasts are resistant to ischemia and can improve ventricular function [186-189]. However, they do not couple with resident cardiomyocytes electromechanically and therefore do not beat in synchrony with the remaining myocardium [190-193]. Tests conducted on bone-marrow-derived hematopoetic stem cells (HSCs) have generated hope by suggesting potential transdifferentiation into cardiomyocytes [194-196], while other studies were unable to confirm this hypothesis [197, 198]. The small amount of detected cardiomyocytes is more likely generated through cell fusion [199]. Bone marrow also contains mesenchymal stem cells (MSCs). The latter might be able to differentiate into cardiomyocytes, but at an extremely low rate [200, 201]. Their beneficial effect can most likely be explained with paracrine growth factor support for other cells present in injured myocardium [202]. Taken together, no consensus exists on whether or not bone-marrow-derived cells are able to improve cardiac function [203-207]. Adult cardiac stem cells represent another potential cell type for cellular cardiomyoplasty [208-211]. However, sourcing, isolating and expanding those cells might be challenging, possibly involving invasive procedures. Moreover, harvesting sufficient numbers seems ironic, given that the heart is known for its lack of regenerative capacity [191]. Promising results have been achieved with embryonic stem cells (ESCs), as they have the unquestioned ability to differentiate into cardiomyocytes and possess the cellular elements necessary for electromechanical coupling with the native myocardium [212-215]. However, hurdles that stand in the way of the clinical use of these cells are immunological rejection, the predisposition to form teratomas [216] as well as ethical considerations. An alternative might be induced pluripotent stem cells (iPS), which are comparable to natural pluripotent stem cells such as ESCs, but are artificially derived from non-pluripotent cells, usually adult somatic cells. That way, researchers have access to pluripotent stem cells, while avoiding the controversial use of embryos [217]. Nelson *et al*. were the first ones to successfully demonstrate iPS-based cardiac repair after myocardial infarction [218]. However, similar to ESCs, iPSs hold an increased risk of tumor formation [218].

A critical factor that determines the success of stem-cell therapy is the retention of the cells. Most intramyocardially injected cells are lost through leakage into the vasculature or squeezed back out of the injection site [219, 220]. The contracting myocardium, being a mechanically taxing environment, contributes to further cell loss after implantation:

Teng *et al*. revealed a cell retention rate of only 11% in the beating porcine heart versus 67% in the non-beating heart [221]. Another study showed that about 1% of infused bone marrow cells are retained in the heart and that less than 3% of MSCs administered by direct injection persist after two weeks [222]. It seems that most of the cells relocate to the lungs, spleen, liver, kidneys and non-infarcted cardiac tissue [223, 224]. Taken together, it can be estimated that about 90% of transplanted cells have disappeared within one week [191]. To transplant adequate numbers of cells into the myocardial region of interest and to achieve maximum cell retention within that area, a sufficiently large cell graft with suitable structural and functional properties is needed [183, 225]. Survival and integration of transplanted cells can be improved by implanting them as monolayer sheets [226] or by embedding them in matrices such as collagen [227, 228], Matrigel [229-231], chitosan [232], fibrin [233-235] or α-cyclodextrin/MPEG-PCL-MPEG self-assembling hydrogel [236].

Despite encouraging results, it is still not fully understood which cell type has the greatest potential to repair myocardium and also it is not verified whether or not injected cells contribute to functional improvement at all. Interestingly, beneficial effects might be a result of any intramyocardial material injection. Wall and colleagues used a finite element model of an ovine infarcted LV to assess the theoretical effect of injecting any non-contractile biomaterial into ischemic myocardium [237]. Functional assessments in most studies are based on ejection fraction (EF), a common clinical metric of heart performance. Since the EF is calculated from geometric factors, increased EF values might not be a reflection of true functional improvement but could just as well be due to an increased wall thickness and therefore changes in ventricular geometry. The sheer presence of a material leads, on top of that, to a local reduction of elevated myofiber stresses [237]. These finite element models provide the hypothetical basis for an increasing interest in injecting decellularized biomaterials to try and prevent progression to heart failure [126].

1.1.2 Biomaterials for the treatment of myocardial infarcts

A biomaterial, by definition, is a non-viable substance that is used in a medical device [238, 239].

In order to enable tissue regeneration, it should allow the substitution of itself by safely degrading at a rate similar to that of the new tissue creation, eventually being completely removed from the body without having produced toxic by-products [238].

Intramyocardial biomaterial injection following MI has shown potential as a method to improve cardiac performance in the face of progressive HF and has the advantage of being less invasive than implanting *in vitro*-engineered tissue or an epicardial patch [126, 240]. Hence, an exciting field of biomaterial research that has opened up and grown rapidly is the use of injectable polymers (i.e. hydrogels). Indeed, initial test results have indicated increased wall/scar thickness [241-244], reduction of adverse LV remodeling [241, 244, 245], attenuated infarct expansion [246, 247] and improvement of functional parameters [241, 242, 247].

Hydrogels are defined as three-dimensional polymer networks that absorb up to thousands of times their dry weight in water [248, 249], which results in properties that are similar to many tissues and as such hydrogels became an attractive extracellular matrix analogue [250-252]. Consequently, they are being used as wound dressings and biomedical implants [253], for tissue engineering [251, 254, 255] and as barrier material to regulate adhesion [256]. Moreover, hydrogels facilitate the incorporation of various chemical functionalities to generate complex architectures; they offer good transport of nutrients to and products from cells (high diffusivity within the polymer network) as well as an aqueous environment that can protect cells and delicate pharmaceuticals [248, 257]. The latter makes hydrogels, apart from the above-mentioned applications, also suitable for drug delivery systems [257, 258]. In fact, the incorporation of pharmaceuticals into hydrogels provides a means for continuous local delivery of low doses. That increases the persistence of a drug at the disease site while confining its availability to a target region, which helps avoiding unwanted systemic side effects adverse to healing [257, 258].

A potential drawback of hydrogels is their low mechanical strength, which might be insufficient for a mechanically taxing environment such as the beating heart. In fact, hydrogels that could be passed through a needle might be too weak to provide structural support. To overcome this challenge, various design strategies have been employed, which allow the formation of the hydrogel structure *following* injection into the myocardium, such as in situ crosslinking [244, 259], photo-induced polymerization [260], self-assembly [261, 262] and thermo-responsiveness [243, 263, 264].

The in situ transformation from liquid precursors to solid final forms has the additional advantage of enabling the minimally invasive delivery of larger implants.

There are several ways of classifying hydrogels. One is based on the mechanism by which the crosslinks within the networks are formed: physical gels ("reversible") shape by molecular self-assembly due to secondary forces, while chemical gels ("permanent") are formed by covalent bonds. Intermediate-type gels polymerize as physical gels but are additionally crosslinked by specific chemical interactions [248, 249]. A perhaps more practical approach to categorizing hydrogels is according to their natural or synthetic origin; selected examples listed in Table 1 and elaborated on below:

Table 1: Examples of hydrogels from natural and synthetic materials

Natural materials	Synthetic materials
Fibrin	Self-assembling peptides (SAP)
Collagen and gelatin	*N*-isopropyl acrylamide (NIPAAm)
Alginate	Poly(ethylene glycol) (PEG)
Hyaluronic acid (HA)	

1.1.2.1 Natural polymer matrices

Fibrin

Fibrin is the major component of blood clots and thus plays an important role in natural wound healing by forming a three-dimensional crosslinked network [126]. It forms a gel by enzymatic cleavage of fibrinogen in the presence of thrombin [251]. During the process of new tissue formation, fibrin gradually becomes degraded by plasmin or matrix MMPs produced in the pericellular milieu of cells invading and replacing the temporary matrix [249]. In terms of clinical applications, fibrin is widely used as tissue sealant in surgery, named "fibrin glue"; a mixture of concentrated fibrinogen and thrombin [265-267]. Because of its slow lysis, fibrin glue has also been explored as provisional reservoir to deliver protein therapeutics [268], cells [269] or DNA of genes [270]. In addition, fibrin glue was found to stimulate capillary ingrowth [271].

Fibrin eventually became the first injectable scaffold to be used to increase cell retention when transplanted into ischemic myocardium and even proved to decrease infarct size when injected alone [235]. Subsequently, fibrin displayed a multitude of beneficial effects [234, 272, 273]. Hence, the injection into one-week-old infarcts prevented wall thinning and maintained fractional shortening over five weeks after injection although the material was resorbed within two weeks [234]. Additionally, it has been shown that fibrin injection is able to reduce infarct size and increase arteriole density, as compared to the control group [272, 274]. In a study performed on infarcted porcine hearts, researchers could confirm increased wall thickness as well as prevention of infarct expansion; however, they were unable to show functional improvement [246].
Overall, fibrin injection is not consistently associated with functional improvement [126], which, in part, could be explained by its limited mechanical strength and duration [251].

Collagen and gelatin

Collagen is the most abundant protein in mammalian tissues [275] and is the main component of the ECM [251]. It meets many of the desired parameters, as it is built from amino acid sequences that are recognized by cells and degraded by enzymes secreted from those cells. Thus, collagen-based gels have been employed for the reconstruction of liver [276], skin [277] and blood vessels [278]. Collagen injection after myocardial infarction has lead to increased ejection fraction relative to the control group at six weeks post-MI. [242]. However, neither angiogenesis nor cell infiltration could be detected in that study. Their lack, however, has not been universally observed, as a different research group was able to demonstrate fibroblast infiltration as well as angiogenesis [274]. When considering it as treatment option, one also has to keep in mind though that collagen gels are mechanically weak and, since derived from animal skin, bone or tendon, potentially immunogenic [249, 279, 280].

Gelatin is a degraded derivative of collagen. Critical properties such as cell adhesiveness and proteolytic degradability are retained in gelatin [249]. Similarly to collagen, gelatin has limited mechanical strength and degrades even quicker than its parent molecule [251]. Its injection into infarcted rat hearts has shown no functional improvement four weeks post-MI [281].

The injection of Matrigel, a porous liquid collagen compound, led to homogeneous engraftment within the ischemic myocardium and adapted to the host organ collagen structure, while preserving cardiac wall geometry [230].

Matrigel injection into ischemic hearts resulted in improved fractional shortening and wall thickness four weeks after treatment [230]. However, according to Wall *et al*. the effects seen by Kofidis and colleagues could be explained by large amounts of material being injected (corresponding to 50% of the normal ventricular wall volume), resulting in geometrical changes instead of the claimed functional regeneration [237]. Moreover, as Matrigel is derived from a mouse sarcoma line, its clinical application remains questionable due to the potential risk of tumor induction [126, 282].

One study compared fibrin with collagen and Matrigel, all of which were injected into one-week-old infarcts of separate groups of rats. The report showed that all three materials generated a similar increase in myofibroblast infiltration and capillary density relative to saline injection, however, the study was lacking data on cardiac function [274]. Fibrin, collagen and Matrigel have the disadvantage of gelling prematurely during catheter delivery due to their rapid gelation kinetics [282]. For fibrin, however, that could be overcome by using double-barreled catheters.

Alginate

Alginate is an anionic linear polysaccharide composed of beta-D-mannuronic acid and alpha-L-glucuronic acid that is found in brown seaweed. When complexed with multivalent cations such as Ca^{2+}, alginate forms a hydrogel [283]. The material properties of alginate have been reviewed and studied extensively [284]. As it is cost-effective, bioinert as well as non-toxic, interest has been generated for its use in the food, pharmaceutical and medical device industry. Thus, alginate-based biomaterials have been applied successfully for the controlled delivery of growth factors [285-287] and drugs [288] as well as for tissue engineering [289, 290]. Based on its unique ability to undergo a phase transition utilizing the calcium present in heart tissue upon injection into the LV wall, its therapeutic potential has also been investigated in the context of MI. It has been shown to reduce post-MI remodeling and dysfunction as well as infarct expansion both in rats [241, 291-293] as well as in swine [245]. Functional improvements after alginate injection could be shown for up to five to eight weeks after treatment, even if the material was injected several weeks after infarct induction [273].

However, alginate may not be an ideal material as it undergoes a somewhat uncontrolled degradation via a process involving loss of divalent ions into the surrounding medium, which eventually results in a decrease in mechanical stability and subsequent unpredictable dissolution [251].

In addition, stimulation of inflammatory cells have been reported [294, 295]. Furthermore, the molecular weights of many alginates are typically above the renal clearance threshold [251].

Hyaluronic acid (HA)

Hyaluronate plays a significant role in wound healing, cell proliferation and differentiation [296] as well as cell adhesion and motility [297, 298]. It has shown promising results when used for tissue engineering of artificial skin [299], dressings for wound healing [300], soft tissue augmentation [301], ophthalmic surgery [302] as well as for the treatment of joints [303] and drug delivery [304-306]. Yet, as for any other biomaterial of natural origin, hyaluronate requires meticulous purification to eliminate impurities and endotoxins that might transmit diseases or elicit an immune response [307]. Furthermore, hyaluronate gels are characterized by low mechanical properties [251].

Ifkovits and colleagues investigated the influence of different mechanical strengths of HA on ovine infarcts, for which Methacrylated Hyaluronic acid (MeHA) with 30% and 60% methacrylate substitution was injected post-MI [308], the higher percentage creating a greater stiffness. While both concentrations showed similar degradation rates, cellular responses as well as tissue distribution patterns, the injection of the stiffer material resulted in less infarct expansion and LV dilation compared to the weaker one and was associated with higher cardiac output and EF after eight weeks [308]. That coincides with the findings of Wall *et al.*, that when it comes to normalizing increased wall stresses, stiffer materials show greater benefits [237].

1.1.2.2 Synthetic polymer matrices

Although synthetic biomaterials are more likely to trigger inflammatory and foreign body reactions, one huge benefit is that every stage of their synthesis can be controlled by the engineer, thus allowing material properties to meet specific design objectives, such as structure (crosslinking density) and tailored properties (degradation, mechanical strength as well as chemical and biological response to stimuli) [255, 279]. Synthetic hydrogels offer the advantage of being biomimetic of the native biochemical and structural matrix composition [282], while eliminating the risk of pathogen transmission and immunogenicity [249]. Three groups of synthetic materials, widely used for experimental myocardial infarct therapy, are briefly described below.

Self-assembling peptides (SAP)

In nature, there is an abundance of materials that self-assemble to create larger structures, including lipids and proteins. Being 8-16 amino acids long, self-assembling peptides are composed of alternating hydrophilic and hydrophobic residues [309]. In water they form stable β-sheets, which upon exposure to physiological salt concentration or pH form a stable hydrogel, consisting of more than 99% water [310, 311]. Adapting that principle to synthetic materials [312], peptides have been developed that are able to self-assemble into macroscopic materials suitable for tissue engineering [313] and cardiac wall therapy [314]. Davis *et al.* could show that the injection of nanofibers into the non-infarcted LV free wall significantly augmented endogenous cell recruitment [315]. They demonstrated in another study the feasibility of sustained IGF-1 delivery and, when combined with cell therapy, improved systolic function after experimental myocardial infarction [316]. In a further study conducted by this group the injection of nanofibers into infarcted hearts showed sustained improvement of fractional shortening over three months, while the injection into uninfarcted hearts resulted in temporarily impaired systolic function [317]. Nanofiber injection into infarcted rat myocardium was unable to increase myocardial cell proliferation and neovascularization [318, 319]. This could perhaps be explained by too little material being injected that, in addition, is not mechanically robust [126].

N-isopropyl acrylamide (NIPAAm)

Thermoresponsive materials, such as NIPAAm, can be dissolved in water below their transition temperature of 32°C but turn into a hydrogel when reaching body temperature [126]. That gel has the disadvantage of being non-degradable, however, that can be overcome by co-polymerization with degradable polymers [320, 321] or incorporation of enzymatically cleavable peptide crosslinkers [322]. The mechanism of temperature-dependent phase transition may be ideal for cell delivery, as the timing of the polymerization is not set, but simply depends on the temperature change upon introduction to the body [251]. The injection of acrylic acid and hydroxyl ethyl methacrylate-poly(trimethylene carbonate) (HEMAPTMC), a co-polymer of NIPAAm has proven to prevent the progression of cardiac dilation as well as post-MI remodeling and has resulted in smooth muscle cell infiltration [243].

Wu *et al*. explored a gel made of Poly(ε-caprolactone) (PCL)-grafted dextran chains, co-polymerized with NIPAAm monomer, which becomes degradable through cleavage of dextran [323]. Its injection into four-day-old MIs lead to significantly improved EF relative to the saline control group and to a considerably thicker LV wall, which was still evident at four weeks post-MI [247]. As all material had disappeared after four weeks, it is unclear, whether the observed effect was due to cell infiltration or an increased collagen deposition. An important factor that needs to be taken into account, is the potential toxicity and carcinogenicity of NIPAAm [324].

Poly(ethylene glycol) hydrogel matrices (PEG)

PEG polymers form aqueous solutions containing linear or branched macromers with reactive groups that can be crosslinked into hydrogels either spontaneously or via photopolymerization. One particular chemistry that is of great interest is the Michael-type addition reaction, as illustrated in Figures 2a and b:

PEG-acrylate:

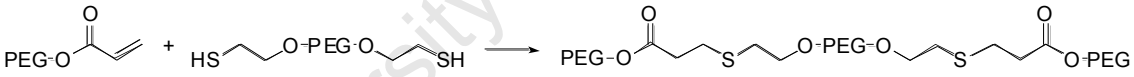

PEG-vinyl sulfone:

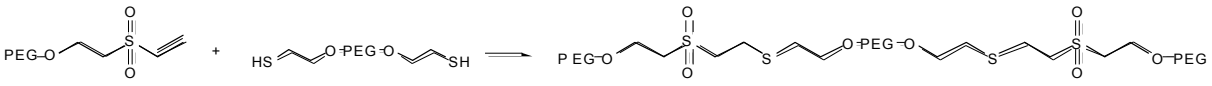

Fig. 2a: Chemistry of Michael-type addition reaction *between acrylate- as well as vinyl sulfone-functionalized multiarm PEGs and thiol-bearing crosslinkers.*

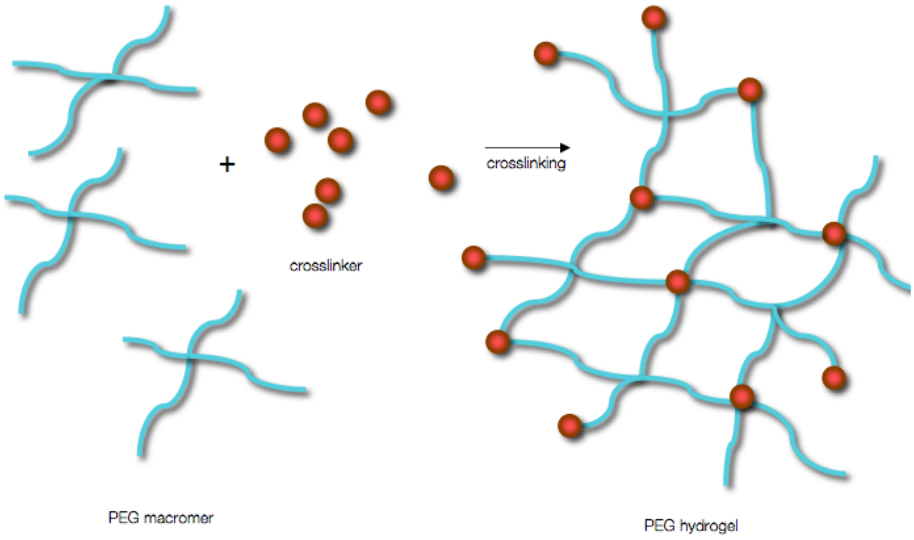

Fig. 2b: Polymerization of multiarm PEG hydrogels. *Here a 4-arm macromer is illustrated, however, the number of arms can vary. Figure modified after Zisch et al. [249]*

PEG macromers have the advantage of being highly hydrophilic, which means that they do not cross cell membranes, while being generally non-adhesive to cells and proteins [249]. As bioactivity is important for cellular adhesion, proliferation, growth and therefore tissue regeneration, its lack can in some cases even be a disadvantage [282]. However, through co-polymerization with other macromolecules, such as the integrin binding peptide RGD, one can easily promote the survival of adherent-dependent cells within otherwise bio-inert PEG hydrogels [350]. Hence, the versatility of the PEG macromer chemistry together with its excellent biocompatibility has, over the past few decades, stimulated significant research and extensive use of numerous intelligently designed PEG hydrogel systems for several medical applications [325-330], such as the control of adhesion formation [344-347], to release adhesion-preventing drugs [348, 349] and to control healing of arterial injuries induced by balloon angioplasty [347].

Christman *et al.* suggested to use an injectable polymer that is non-degradable for long-term beneficial effects on post-MI heart remodeling [240]. Hence, to our knowledge, we were the first laboratory to use the Michael-type addition reaction to introduce non-degradable PEG to the heart [244].

The intramyocardial injection of a PEG-based hydrogel following permanent coronary artery occlusion was used in order to prevent post-infarct remodeling and progression to heart failure. The thiol-bearing crosslinker caused spontaneous in situ polymerization and was non-degradable. Thus, the PEG hydrogels remained at the injection site indefinitely and showed promising results at 28 days post-MI (reduced end-diastolic diameters). However, after three months, despite the inert nature of PEG hydrogels, an extensive macrophage response was detected [244], which may be a prove for the damaging role that chronic inflammation can play.

Therefore a degradable PEG hydrogel might be superior to a non-degradable one, which is why numerous biomaterials have been designed to degrade by ester hydrolysis [255]. Yet, more common *in vivo* is the enzymatic cleavage of structural proteins of the extracellular matrix, such as collagen, by cell-secreted proteases [331-334]. Cell-induced proteolysis is essential for 3-D cell invasion, otherwise the ECM would have a barrier function and thus hinder migration [335]. Consequently, PEG hydrogels with biological functionalities specifically associated with cell migration have been developed, making them sensitive to degradation by MMP [336-338], plasmin [339] or both of these protease families [331, 340, 341]. That way, the degradation process is directly linked to the healing progress of the responding tissue. This “cell-dictated” hydrogel degradation is extremely useful for tissue regeneration as it eliminates the risks of incorrect network degradation or therapeutic liberation profiles and is therefore strongly desired in essentially every *in vivo* tissue engineering approach [342].

After degradation, PEG hydrogels are eventually excreted via urine or feces [343].

1.1.2.3 Host response to biomaterials

Biocompatibility is crucial for the *in vivo* use of any biomaterial. Although commonly used biomaterials are supposed to be physically and chemically stable, inert as well as nontoxic, a host inflammatory reaction is a natural response to tissue damage and the presence of a foreign object [351, 352]. Yet, extent and duration of the inflammatory process directly influence biomaterial integrity [353] and can result in serious iatrogenic consequences such as osteolysis next to artificial joints, stress cracking of pacemaker leads as well as capsule contracture of mammary prostheses [354]. Inflammatory responses to biomaterials involve a number of dynamic, interdependent and multi-factorial reactions [355]:

Firstly, biomaterials spontaneously acquire a film of nonspecific host protein immediately upon implantation; a process that does not occur during physiological wound healing [354, 356]. The three predominating host plasma proteins are albumin, IgG and fibrinogen [357, 358]. Those proteins, found on the biomaterial surface, are recognized by leukocytes, which subsequently adhere via several adhesion ligand-receptor superfamilies [359]. Since the implant is considerably larger than the adhered macrophages, they are unable to phagocytose the foreign body [356]. That triggers a chronic inflammation at the biomaterial surface as well as the fusion of macrophages, which form multinucleated foreign body giant cells (FBGC); cells that are frequently observed for the duration of the implant [360]. The formation of FBGCs is unique to the macrophage phenotype, thus their presence can be exploited as a histopathological marker for chronic inflammatory or foreign body reaction [361]. The final step of the foreign body reaction is reached as soon as the implant is surrounded by a dense, avascular, fibrous capsule, typically 50-200µm thick [356].

Non-fouling coatings (i.e. coatings that are resistant to protein-adsorption), including hydrogels, polymeric films and brushes, have been investigated to modulate inflammatory responses to implanted biomaterials [355]. Of all hydrogels, PEG is particularly known for its protein and cell resistance [362-368], which is believed to be a result of its hydrophilicity (hydrophilic molecules stay outside the cell's plasma membrane) as well as the PEG chain length and density [257, 369]. One of the first experiments with PEG was performed by Merrill *et al.* in 1982, showing that the adsorption onto glass surfaces prevented adherence of proteins [370]. Ever since, various forms of PEG modification became a popular means to render a surface protein resistant and to enhance biocompatibility [279].

1.1.2.4 Timing

Countless models have been tested thus far to try and prevent the progression to HF post-MI. In the search for treatment alternatives, infarcted hearts have been treated with different amounts of various cell types, alone or embedded into a range of biomaterials or with a variety of biomaterials alone. Although it might be a crucial factor, influencing the success of a treatment, the timing of biomaterial injection after a myocardial infarction has, to our knowledge, not yet been systematically investigated. In fact, across different studies, biomaterials have been injected at various time points, ranging from minutes to weeks or even months after myocardial infarction.

That complicates, perhaps even makes it impossible, to compare the outcome of those studies and to draw conclusions about their potential as treatment alternative.
A disadvantage that might relate to delayed injection is the increased difficulty to salvage myocardial tissue. Biomaterial delivery immediately after experimental infarct induction, on the other hand, might not be able to mimic a clinical setting, as it is much more likely that a patient will be treated hours, if not days (if the infarct went unrecognized) after a myocardial infarct has occurred.

The following tables (2 a and b) give an overview of a selection of studies that have been conducted as well as the time point, at which the respective biomaterial was injected:

Table 2a: Examples of studies with intramyocardial biomaterial injection immediately post-MI

Immediate biomaterial injection			
Group	Transplanted material	Outcome	Reference
Lin *et al.*	Self-assembling peptide nanofibers were injected with autologous bone marrow mononuclear cells	Improved cell retention and post-MI cardiac function	[314]
Davis *et al.*	Self-assembling peptide nanofibers were injected with neonatal cardiomyocytes and IGF-1	Improvement of post-MI systolic function	[316]
Hsieh *et al.*	Self-assembling peptide nanofibers were used for the delivery of PDGF	Long-term improvement of post-MI cardiac performance	[317]
Segers *et al*.	Self-assembling peptide nanofibers were used for the delivery of SDF-1	Recruitment of stem cells and improved post-MI cardiac function	[319]
Kofidis *et al.*	Injection of Matrigel with embryonic stem cells	Mice treated with Matrigel + ESCs had superior post-MI function relative to contro groups	[230]
Dobner *et al*.	Injection of a synthetic non-degradable PEG hydrogel	Transient reduction of EDD	[244]
Shao *et al*.	Gelatin hydrogel was used for the delivery of bFGF	Incorporation of bFGF in gelatin was superior to either of the components alone and enhanced arteriogenesis and post-MI cardiac function	[281]
Ifkovits *et al*.	Injection of HA 30min post-MI	Depending on material properties significantly increased wall thickness and post-MI functional improvement	[308]

Table 2b: Examples of MI studies with delayed intramyocardial biomaterial injection

Delayed biomaterial injection			
Group	Transplanted material	Outcome	Reference
Christman *et al*.	Fibrin glue and skeletal myoblasts were injected one week post-MI	Preserved infarct wall thickness and post-MI cardiac function as well as increased cell transplant survival and smaller infarct size	[234, 235]
Christman *et al*.	Fibrin glue-based delivery of pleiotrophin, injected one week post-MI	Combined delivery enhances pleiotrophin plasmid efficacy	[272]
Dai *et al*.	Collagen injection one week post-MI	Thickened infarct scar and improved LV function	[242]
Landa *et al*.	Calcium-crosslinked alginate was injected either one week or two months post-MI	Prevention of adverse cardiac remodeling and dysfunction in both recent and old infarcts	[241]
Leor *et al*.	3D alginate scaffold was implanted with fetal cardiac cells one week post-MI	Stimulated neovascularization and attenuated LV dilatation	[291]
Yu *et al*.	Injection of either alginate or fibrin glue five weeks post-MI	Increased arteriogenesis as well as restoration of LV geometry and function	[273]
Huang *et al.*	Comparison of collagen, fibrin and Matrigel, injected one week post-MI	Similar degree of angiogenesis in all three groups	[274]
Fujimoto *et al*.	Degradable, thermoresponsive hydrogel injected two weeks post-MI	Increased wall thickness and higher capillary density relative to saline control as well as preserved LV cavity area and contractility	[243]

To our knowledge, so far only two groups injected biomaterials (both alginate) at two different time points as part of the same experiment:

Ruvinov *et al*. injected immediately as well as six days post-MI. Yet, potential differences in outcome were not directly compared. Instead, the rats that were treated immediately post-MI were killed one week after the biomaterial injection, while rats, which were injected six days after infarct induction were killed four weeks after the treatment [293]. Landa and co-workers treated the rats either one week or two months after infarct induction, in both groups animals were killed eight weeks after treatment. The improvements in old infarcts were less pronounced and hence, Landa suggested that earlier injection might achieve a superior effect on the prevention of remodeling, but that the optimal timing for implant delivery certainly requires further investigation. Yet, the main aim of their study was to demonstrate feasibility rather than primarily comparing the outcome of the two different time points [241].

1.2 Project aims

Not only are PEG hydrogels considered one of the most inert synthetic biomaterials to date [371], they also rank amongst the stiffest mentioned in Wall's paper [237], who had shown that the firmest materials show the greatest benefit for prevention of post-MI remodeling.

As non-degradable PEG hydrogels were shown to elicit an extensive inflammatory response after intramyocardial injection, hydrolytically and enzymatically cleavable PEG hydrogels need to be characterized *in vitro* as well as *in vivo,* with the aim of identifying the most compatible degradable PEG hydrogel for intramyocardial injection.

Secondly, as there is no consensus in the present literature on the timing of biomaterial implantation, which currently ranges from minutes to two months post-MI, it needs to be investigated if the time point of the biomaterial injection has an influence on the success of the treatment.

1.3 Results and discussion

1.3.1 Preliminary *in vitro* characterization of PEG hydrogels

A study previously conducted in our laboratory, using 20PEG-8VS crosslinked with 2nPEG-2SH, revealed an extensive macrophage response [244]. The non-degradable gel eventually caused scarring and chronic inflammation in uninfarcted myocardium and may have also contributed to the loss of an initial functional improvement observed for infarcted hearts injected with PEG gel. In an attempt to avoid these adverse effects, the focus of the present study was shifted towards the utilization of a degradable PEG hydrogel for the treatment of myocardial infarction.

A selection of degradable PEG gels was investigated to determine the optimal composition for myocardial infarction therapy. This is crucial, as the mechanical properties of hydrogels largely depend on parameters such as the gelling time, amount of swelling, rigidity and degradation rate - all of which are determined by the crosslink density [251].

The use of a 4-arm crosslinker should polymerize gels faster. There is also the possibility they may crosslink macromers more efficiently than 2-arm crosslinkers and thus elevate the number of crosslinks obtained. Hence, a hydrogel that is polymerized with a 2-arm crosslinker may be “softer” than one with a 4-arm crosslinker, which would then be a more rigid gel with potentially greater strength. Polymers with a low crosslink density are preferred for applications, where fast ingrowth and migration of cells is needed, while more rigid gels might be favored for mechanically taxing environments.

20PEG-8Ac hydrogels were crosslinked with different ratios of 10nPEG-4SH (4-arm crosslinker) and 2nPEG-2SH (2-arm crosslinker) and were compared to 20PEG-8VS crosslinked using a peptide with MMP-1 recognition site (MMP-1 substrate [MMP-1s]), as detailed in chapter 5.1.2. The hydrogels were assessed with respect to the above-mentioned properties. 20PEG-8VS crosslinked with 2nPEG-2SH was added as non-degradable control.

Acrylate-based crosslinks with sulfhydryl are hydrolytically unstable, degrading due to hydrolysis. Vinyl sulfones, on the other hand, form a stable permanent covalent linkage.

1.3.1.1 Gelling time

Table 3: Gelling times

Pre-polymer	Crosslinker	Gelling time
20PEG-8Ac	100% 4-arm	3'40min
	75% 4-arm, 25% 2-arm	3'00min
	50% 4-arm, 50% 2-arm	3'45min
	25% 4-arm, 75% 2-arm	6'00min
	100% 2-arm	9'30min
20PEG-8VS	100% 2-arm	2'30min
	MMP-1s	9'30min

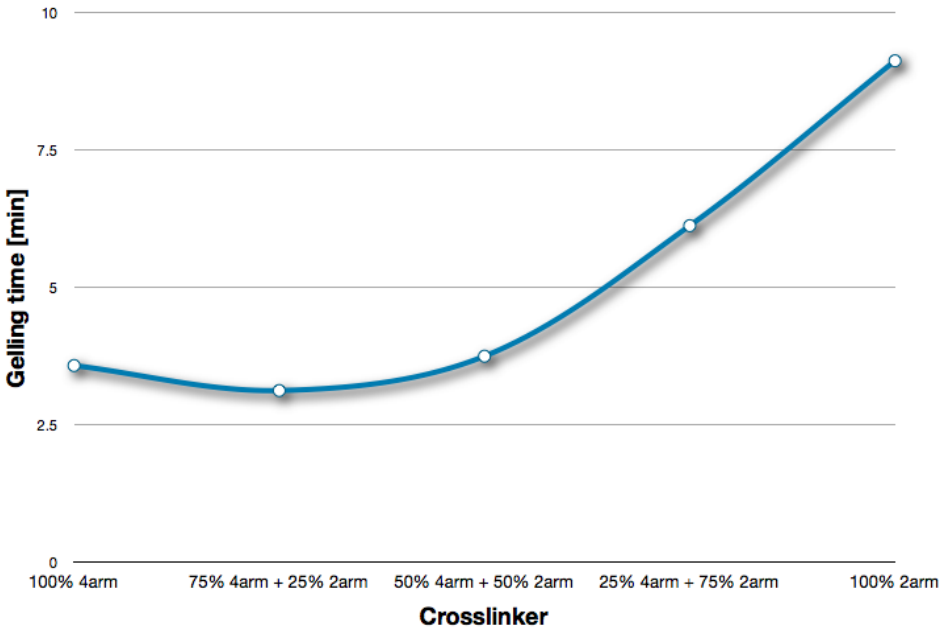

Fig. 3: Gelling time *(illustrated for 20PEG-8Ac)*

The gelling time indeed did depend on the number of arms of the crosslinker, as demonstrated in Table 3 as well as in Figure 3. Thus, the use of a crosslinker with more arms did accelerate the polymerization process.

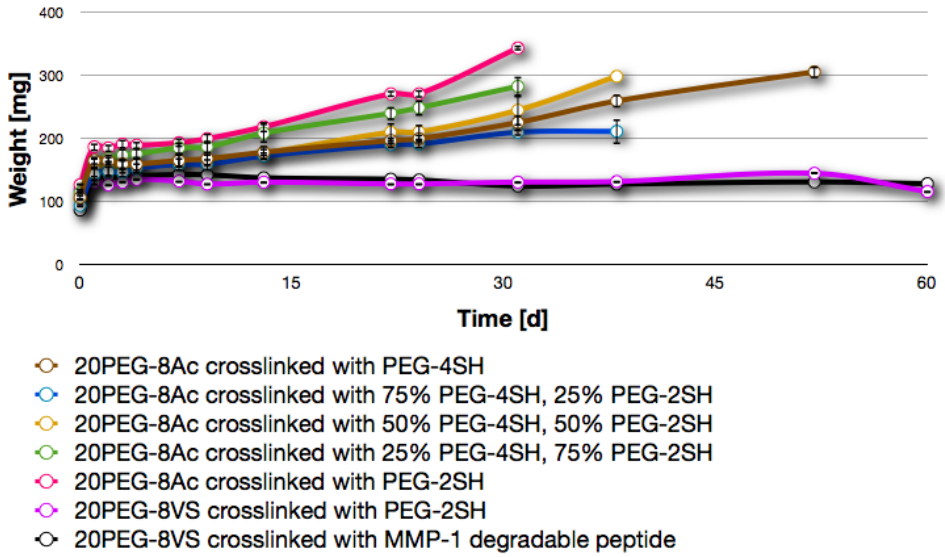

Fig. 4: Amount of swelling and time to degradation, comparing various degradable PEG gels

1.3.1.2 Swelling

The first measurement after 24 hours, before any swelling due to degradation could occur, showed significantly increased swelling of 20PEG-8Ac crosslinked with PEG-2SH relative to MMP-1 degradable 20PEG-8VS ($p<0.05$). According to the *Flory-Rehner Theory*, crosslinked polymers absorb solvent, which diffuses into the gel network and causes swelling [373, 374]. This is a consequence of positive entropy change. The gels do not dissolve but as the volume increases, the network chains are stretched and straightened and an elastic retracting force develops. The chain deformation causes a decrease in entropy; consequently the swelling process slows down. Equilibrium is achieved when the opposing forces are balanced [375]. Network chains of gels with higher crosslink density can stretch less and therefore swell to a lesser extent.

Most likely vinyl sulfones react more efficiently with sulfhydryls than acrylate, which might explain why the gels swelled less [372]. Thus it appears that vinyl sulfone-based gels have a higher crosslink density and are potentially stiffer (Figure 4).

1.3.1.3 Degradation

As crosslinks break down, more swelling occurs. Hence, further swelling indicates ongoing degradation. The endpoint was observed when the gel eventually became too pliable to be handled, i.e. for its weight to be measured. As shown in Figure 4, one of the factors that determined the span of time until degradation took place was the type of crosslinker the hydrogel was polymerized with. PEGs that were mixed with a 2-arm crosslinker took about one month to degrade *in vitro*, while those crosslinked with a 4-arm one could be handled for more than 50 days. Thus, hydrogels with a lower crosslink density degraded faster because of their increased tendency to swell, which resulted in more hydrolytically degradable bonds being exposed to water at a given time. Moreover, hydrogels crosslinked with fewer arms de facto have less bonds that need to be degraded for the gel to break down. Another aspect influencing the degradation was the nature of the macromer: 20PEG-8VS, crosslinked with PEG-2SH was non-degradable, while 20PEG-8Ac, irrespective of the crosslinker, would degrade by hydrolysis.

As expected, 20PEG-8VS polymerized with the MMP-1s, which would be cleaved *in vivo*, remained non-degradable *in vitro*, as the solvent (iPBS) was lacking the MMP-1 enzyme. Hence, measurements were discontinued on day 60.

As shown in this study, stiffness and degradation of PEG hydrogels can be controlled by the choice of macromer and crosslinker. This is a clear advantage synthetically derived hydrogels have over natural polymer matrices [251, 255, 279] and one of the reasons that justifies the use of PEG in the present study. Moreover, the application of synthetic hydrogels eliminates the risk of pathogen transmission and immunogenicity [249].

Another crucial factor is the biocompatibility of hydrogels, relating to the biomaterials ability to exist within the body without damaging adjacent cells or eliciting a response that impacts on its desired function [251]. Although naturally derived polymers typically offer superior biocompatibility to synthetic ones [255, 279], PEG hydrogels are an exception from this; due to their hydrophilicity as well as to the PEG chain length and density they are known for their protein and cell resistance and hence are often used as non-fouling coatings for implants to prevent foreign body responses [257, 363-370].

Therefore, using a PEG hydrogel allowed the combination of having an engineerable biomaterial that typically displays excellent biocompatibility.

Out of the previously investigated gels (Figure 4), it made most sense to further test the "softest" hydrogel that caused most swelling and degraded fastest (hydrolytically degradable 20PEG-8Ac crosslinked with 2nPEG-2SH) against the most rigid degradable PEG (enzymatically cleavable 20PEG-8VS crosslinked with MMP-1s). Their biocompatibility was compared to 20PEG-8VS crosslinked with 2nPEG-2SH, which served as non-degradable control.

1.3.2 Subcutaneous assessment of biocompatibility

The implantation of PEG hydrogel discs underneath the dorsal skin of rats was a feasible screening method, as it puts less strain on the animal than an intramyocardial injection would, while a larger number of gels could be tested simultaneously. Six gels were used per group and three gels were implanted per rat as described in chapter 5.2.2.2. In a wound healing situation such as this one, the number of monocytes typically peaks one to two days after the injury has occurred [376], before they mature into macrophages in the wound site. Hence, after four days, the gels together with surrounding tissue were explanted, processed and analyzed based on ED1 staining, as described in 5.3.1.5. That way, macrophages could be visualized, depicting the extent of the inflammatory reaction.

As illustrated in Figure 5, only low levels of macrophage response could be detected histologically, with hardly any difference between the three investigated groups. Those inconclusive results could perhaps be attributed to subcutaneous implantation not being able to offer an accurate reflection of the immune response one would get if one was to implant into muscle tissue, which typically has a much better blood supply. Hence, it was necessary to re-assess the biocompatibility intramyocardially.

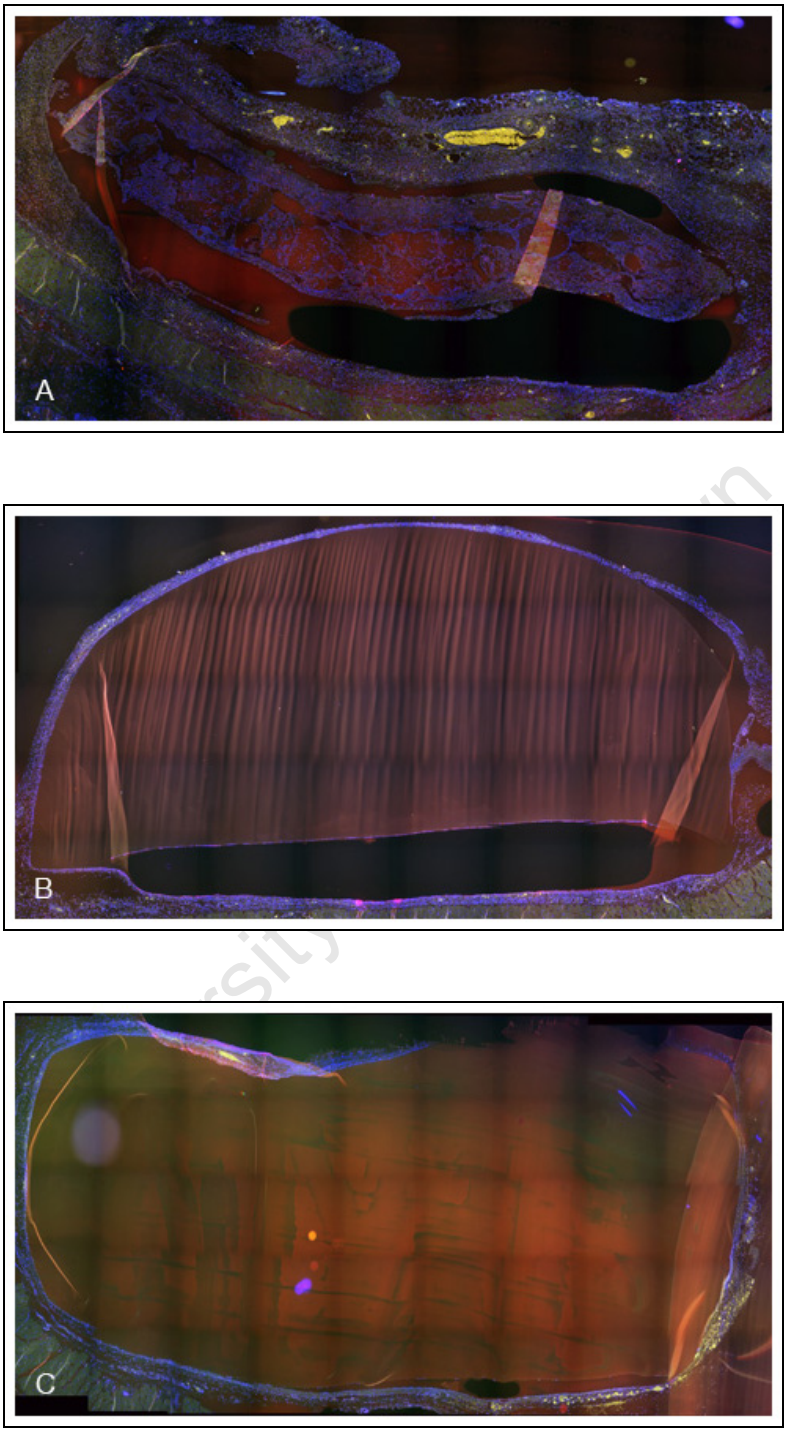

Fig. 5: Stitched microscopic images of ED1 stained PEG hydrogel discs. *(A): 20PEG-8Ac hydrogel crosslinked with 2nPEG-2SH; (B): 20PEG-8VS crosslinked with MMP-1s; (C): 20PEG-8VS crosslinked with 2nPEG-2SH.*
Original size of hydrogel discs: 1mm (thickness), 0.8cm (diameter). Nuclei stained blue, macrophages red.

Although no conclusion could be drawn with respect to biocompatibility, the subcutaneous assessment confirmed previous *in vitro* results.

As illustrated in Figure 5, after only four days, substantial tissue ingrowth could be seen in the 20PEG-8Ac hydrogel crosslinked with 2nPEG-2SH (picture A), in accordance with the findings described in chapter 1.3.1. There, the same gel appeared to be the "softest", allowing most swelling to occur and degrading fastest – ideal for tissue ingrowth and rapid cell migration. Also consistent with the results in 1.3.1, both 20PEG-8VS crosslinked with MMP-1s (picture B) as well as crosslinked with 2nPEG-2SH (picture C) proved to be rigid gels with high mechanical strength, which hardly swell but instead kept their shape.

1.3.3 Intramyocardial evaluation of biocompatibility and time to degradation

As the non-degradable 20PEG-8VS crosslinked with 2nPEG-2SH had already been shown to elicit an extensive macrophage response [244], only the degradable 20PEG-8Ac crosslinked with 2nPEG-2SH and 20PEG-8VS crosslinked with MMP-1s were implanted intramyocardially to gain information about their biocompatibility. Furthermore, both hydrogels were evaluated with respect to the time until degradation *in vivo*.

Therefore, rats were operated on as specified in chapter 5.2.2.3. However, for this experiment, sham rats were used to avoid confusion of a foreign body reaction with inflammation due to a healing infarct. Of the respective hydrogels, 100µl were injected per heart. Hearts were explanted four days, one week, two weeks and four weeks after hydrogel injection.

The explants were stained with ED1 (see 5.3.1.5) to assess macrophage response, while the explantation at different time points allowed for an assessment of the amount of hydrogel left after a certain time and therefore the *in vivo* degradation rate. Three rats were explanted per time point. Representative pictures are shown in Figure 6:

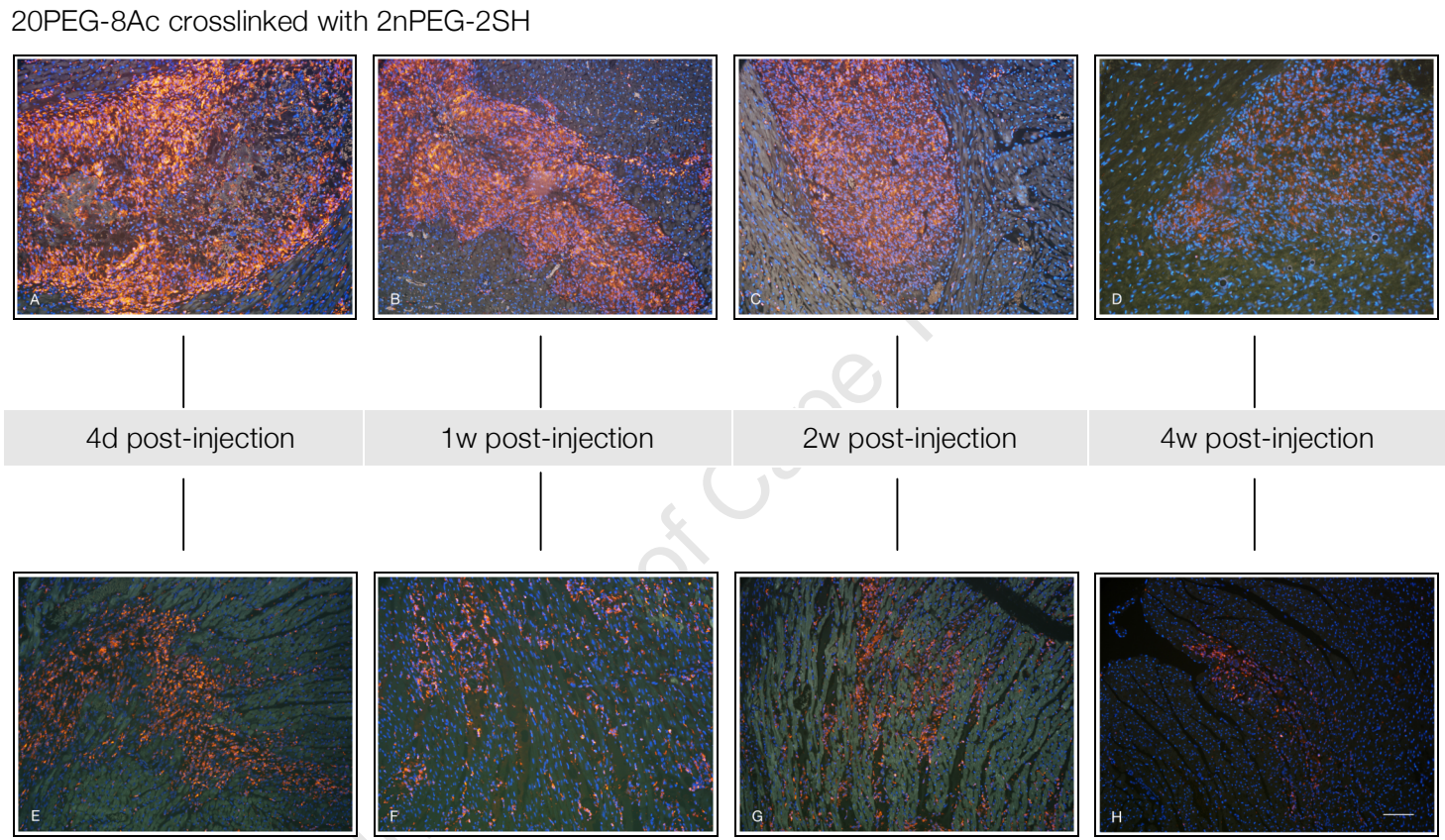

Fig. 6: ED1-based intramyocardial evaluation of biocompatibility and time to degradation*. Representative microscopical images of ED1 stained myocardium containing PEG hydrogel. Upper row: 20PEG-8Ac crosslinked with 2nPEG-2SH, explanted after: (A) four days, (B) one week, (C) two weeks, (D) four weeks. Lower row: 20PEG-8VS crosslinked with MMP-1s, explanted after: (E) four days, (F) one week, (G) two weeks, (H) four weeks.*
Nuclei stained blue, macrophages red. Bar represents 100µm.

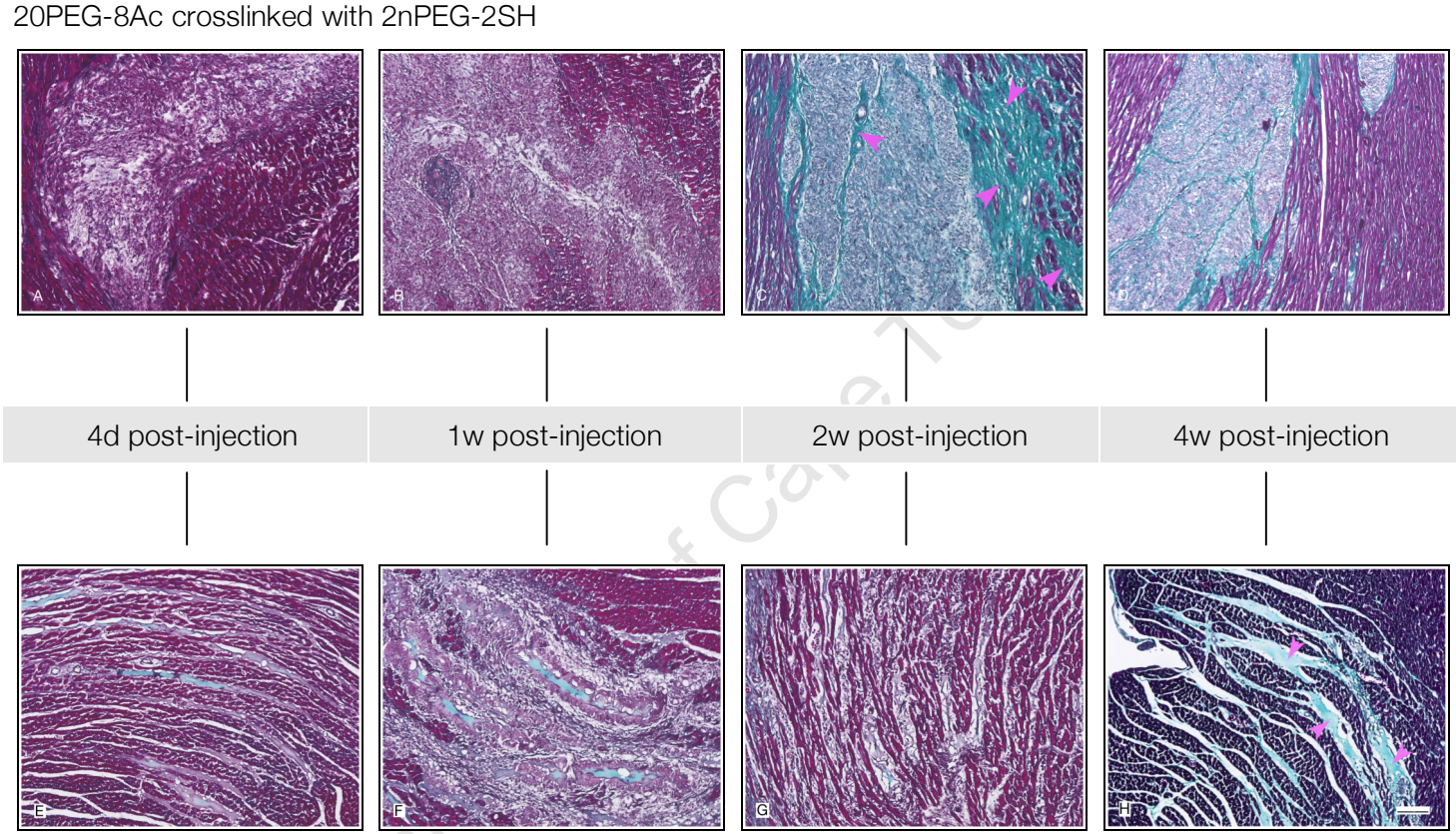

Fig. 7: Masson's Trichrome-based intramyocardial evaluation of biocompatibility and time to degradation*. Representative microscopical images of MT stained myocardium containing PEG hydrogel. Upper row: 20PEG-8Ac crosslinked with 2nPEG-2SH, explanted after: (A) four days, (B) one week, (C) two weeks, (D) four weeks. Lower row: 20PEG-8VS crosslinked with MMP-1s, explanted after: (E) four days, (F) one week, (G) two weeks, (H) four weeks. Muscle tissue stained purple, collagen fibers green. Bar represents 100µm.*
Arrows in picture C mark collagen fibers, arrows in picture H indicate PEG hydrogel.

Based on the amount of macrophages that could be seen after ED1 staining, some significant differences between the two hydrogels became apparent, as demonstrated in Figure 6. Firstly, the immune response elicited by 20PEG-8VS crosslinked with MMP-1s was considerably milder and more localized than the one caused by 20PEG-8Ac crosslinked with 2nPEG-2SH, although both showed evidence of a decline in severity over time. Secondly, the inflammatory reaction after injection of 2nPEG-2SH crosslinked 20PEG-8Ac was widespread and persisted at the injection site throughout the four-week follow up period although the gel was completely degraded between one and two weeks. In contrast, MMP-1 cleavable hydrogels could still be detected after four weeks in the myocardium, with almost no immune response left at that time (Figures 6 and 7).
Encapsulation of an implant by fibrous tissue is a common sign of a foreign body reaction, typically demarcating its final stages [356]. Masson's Trichrome stained micrographs showed the appearance of scar tissue around 20PEG-8Ac implants, beginning after about two weeks, although the hydrogel was already degraded by then. In contrast, throughout that month no scar tissue had formed around MMP-1s crosslinked PEG (Figure 7).
It is possible that the acrylate moiety is more inflammatory than the vinyl sulfone moiety, or that the latter reacts more effectively with its crosslinkers, therefore preventing unbound, loose ends of the crosslinkers to cause inflammation.

In the search for a degradable PEG hydrogel that is most biocompatible and that can provide the infarcted myocardium with adequate mechanical support, MMP-1 degradable 20PEG-8VS appeared to be the optimal material tested. Additionally, as the degradation rate of this hydrogel depends on the migration of cells that secrete MMPs (originally to cleave peptide sequences in the fibrin network), it will only disappear at a rate that is similar to the new tissue formation. Moreover, MMP-1 degradable PEG having a high crosslink density, preventing it from extensive swelling, decreases the likelihood of surviving cardiomyocytes being forced apart, lessening their ability to generate force effectively. Lastly, the relatively long gelling time of MMP-1 degradable PEG hydrogels (9'30min) enables comfortable handling and injection, before the components polymerize.

However, before MMP-1s crosslinked PEG hydrogels could be evaluated as treatment option after myocardial infarction, adverse effects on the function of healthy hearts needed to be excluded.

1.3.4 Effect of MMP-1s crosslinked 20PEG-8VS on the function of healthy hearts

Rats underwent sham operation as detailed in chapter 5.2.2.3 and were then randomized to receive an intramyocardial injection of either 100µl MMP-1 degradable PEG hydrogel or 100µl of saline as control. At two and four weeks after the injection, echocardiography was performed to assess myocardial function as explained in 5.2.3. The experiment was terminated after four weeks.

The average fractional shortening (FS) of rats two weeks after intramyocardial saline injection was 46.3% (±1.03%) and after injection of 20PEG-8VS crosslinked with MMP-1 degradable hydrogel 43.02% (±2.58%) (Figure 8) as well as after four weeks 46.5% (±0.94%) (saline group) and 44.2% (±2.46%) (hydrogel group) (Figure 9).
No significant functional difference could be detected between the two groups; neither at two ($p=0.26$) nor at four weeks ($p=0.4$) after the respective injection.

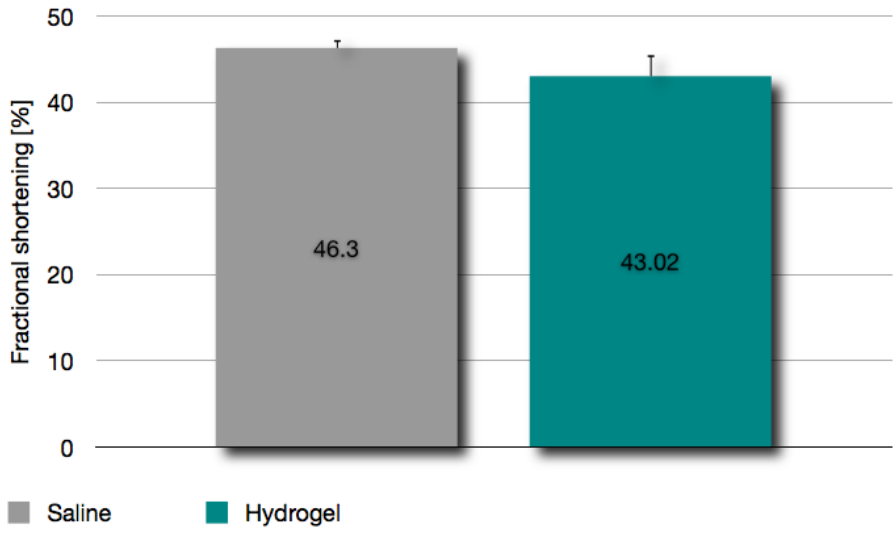

Fig. 8: Effect of intramyocardial hydrogel injection on the function of uninfarcted hearts, 14 days after the injection. There was no significant functional difference between injection of saline and injection of MMP-1 degradable PEG hydrogel (p=0.26).

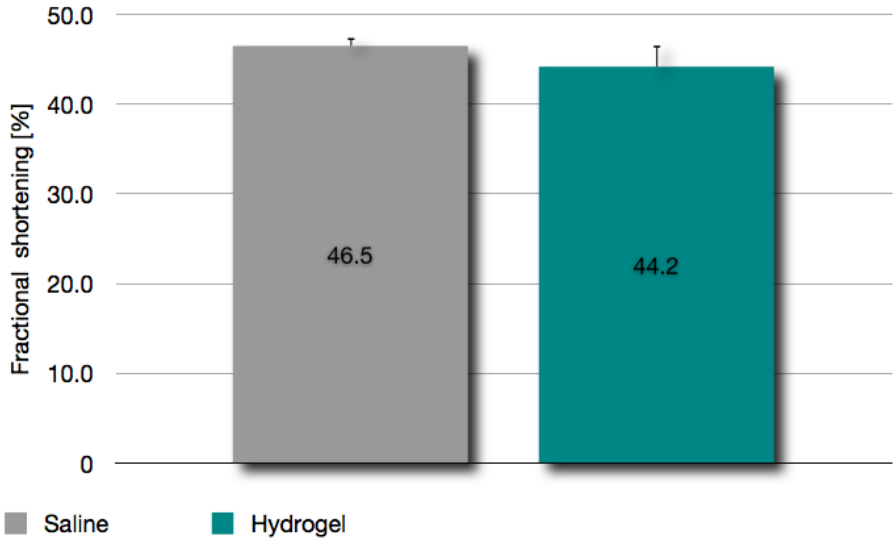

Fig. 9: Effect of intramyocardial hydrogel injection on the function of uninfarcted hearts, 28 days after the injection. No significant functional difference between injection of saline and injection of MMP-1 degradable PEG hydrogel (p=0.4)

MMP-1 cleavable PEG hydrogel proved to not have any adverse effects on the function of healthy hearts. Taking into account its excellent biocompatibility and mechanical strength that could help support infarcted myocardium, the feasibility of MMP-1 degradable PEG hydrogel for myocardial infarct therapy was then tested in a rat infarct model.

1.3.5 Investigation of MMP-1 degradable PEG hydrogel for treatment of myocardial infarction

To assess the value of enzymatically degradable PEG hydrogel for myocardial infarct therapy, 100µl of 20PEG-8VS crosslinked with MMP-1s were injected into rat myocardium immediately after infarct induction and were compared to the same amount of saline as control as detailed in chapter 5.2.2.3. To investigate if the time point of a biomaterial application impacts on cardiac function, immediate hydrogel injection was directly compared to the same treatment administered after seven days. At two and at four weeks post-MI induction cardiac function was assessed with echocardiography, before the experiment was terminated four weeks post-MI.

The study was designed as follows:

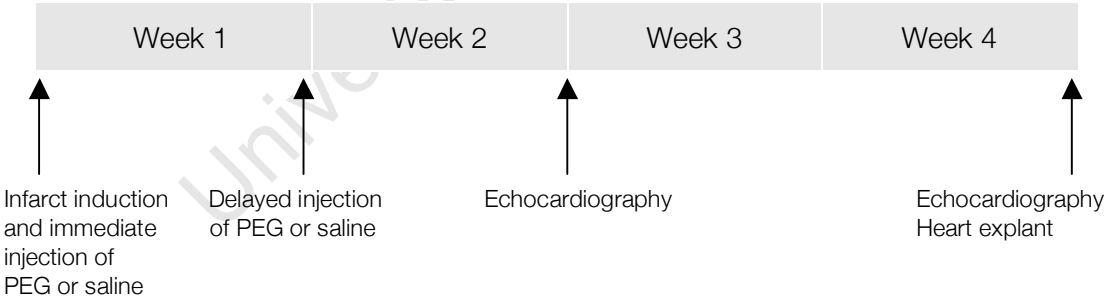

Aiming to avoid false positive results and to minimize variability between the four groups, only rats with a minimum of one eighth of the myocardium being infarcted (12.5%) were included in this study. Calculations of the infarct size were based on histomorphometric analyses and could therefore only be performed after the hearts were explanted. That resulted in an inconsistent number of replicas per group: saline delayed injection (n=7), saline immediate injection (n=8), PEG hydrogel delayed injection (n=9), PEG hydrogel immediate injection (n=8).

After the infarct size was assessed, echocardiography results of the pertinent rats were revealed for analysis.

1.3.5.1 Functional assessment

Table 4: Echocardiographic assessment of myocardial function at two and four weeks post-MI. *ESD: end-systolic diameter in mm; EDD: end-diastolic diameter in mm; FS%: percent of fractional shortening*

Weeks	Parameter	Saline 0d	Hydrogel 0d	Saline 7d	Hydrogel 7d
2	ESD	4.9 ± 0.11	5.2 ± 0.21	5.0 ± 0.19	4.3 ± 0.25 * †
	EDD	7.6 ± 0.12	7.8 ± 0.19	7.3 ± 0.16	7.2 ± 0.23
	FS%	34.9 ± 1.28	33.2 ± 1.69	32.0 ± 2.33	39.8 ± 2.05 * †
4	ESD	5.2 ± 0.24	5.6 ± 0.25	5.5 ± 0.23	4.7 ± 0.2 * †
	EDD	8.1 ± 0.15	8.4 ± 0.19	8.0 ± 0.19	7.8 ± 0.22
	FS%	35.9 ± 2.41	33.3 ± 1.82	31.9 ± 2.07	40.6 ± 1.36 * †

**p<0.05 immediate vs. delayed PEG-treatment of infarcted hearts*
†p<0.05 delayed treatment vs. saline control

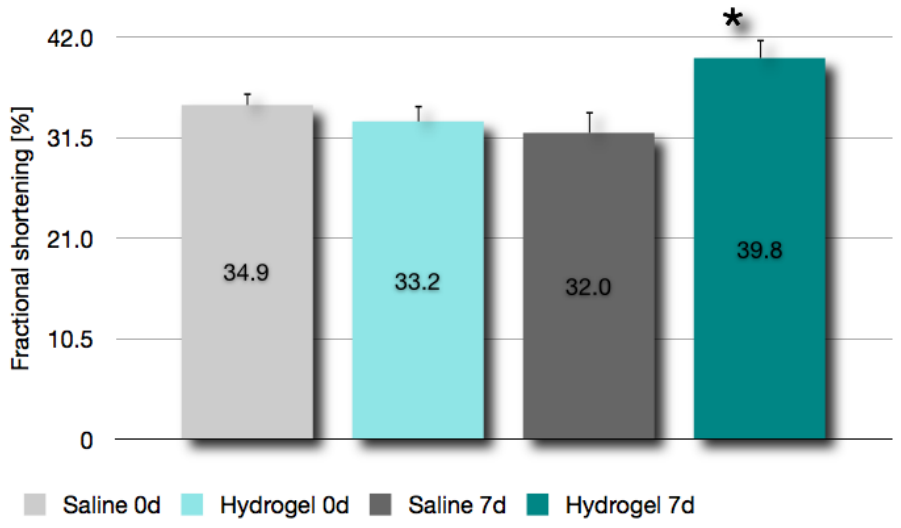

Fig. 10: Effect of intramyocardial hydrogel injection on fractional shortening (FS), 14 days post-MI. *FS after delayed hydrogel injection was significantly improved relative to immediate treatment and saline control group (p<0.05), n=7-9.*

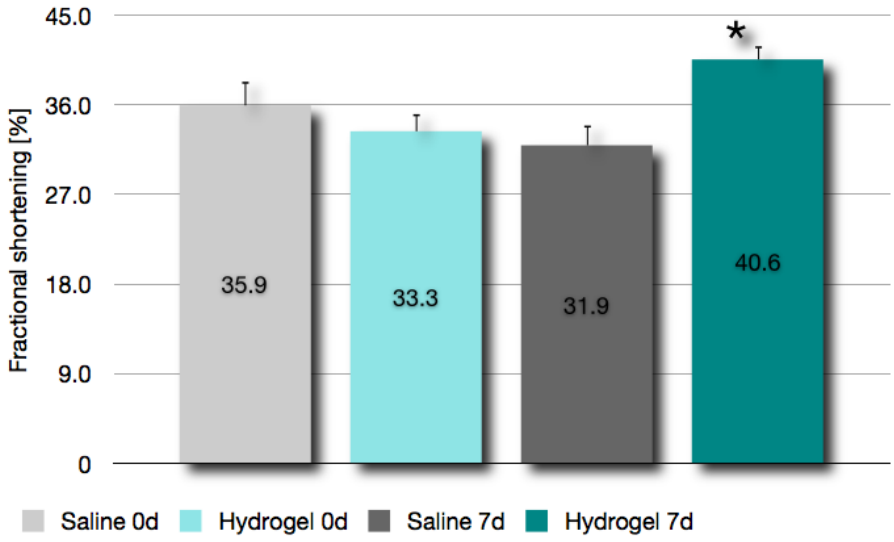

Fig. 11: Effect of intramyocardial hydrogel injection on fractional shortening (FS), 28 days post-MI. *FS after delayed hydrogel injection was significantly improved relative to immediate treatment and saline control group (p<0.05).*

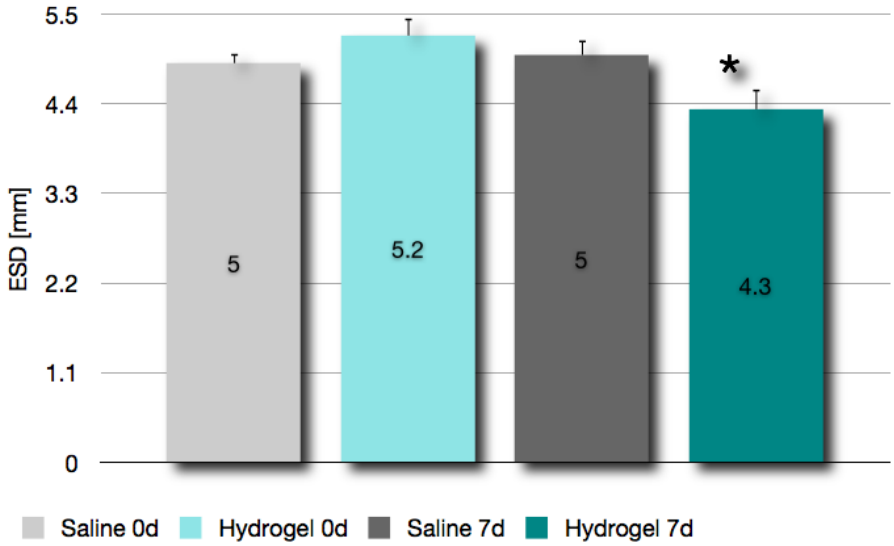

Fig. 12: Effect of intramyocardial hydrogel injection on end-systolic diameter (ESD), 14 days post-MI. *ESD after delayed hydrogel injection was significantly improved relative to immediate treatment and saline control group (p<0.05).*

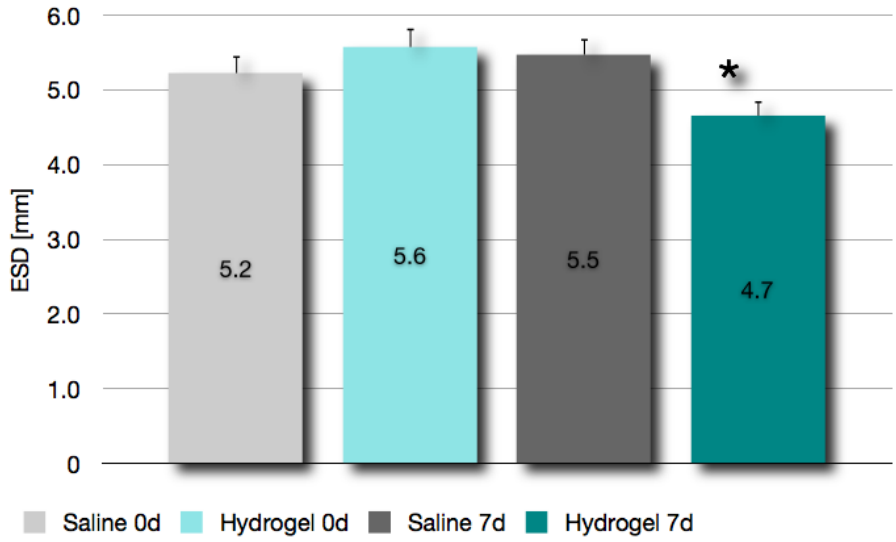

Fig. 13: Effect of intramyocardial hydrogel injection on end-systolic diameter (ESD), 28 days post-MI. *ESD after delayed injection was significantly improved relative to immediate treatment and saline control group (p<0.05).*

The diameters of PEG hydrogel injected hearts at end-diastole (EDD) were smallest in the group that received delayed treated with MMP-1s crosslinked PEG hydrogel at both two and four weeks, as outlined in Table 4. However, differences were not statistically significant.

At two weeks post-MI, delayed hydrogel treatment resulted in significantly smaller left-ventricular end-systolic diameter (ESD) as compared to immediate treatment and saline control ($p<0.05$). Also at four weeks, ESD values were significantly reduced relative to both immediate treatment and saline control ($p<0.05$).

The group that received the treatment delayed by seven days had significantly higher fractional shortening values relative to immediate treatment and saline control ($p<0.05$) after both two and four weeks.

The time point of intramyocardial biomaterial injection indeed had an impact on post-MI cardiac performance, with delayed treatment being superior to immediate one (Figures 10-13).

1.3.5.2 Infarct size and scar thickness

The hearts were explanted after four weeks and stained as described in chapter 5.3.1.3 as well as 5.3.1.4.

The infarct size was calculated as explained in chapter 5.3.1.8 and, as discussed above, only rats with a minimum of one eighth (12.5%) of the myocardial wall being infarcted were included in this study. The overall average infarct size amounted to 20.85% and did not differ significantly between any of the groups ($p>0.1$). Average infarct size after immediate saline injection was 21.8% (±2.54%), after immediate MMP-1 injection 22.0% (±2.4%), after delayed saline injection 17.7% (±1.94%) and after delayed MMP-1 injection 21.9% (±1.68%).

Interestingly, the average scar thickness, calculated as detailed in chapter 5.3.1.8, was significantly thicker in the group that received delayed PEG injection compared to immediate PEG injection and saline control ($p<0.05$), as shown in Figure 14.

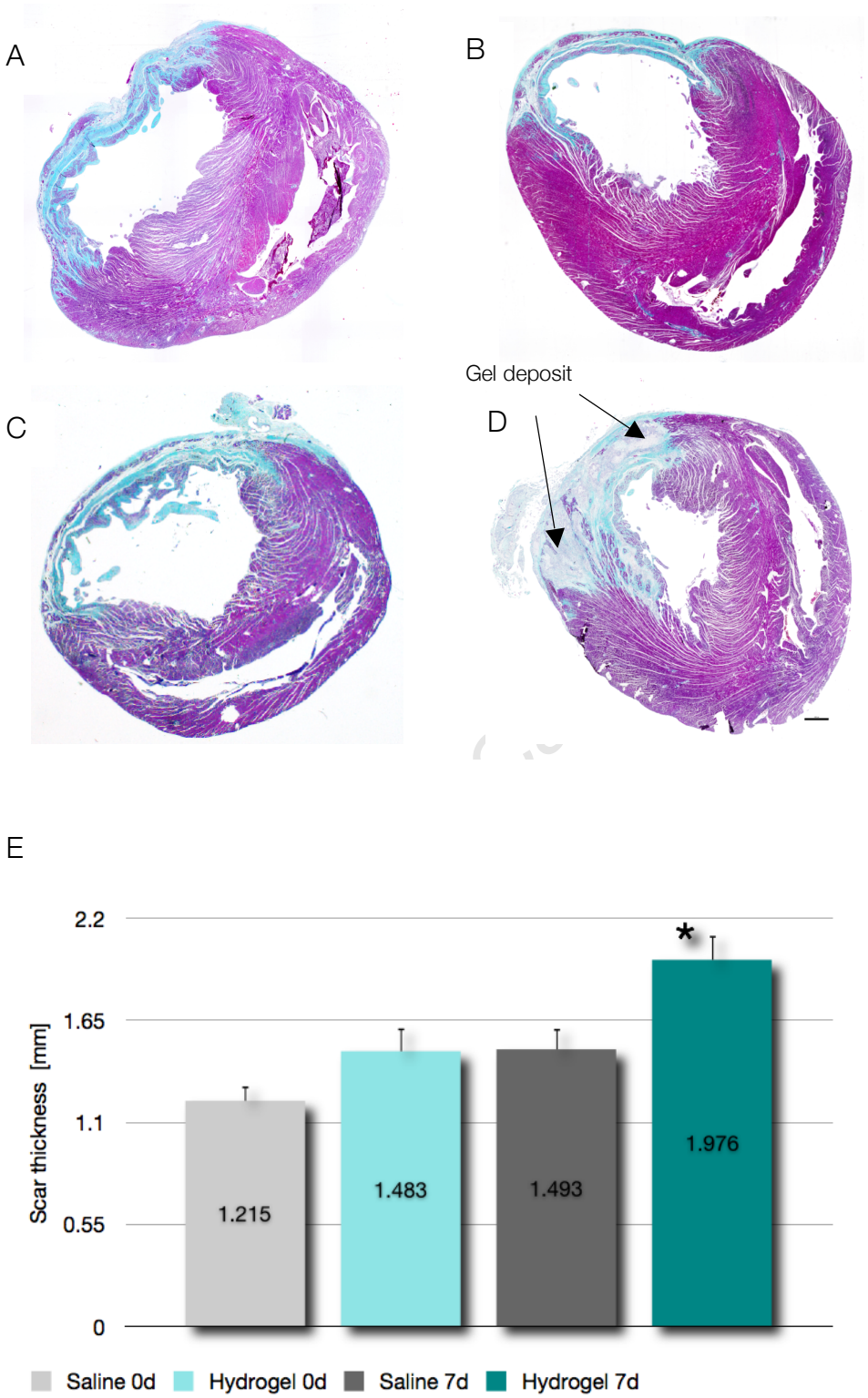

Fig. 14: Scar thickness. *Delayed injection of MMP-1 degradable PEG hydrogel resulted in a significantly thicker scar. Representative micrographs of MT stained infarcted hearts at four weeks after (A) immediate and (B) delayed injection of saline as well as after (C) immediate and (D) delayed treatment with 20PEG-8VS/MMP-1. Bar represents 1mm (E) Thickness of the infarcted myocardial wall was quantified based on histomorphometric analyses. (Chapter 5.3.1.8). Arrows indicate gel deposit. *p<0.05 versus immediate treatment and saline control.*

In accordance with functional assessment that showed most improvement after delayed biomaterial injection, the thickness of the infarcted scar was only increased in the group where the biomaterial was administered after one week.

1.3.5.3 Assessment of hydrogel distribution using Alexa Fluor®

Micrographs of hearts that were explanted at four weeks after infarct induction indicated potential gel deposits that were present after delayed, but not after immediate injection, as possible explanation for the observed superior effect of delayed treatment (see arrows Figure 14). In order to substantiate that presumption, intramyocardially injected MMP-1 degradable hydrogels were visualized by covalent attachment of a far-red fluorescent label (Alexa Fluor®) as detailed in chapter 5.2.2.3 before injection into infarcted rat hearts; either immediately or seven days post-MI.

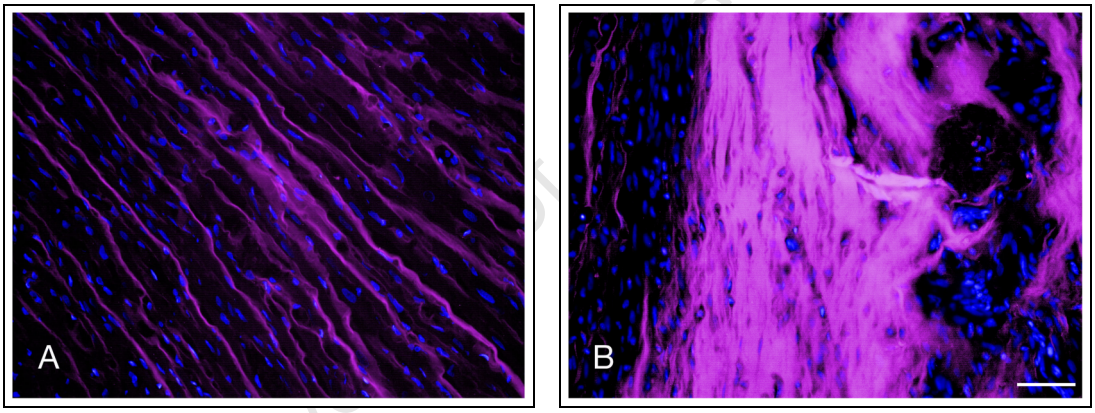

Fig. 15: Distribution pattern of Alexa Fluor®-labelled MMP-1 degradable hydrogel immediately after intramyocardial injection. *Injection took place (A) immediately post-MI and (B) seven days after infarct induction.*
Nuclei stained blue, hydrogel purple. Bar represents 50µm.

Explantation immediately after hydrogel injection revealed completely different distribution patterns: hydrogel that was injected with a delay of seven days formed a bulky deposit, as opposed to immediately injected PEG, which polymerized in fine layers (Figure 15). To investigate if the divergent distribution pattern also had an impact on the degradation of the gel, hearts were explanted instantly after immediate post-MI injection as well as after three, seven, 14 and 28 days. Following delayed PEG injection, three hearts were explanted instantly, as well as two and four weeks after infarct induction (Figure 16):

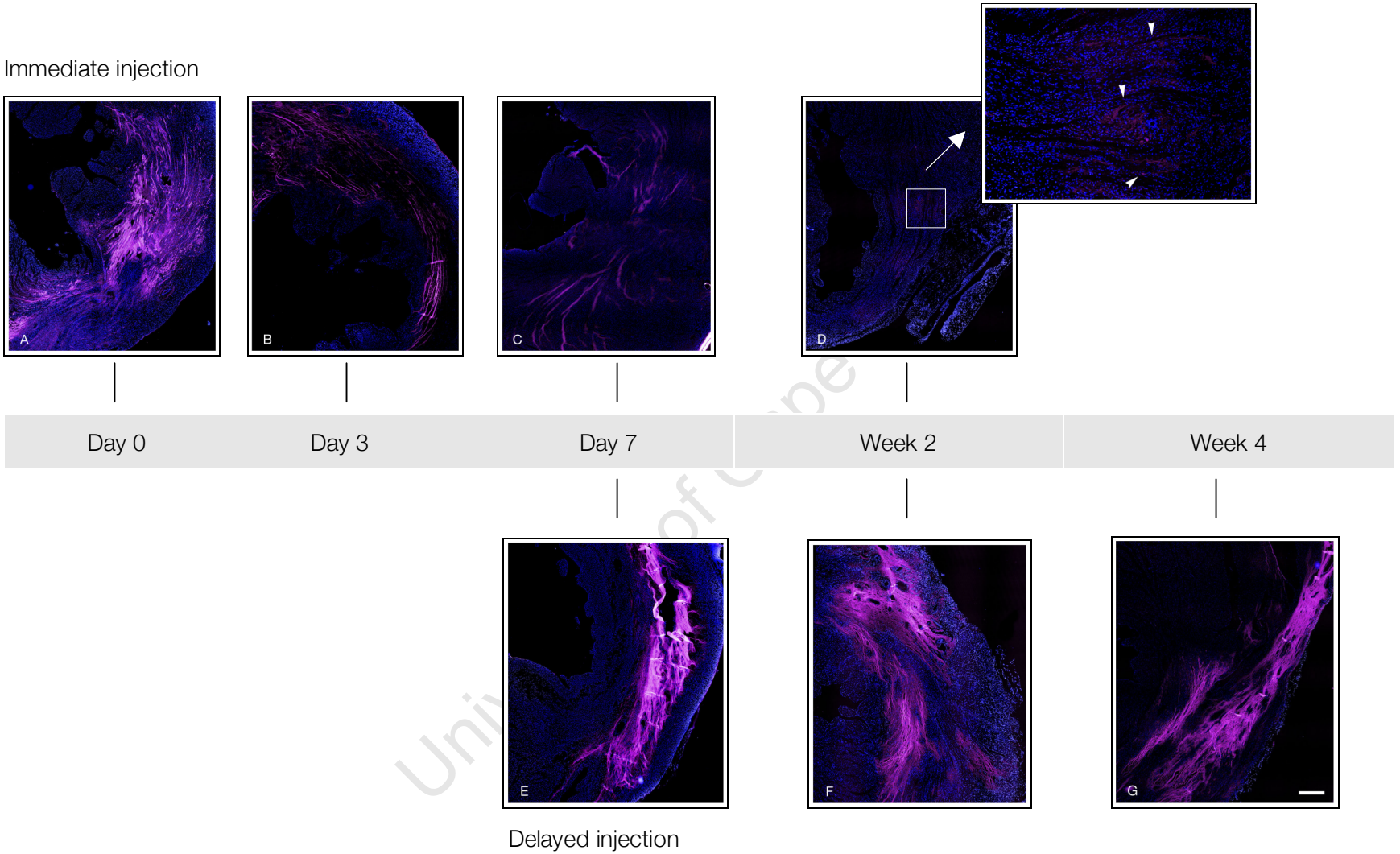

Fig. 16: Degradation of MMP-1 cleavable hydrogel, labelled with Alexa Fluor•. *Immediate injection, explanted after (A) injection (B) three days (C) seven days (D) two weeks and delayed injection, explanted after (E) injection (F) two weeks post-MI and (G) four weeks post-MI. Bar represents 500µm. Arrows indicate potential gel deposits. Nuclei stained blue, hydrogel pink. Four-week data of immediately injected gel not shown due to its absence.*

Immediately injected gel thereafter completely degraded within two weeks post-MI, while hydrogel that was administered with a delay of one week appeared hardly changed three weeks after delivery (equals four weeks post-MI) (Figure 16). The bulky distribution would be observed throughout the time period. Interestingly, MMP-1 degradable PEG that was previously injected into uninfarcted hearts was still visible after one month (Figure 7), indicating a different degradation rate in healthy myocardium.

The difference in degradation rate could be explained, at least in part, by the cardiac tissue structure into which the hydrogel gets injected: administering a hydrogel in freshly infarcted myocardium that was damaged only a few minutes ago, means injecting into a tissue that is still "intact", as the disruption of structural protein only starts occurring at least half an hour after infarct induction [58, 68-70]. That results in the gel "flowing" in between cardiomyocyte bundles before it polymerizes. After one week, at the end of the necrotic phase [58], the gel most probably gets injected into an edema – which may allow for the formation of a bulky deposit.

Being distributed finely, the surface to volume ratio of the immediately injected gel would be much larger relative to that of the bulk form of the delayed injections. Hence, more of the MMP-1 degradable crosslinks get exposed to enzymatic cleavage, which results in a faster degradation.

1.3.5.4 Corrosion casting

Typically used to reproduce the vascular system of organs or animals, vessels can be injected with a plastic polymer that fills the space and rapidly polymerizes.
Once the surrounding tissue has dissolved with an alkali solution, the cast remains and represents the precise structure of the vascular system. Subsequently, the corrosion cast can be studied using a scanning electron microscope (SEM), which produces images of sample surfaces that have a very high resolution and a large depth of field, even capable of revealing details of less than 1nm in size [377]. Since the reagents used to form the corrosion cast had a polymerization time that was similar to that of PEG hydrogel, this was a suitable method to further investigate by 3D visualization the infiltration pattern that result from biomaterial injections at different time points.

Rats were infarcted as explained in chapter 5.2.2.3 and randomized to be injected with Mercox resin either immediately (n=3) or one week post-MI (n=3). The hearts were explanted a few minutes after the respective injection and were treated as described in chapter 5.3.3 before the cast was viewed under the SEM.

Immediately injected corrosion cast polymerized in fine layers in between cardiomyocytes, confirming the histological finding of the previous experiment (Figure 17). It was not possible to retrieve a sufficient amount of delayed injected resin for it to be captured on the SEM. A possible explanation for this is that a slightly bigger needle was needed to inject the more viscous resin and this may have resulted in the injectate leaking out into the ventricle, possibly reflecting the fragility of the infarcted wall at this stage of healing.

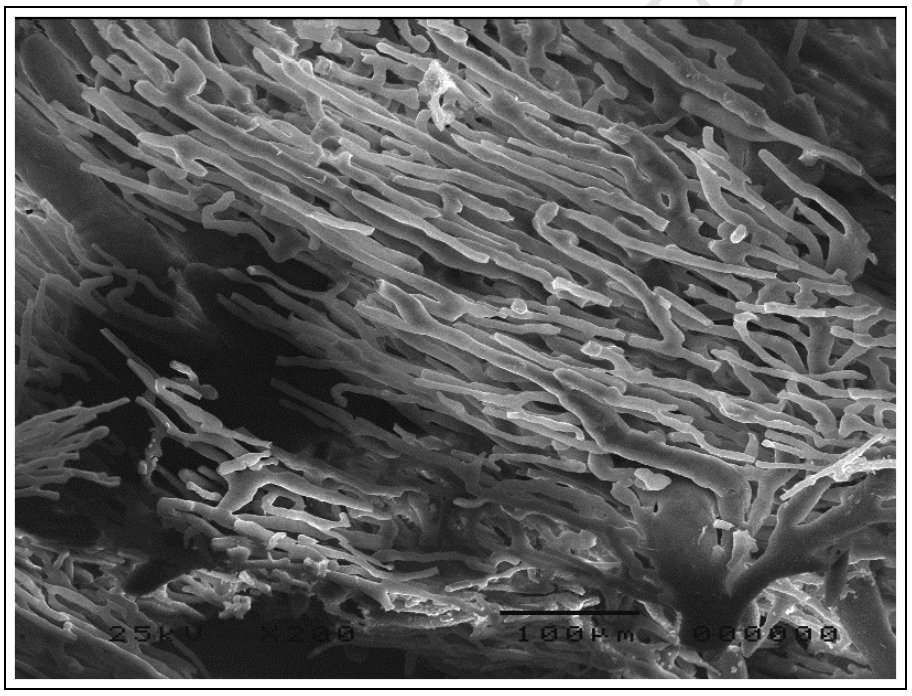

Fig. 17: SEM picture of corrosion cast, injected immediately post-MI

1.3.5.5 Assessment of retention of gel within the heart after injection

Histology indicated a possibly more efficient incorporation of hydrogel after delayed injection as opposed to immediate treatment, as shown in Figure 15. Hence, in order to quantify the amount of gel at the two investigated time points, the gels were labelled with lead. The decision to do so was based on the high affinity of lead for sulfhydryl molecules [378] and the high sensitivity and accuracy of ICP-MS (inductively coupled plasma mass spectroscopy) detection of lead in solution.

The hydrogels were crosslinked with a 4-arm PEG-SH crosslinker to allow for maximum loading of lead without substantial disruption of hydrogel structure. The optimal concentration of lead loading in the hydrogel was 0.5mM that is equivalent to one lead molecule per molecule of PEG-VS. Higher loadings resulted in gels that gelled inadequately. A hydrogel loaded at a 1:1 ratio gelled properly in a time equivalent to peptide crosslinked hydrogels.

An initial study confirmed that the lead was relatively tightly bound with only 3.3% (±0.65%) of lead loaded eluting after incubation of gels in H_2O for 24 hours at room temperature. After injection of lead labeled gels into excised dead hearts (n=3), 81.8% (±0.4%) of lead delivered was recovered after exhaustive tissue hydrolysis. To establish a baseline for potential retention of unincorporated lead label, beating hearts in rats were injected with an equivalent amount of PEG-SH crosslinker labeled with lead alone (n=3). After 30 min, hearts were excised and 5.5% (± 2.6%) of lead loaded remained within the heart. Finally infarcted rat hearts were injected with lead labeled hydrogels and hearts were again excised 30 min after injection. Only 11.7% (±3.9%) of lead loaded remained within the heart. This amount was not significantly more than that found in hearts injected with lead labeled crosslinker (p=0.33).

Thus though it was possible to label PEG hydrogels with lead, in the environment of a beating, infarcted heart the label was removed. It is not clear why this displacement occurred as these gels certainly gelled within heart tissue. It is possible that a circulating thiol containing compound (such as glutathione) may have competed for binding but this seems unlikely as in such a scenario it is likely that gel polymerization in general would be compromised. Whatever the precise reason for the outcome, it was clear that lead labeling was inadequate for the task of assaying differences between gel delivery efficiency under variable delivery conditions. The potentially more efficient incorporation of gel after delayed injection thus remains an uncorroborated observation.

1.3.5.6 Inflammation

Another possible explanation for the faster degradation of the immediately injected gel was inflammation. Immediately injected gel would not only encounter the naturally occurring foreign body reaction, but would also be subjected to a one-week inflammatory reaction due to the healing process of the ischemic tissue.

In contrast, hydrogel that gets injected with a one-week delay, when the necrotic phase has subsided [58], would be subjected to a shorter period of exposure to additional MI-induced inflammation.

As illustrated in Figure 18, immediately post-MI injected hydrogel polymerized in fine layers in between the cardiomyocyte bundles (A). Since the sample had been explanted only a few minutes after the biomaterial application, no inflammatory reaction could be detected yet. Three days after immediate PEG injection, macrophages migrated towards the foreign body and could be visualized around the hydrogel (B) as well as in areas that are remote from the polymer (C). Distant from the hydrogel, neutrophils were detected too (C). After one week, the biomaterial was completely surrounded by macrophages (D), while neutrophils could, again, only be detected unrelated to the hydrogel (E). Two weeks after infarct induction and biomaterial injection, the macrophage response persisted (also shown in Figure 6), although remaining small gel deposits that might still be present after 14 days (Figure 16) could not be detected (F). However, this could be a consequence of the Alexa® signal being impaired by immunohistochemistry. One month after immediate injection also the macrophage response had subsided (G).
Injected with a one-week-delay and hence into an edema, PEG gel formed a bulky deposit, with single macrophages being visible entrapped within the gel and surrounding it (H). Neutrophils were also observed (data not shown). Entrapped macrophages could still be seen at the two-week time point but could also be observed in the periphery (white arrow) of the gel (I and J). A month after infarct induction and therefore three weeks after biomaterial application, the amount of gel appeared to be unchanged, causing a moderate immune response in some areas (K) and an intense response in other regions (L). However, the stability and integrity of the hydrogel structure did not seem to be compromised.

Overall, the predominant response at all time points was macrophage-based, indicative of a foreign body reaction to the gel, irrespective whether the gel was injected immediately or seven days after infarct induction. Neutrophils could be detected at three and seven days, but at much lower levels than macrophages and not associated with gels (Figure 18).

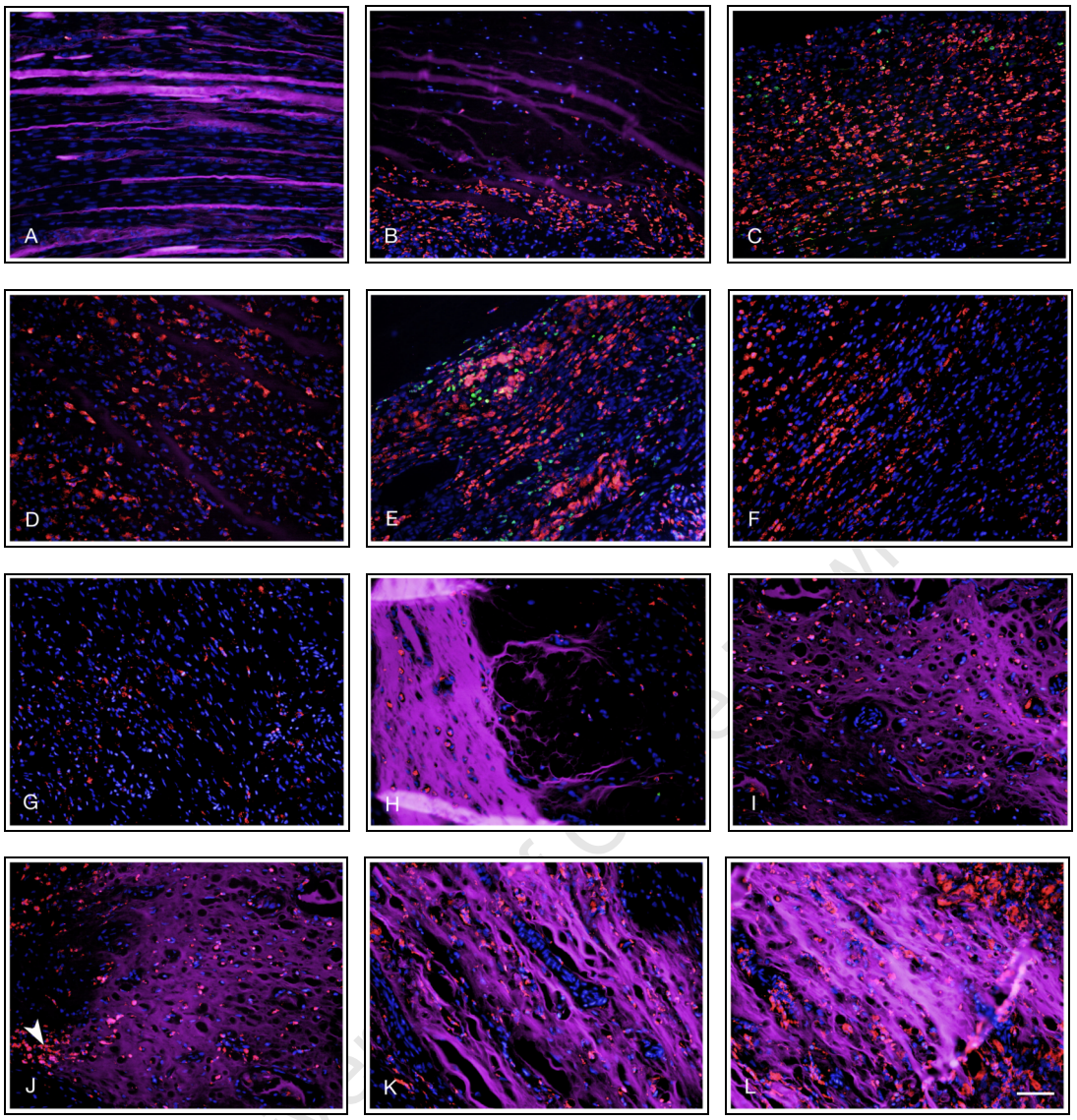

Fig. 18: Inflammatory reaction after immediate and delayed hydrogel injection. *Micrographs show immediately post-MI injected MMP-1 degradable PEG hydrogel, explanted (A) immediately after injection, (B) and (C) after 3d, (D) and (E) after 7d, (F) after 14d and (G) after 28d. Micrographs of delayed injected MMP-1 sensitive PEG hydrogel, explanted (H) immediately after the injection (= seven days post-MI), (I) and (J) one week after the injection (= two weeks post-MI), (K) and (L) three weeks after the injection (= four weeks post-MI).*
Nuclei stained blue, hydrogel purple, macrophages red and neutrophils green. Bar represents 50µm.

As shown in the present study, neutrophils typically disappear one week post-MI in rats, while macrophages persisted for a greater period of time and associated with biomaterial. Based on the time points that were chosen, an earlier neutrophil-based attack on the hydrogels cannot be excluded. Evidence suggests that the response to the hydrogels was a relatively moderate foreign body-type response for both time points of injection.

1.3.6 Summary

Remodeling following myocardial infarction has been shown to cause a progressive decline in LV performance due to a series of histopathological and structural changes, leading to heart failure [55-57] in the majority of infarct patients [164]. The delivery of biomaterials (hydrogels) appears to be a promising approach, as first results indicated an increased wall/scar thickness [241-244], reduction of adverse LV remodeling [241, 244, 245], attenuated infarct expansion [246, 247] and improvement of functional parameters [241, 242, 247].

However, there is no consensus in the present literature on the influence of timing on the success of the treatment. Thus, the aim of this investigation was to evaluate MMP-1 degradable PEG hydrogel in view of its compatibility and to directly compare the effect of its injection immediately or seven days post-MI on pathological remodeling.

Indeed, with this study it could be shown for the first time that the intramyocardial injection of MMP-1 cleavable PEG gel is feasible and lead to a retardation of post-MI remodeling, if administered with a one-week delay. That conclusion could be drawn from the first direct comparison of different time points for treatment administration.

One motivation for choosing PEG hydrogels is their high mechanical strength, which makes them ideal for taxing environments such as the beating heart. In fact, according to Wall *et al*., PEG hydrogels are more resilient than naturally derived polymers such as collagen, alginate and fibrin and thus rank amongst the stiffest biomaterials [237]. A recent study showed that elevated levels of ST2, a marker for biomechanical strain, correlates significantly with a higher prevalence of cardiovascular death and heart failure post-MI [379]. Hence, increased mechanical stability is desired to provide meaningful stress relief for cardiomyocytes [240]. Out of the PEG hydrogels tested in the present study, MMP-1s crosslinked PEG proved to swell least, which points towards a high crosslink density and therefore a “rigid” gel, which is in good accordance with the desire of using a “stiff” material. Another reason for which PEG hydrogels were chosen in this experiment, is their bioinert nature [362-368] that made PEGs even become a popular means to render a surface protein resistant and to enhance biocompatibility [279]. However, a study previously conducted in our laboratory, using non-degradable PEG hydrogel, showed an extensive macrophage response, possibly due to the biomaterial remaining in situ indefinitely [244].

Thus, the focus of the study at hand shifted towards the investigation of degradable PEG hydrogels, the mechanical properties of which (such as amount of swelling, rigidity and time to degradation) can be controlled precisely, while a chronic inflammatory reaction can be avoided. The gel with the lowest crosslink density (hydrolytically cleavable 2-arm crosslinked PEG) proved to be the one that swelled most and thus allowed most rapid tissue ingrowth. It degraded at 30 days *in vitro* (Figure 4) and two weeks *in vivo* (Figure 7), this difference most likely related to the foreign body reaction and the heart being a more taxing environment. The enzymatically degradable MMP-1 sensitive PEG hydrogel had a much slower degradation rate and appeared to be the more rigid gel – ideal for a mechanical taxing environment such as the beating heart. Hydrolytically degradable PEG caused an extensive macrophage response when injected intramyocardially, which caused scarring in the long run. Enzymatically cleavable PEG, on the other hand, only caused a mild and localized immune reaction that subsided within a short period of time without resulting in scarring of the myocardium. This possibly reflects the acrylate moiety being more pro-inflammatory than vinylsulphone. Hence, the investigation of MMP-1 degradable PEG hydrogel as biomaterial for intramyocardial post-MI injection was pursued further.

In contrast to other hydrogels such as self-assembling peptides, which can cause functional impairment when injected into sham animals [317], MMP-1 cleavable PEG injected into uninfarcted rats showed no evidence of adverse effects on myocardial performance in the study at hand. Based on that, the value of enzymatically degradable PEG for myocardial infarct therapy was evaluated.

The injection of MMP-1 degradable PEG gel into a one-week-old myocardial infarct was effective in ameliorating cardiac performance, as indicated by the fractional shortening, a commonly used clinical parameter used for the evaluation of myocardial function. Interestingly, although infarct patients commonly benefit from timely intervention [136-138, 143], delayed treatment was superior to immediate one in this study.

In an attempt to elucidate these results, explanted hearts were analyzed histologically, and revealed a significantly thicker scar after delayed injection, relative to immediate treatment and to saline control group. When injected after one week, the hydrogel was able to prevent wall thinning and to offer mechanical support to the weakened wall, which resulted in ameliorated function.

These findings were in accordance with the literature, where increased mechanical stability results in relief of stress on the remaining healthy cardiomyocytes and consequent prevention of heart failure [240, 379].

To gain a better understanding of the hydrogels geometry that lead to the difference in scar thickness, PEG was visualized with the use of a label covalently conjugated to the gel. Apart from revealing a well-dispersed distribution pattern after immediate injection and the formation of bulky deposits after delayed treatment, the explantation at different time points also indicated a much faster degradation of the immediately injected gel. That can be explained with a relatively bigger surface area and hence increased exposure of enzymatically labile bonds. Understandably, a faster degrading gel resulted in less mechanical support to the infarcted wall. The distribution pattern was confirmed with the corrosion cast method that, once again, showed fine distribution, the resin flowing in between an intact cardiomyocyte structure if administered immediately after infarct induction (fibrils of 10-50μm were observed). However, it is not possible to comment on the distribution after delayed injection, as most of the resin, being a slightly more viscous solution and requiring a bigger needle to be injected, was lost into the ventricle or the circulation and could therefore not be assessed. This also indicated the fragility of a one-week-old infarcted wall.

Labeling gels with lead and subsequent analysis of its concentration was an attempt to quantify the retention of the gel in the myocardium after injection at different time points. However, due to removal of the label when injected into a beating heart, the experiment failed to provide information about potential differences between immediate and delayed injection with respect to the amount of gel left.

Another potential explanation for superior outcome after delayed treatment was inflammation, with immediately injected gels being subjected to the inflammatory, necrotic phase; in addition to the naturally occurring foreign body response. This theory, however, did not provide a clear explanation for the observed differences in degradation rates, as the foreign body-type response was very similar for both implant times, with macrophages being the predominant response at all time points, while neutrophils were observed in both groups at much lower levels than macrophages and not associated with gels. Influence of neutrophils, however, cannot be precluded.

Instead, evidence indicates that the divergent distribution patterns and surface to volume ratio are the most likely explanation for the observed phenomenon. Although biomaterials have been injected immediately post-MI [281, 314, 316, 317, 319], after one week [234, 235, 242, 272, 274, 291], after two weeks [243] or even after five weeks [273], most of these groups neither visualized the distribution pattern of the polymer nor did they intend to investigate the impact of timing on functional parameters. Other intramyocardially injected polymers very likely behave similarly to the MMP-1 degradable PEG used in the present study, as Dobner *et al.,* using a non-degradable PEG [244] and Ifkovitz *et al.* injecting Hyaluronic acid [308] showed the same fine-layered distribution after immediate administration that has been demonstrated in the present study.

Interestingly, also for intramyocardial stem cell therapy there seems to be a timing factor, with early administration (three days post-MI) of bone marrow cells being superior to delayed one [380]. Hence, optimal timing might vary between different treatment modalities but certainly does influence treatment outcome.

It is possible that the lower degradation rate of the delayed injected hydrogel is not entirely responsible for the functional improvements observed. In a study previously conducted in our laboratory, investigating an immediately injected non-degradable PEG gel, no functional improvement (as indicated by fractional shortening) could be observed [244]. This potentially points towards the different hydrogel structure alone, resulting from injections at different time points - not just their degradability - as a crucial factor in the reduction of adverse LV remodeling as well as functional improvement. Finite element modeling and biomechanical testing to try to determine other possible mechanisms behind the observed functional improvement are currently under way.

One has to be careful though when translating results from rats to humans - despite the similarities between the rodent and human vascular system [381, 382]. While for animal studies a homogeneous group of healthy and young animals without concomitant illnesses is being used, cardiac patients with heart failure typically are middle-aged and suffer from co-existing diseases [55, 383]. Animals are usually not being treated with additional medication, while patients might very well receive simultaneous treatments that may influence the outcome of the investigation. Another aspect is the timing of intervention.

Even though it may vary between different studies, it is similar for each animal within an experiment, while the timing of intervention in clinical trials by necessity fluctuates between the included patients. Lastly, infarct sizes in small animals often range from 20 to even 60% of the LV being ischemic, when in humans 13-16% appear to be a "common" interval.
Nevertheless, for more than 40 years, basic and translational scientists successfully used small animal models for cardiovascular research [384], before treatments could be applied to larger animals and eventually humans.

The findings of this experiment, which was conducted in a randomized and strictly blinded fashion in order to eliminate any subjective bias (see chapter 5.2.2.3 and 5.2.3), have practical relevance especially for those myocardial infarct patients, who could not benefit from timely treatment initiation. This is particularly the case in patients whose infarct went unrecognized due to age, female sex or concomitant diseases such as DM [47-49], leading to a time delay of possibly several days before seeking medical attention [143].
Further research will have to determine if the results found in the present study can be translated universally to other intramyocardially injected biomaterials and if their delayed application remains superior long-term.

2 Utilization of MMP-1 degradable PEG hydrogels for controlled local drug release

2.1 Introduction

2.1.1 Corticosteroid administration after myocardial infarction

Corticosteroids are potent anti-inflammatory, anti-rheumatic and immunosuppressive agents that are being used for the treatment of a wide range of disorders such as asthma [385], allergic reactions [386] or rheumatoid arthritis [387] - to mention a few.

In 1953, Johnson *et al.* were able to show that corticosteroids reduce myocardial infarct size in dogs, which was confirmed 20 years later by Libby and colleagues [388, 389]. Since then, this group of drugs has been investigated extensively to gain a better understanding of their mode of action and to assess their potential value for myocardial infarct therapy.

Corticosteroids act by binding to glucocorticoid receptors, which, in turn, bind to DNA sequences, containing glucocorticoid response elements (GRE) and subsequently initiate the expression of target genes [390]. Hafezi-Moghadam *et al.* were able to show that this results in the stimulation of phosphatidylinositol 3-kinase (PI3-kinase) and protein kinase Akt, a fast activation of eNOS and subsequent NO formation [391]. The latter triggers soluble guanylate cyclase (sGC), which mediates a majority of the effects of NO, including vasodilation as well as the inhibition of platelet and neutrophil adhesion [390]. In view of that, Chen and colleagues injected adenovirus carrying human eNOS gene four days prior to coronary occlusion directly into rodent myocardium, which lead to inhibition of MAPK signaling and resulted in significantly reduced infarct sizes as well as improved contractility one week post-MI [392]. Cardioprotective effects, resulting from dexamethasone-induced inactivation of MAPK, could be confirmed by Lochner and colleagues [393].

Investigations have shown that NF-κB activation might play a central role in cardiac injury due to intracellular calcium overload [394], resulting in harmful long-term consequences [109].

The fact, that corticosteroids augment the expression of annexin1 as well as the inhibition of NF-κB might therefore be the basis for another explanation of their beneficial effect [390, 395, 396], because the administration of annexin1 diminishes both inflammatory response caused by myocardial ischemia as well as infarct size [391, 397], while the inhibition of activated NF-κB has proven to be cardioprotective [398]. Furthermore, it could be demonstrated that the application of glucocorticoids results in a significantly decreased ischemic area after either permanent coronary artery occlusion or after reperfusion [399], possibly due to induction of the cardioprotective heat shock protein 72 (HSP72) [400]. Although in another study dexamethasone neither had hemodynamic effects in sham operated nor in infarcted animals, the administration of the drug resulted in the normalization of elevated ST-segments and prevented the increase of Creatine phosphokinase (CPK), an enzyme indicative of muscle damage [401].

Various clinical studies were conducted in the 1950's, -60's and -70's, showing reduced mortality of infarct patients after corticosteroid administration [402-404]. In one study for example, 849 patients with confirmed MI received methylprednisolone, which resulted in a significant mortality reduction for patients suffering inferior/posterior transmural infarctions [405]. Yet, those positive results couldn't be confirmed universally [406]. Methylprednisolone has been administered in 42 MI patients and has shown no beneficial effect two weeks after infarction [407]. Similarly, two high doses of the drug were given to 14 patients with MI, while 15 other MI patients served as control group. No significant difference could be observed between the two cohorts with regards to infarct size (assessed on the basis of serum enzyme levels), arrhythmias, HF or mortality. Hence, the authors concluded that the use of corticosteroids post MI has neither deleterious nor beneficial effects [408].

Despite all encouraging results, corticosteroids have long been the subject of controversy, as some studies were simply not able to confirm their cardioprotective property [409, 410]. In fact, their application has even been associated with the development of cardiac aneurysms and potentially fatal cardiac ruptures due to reduced wound healing [411].

Mannisi *et al.* conducted a study, where rats were treated with either methylprednisolone or saline within 24 hours of infarct induction. Infarct sizes were similar in both groups but already at three days post-MI, rodents that were treated with steroids had a significantly thinner infarct wall thickness relative to the control group [412]. That could be attributed to steroids preventing water increase and therefore edema, which would naturally reinforce the necrotic infarct against expansion by increasing infarct stiffness [58].

In summary, dyslipidemia and hypertension as well as LV free wall rupture due to delayed myocardial scar formation could be identified as the potential main adverse effects of corticosteroids on the cardiovascular system [413], which is why their use for myocardial infarct therapy has been met with scepticism.

2.1.2 Controlled release of dexamethasone utilizing PEG hydrogels

One way of avoiding adverse effects of corticosteroids, such as the tendency to thin the infarcted wall, potentially even causing cardiac rupture, is to incorporate them into a hydrogel, which is able to strengthen the damaged myocardium, while the drug is being released.

Degradable polymeric biomaterials seem to facilitate the most effective use of agents by offering sustained concentrations, i.e. avoiding potentially toxic over-dosing that can occur at the beginning of a treatment period and preventing ineffective under-dosing that can occur at the end of it [257]. Furthermore, by providing high concentrations of the drug only in the local vicinity of the drug-release depot, unwanted concentrations distant from the disease site and systemic side effects can be averted, as the slow and controlled release would reduce the dose that is encountered by the body at a given time.

The incorporation of agents, such as growth factors or drugs can be achieved either by entrapment or by tethering, as illustrated in Fig. 19:

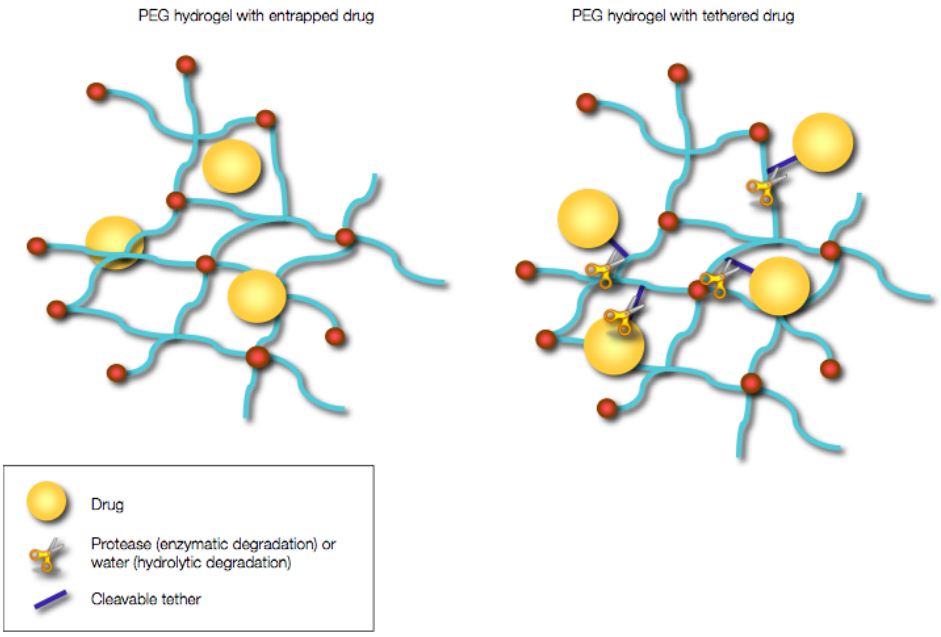

***Fig. 19: Incorporation of drugs**. Drugs can be loaded into PEG hydrogels either via in situ entrapment or via tethering. For the latter, drugs are being modified with crosslinkable and cleavable tethers and can be released once the tethers are degraded either hydrolytically or enzymatically. Figure modified from Lin et al. [342]*

This concept has already been explored in experimental MI settings, where different growth factors were administered together with various biomaterials, the latter serving as depot for their sustained delivery [126].

That way, VEGF and PDGF, both playing key roles in vessel formation, have successfully been delivered to ischemic myocardium [292, 317, 318, 414, 415]. Similarly, basic fibroblast growth factor (bFGF) [281], erythropoietin (EPO) [281, 416], insulin-like growth factor (IGF-1) [316] and stromal cell-derived factor 1 (SDF-1) have been investigated [319] and shown, that the combined delivery of growth factors with biomaterials is superior to the injection of free growth factors in saline and may have the potential to improve cardiac function post-MI.

Also Dexamethasone has been incorporated and released from biomaterials, however, mainly to successfully attenuate foreign body reactions of the tissue around implants [417-423].

2.2 Project aims

The danger of a possible cardiac rupture still being the number-one-concern, a meta-analysis conducted in 2003 by Giugliano *et al.,* involving 11 controlled trials with a total of 2646 patients, showed that corticosteroid treatment after myocardial infarction was associated with a 26% reduction in mortality, while no clear association with myocardial rupture could be proven [424]. Hence, it has been suggested to further investigate the administration of dexamethasone as part of the treatment of acute coronary syndrome [425].

By incorporating the drug into a hydrogel, the infarcted wall could be stabilized, which would prevent possible adverse effects such as the thinning or even rupturing of the damaged tissue. Simultaneously, beneficial results such as diminished infarct size or reduced post-MI mortality rate could be achieved.

Hence, the aim of this experiment was to incorporate dexamethasone into MMP-1s crosslinked and therefore enzymatically degradable PEG hydrogel, comparing both entrapment and tethering. It would be interesting to know if the way the drug is loaded into the gel as well as its dosage impact on the pace of dexamethasone release *in vitro* and *in vivo*. Moreover, the effects of controlled, locally delivered dexamethasone, slowly released into infarcted myocardium on post-MI remodeling should be investigated.

2.3 Results and discussion

2.3.1 Assessment of *in vitro* dexamethasone elution

PEG hydrogels have already been established as controlled release devices, the rate of drug elution depending on the method of preparation, the crosslinking density as well as drug solubility [325, 342, 426].

In the present study, dexamethasone was either covalently attached to PEG as detailed in chapter 5.4.1 or it was entrapped in the hydrogel as explained in chapter 5.4.2. For the latter, dexamethasone was distributed within the gel while it polymerized, so that the drug was physically caught in between the polymer network of the PEG. Dexamethasone is practically insoluble in water and therefore it precipitates from the organic vehicle upon addition to the hydrogel. Due to their size, the precipitates are then physically entrapped within the hydrogel, which has porosity dimensions in the nanometer range. Its release, however, also depended on the swelling of the hydrogel, resulting in stretched and straightened network chains that facilitated dexamethasone diffusion. In contrast, the release of the covalently bound steroid was reliant on the degradation of ester links that were created between the agent and the polymer network of the PEG. Those ester bonds were hydrolytically cleaved by water. Either way, if successful polymerization occurred, effective inclusion or coupling of dexamethasone to the hydrogel ensued.

In order to obtain an indication for the rate, at which dexamethasone was going to be released from hydrogels *in vivo*, the elution was initially measured *in vitro*. As it is very difficult to mimic *in vitro* the cell-driven enzymatic degradation of MMP-1 sensitive hydrogels, the two extremes - non-degradable 20PEG-8VS and hydrolytically cleavable 20PEG-8Ac - were utilized to attempt to model the *in vivo* release *in vitro*.

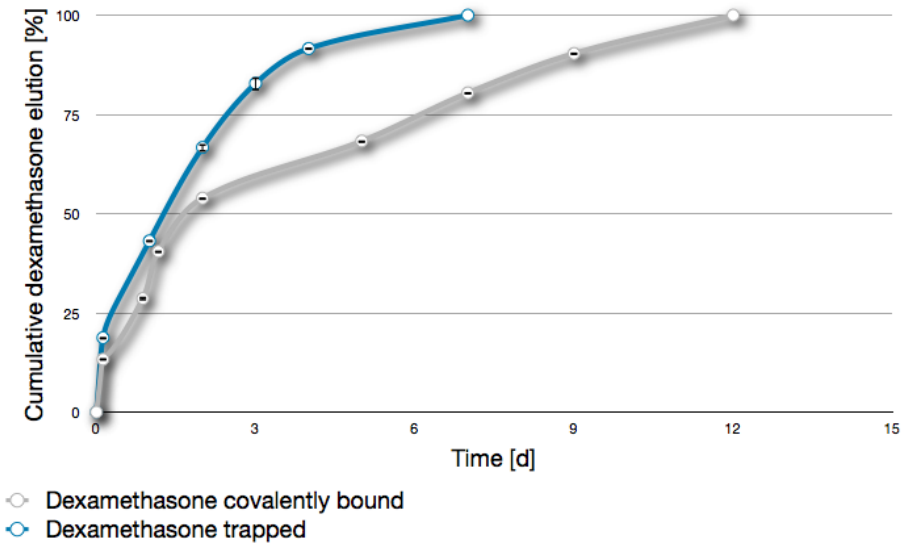

Fig. 20: Dexamethasone elution from 20PEG-8Ac. *(n=3), error bars indiscernible*

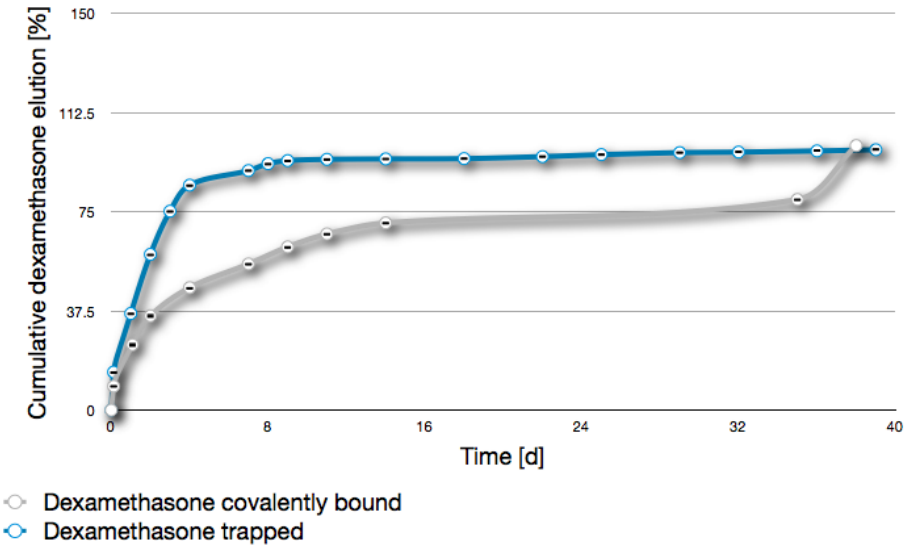

Fig. 21: Dexamethasone elution from 20PEG-8VS. *(n=3)*

The release of entrapped dexamethasone was compared to its elution when tethered to the hydrogel network, investigating both hydrolytically degradable and non-degradable PEG (Figures 20 and 21).

For both hydrogels, an initial burst release was observed, most probably related to the elution of unbound dexamethasone. The release then protracted, with the covalently bound glucocorticoid eluting at a slower pace compared to the entrapped drug, as ester bonds had to break down for the steroid to be released. As shown in Figure 20, entrapped dexamethasone was eluted from the hydrolytically degradable gel within one week, congruent with the pace it was released at from the non-degradable one (Figures 21 and 22). The elution of the covalently bound drug from the degradable hydrogel took 12 days to be completed and coincided with the breaking down of the PEG (Figure 20), whereas from the non-degradable PEG less than 80% of the covalently bound dexamethasone was eluted after 35 days (Figure 21). As the aim was to investigate the rate of elution rather than its overall duration, the experiment was discontinued by chemical degradation of the PEG (see chapter 5.4.2), which resulted in the release of the remaining dexamethasone.

While the release of a covalently bound drug from non-degradable PEG solely depends on the breaking of ester bonds, its elution from a degradable gel is accelerated by the additional degradation of the gel itself, which explains the different rate at which dexamethasone was eluted from degradable versus non-degradable PEG.

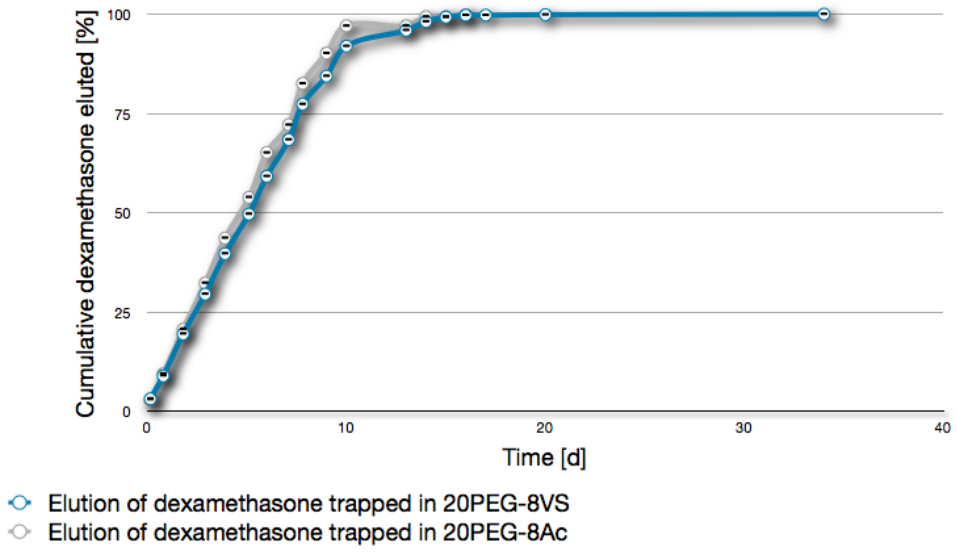

Fig. 22: Elution of entrapped dexamethasone, directly comparing degradable and non-degradable PEG hydrogels. (n=3)

The previous study indicated that hydrogel injected immediately after infarction had a large surface to volume ratio. As argued below immediate delivery of dexamethasone is probably most the most effective approach and thus it was determined whether the surface to volume ratio of the hydrogel would have an effect on the rate dexamethasone was eluted, gels with a larger surface possibly accelerating drug release. Hence, non-degradable PEG gels were formed as droplets and were compared to flattened discs, that had been polymerized in between glass slides, thus having a surface area to volume ratio that was increased by about 2.5fold.

Also, it needed to be considered that entrapping different amounts of dexamethasone within a PEG gel might have an impact on the rate of agent release, due to potential differences in precipitate formation. As detailed in chapter 5.4.2, both droplets and flat discs were loaded either with 150µg or with 500µg of dexamethasone. The drug release was measured and is illustrated in Figure 23:

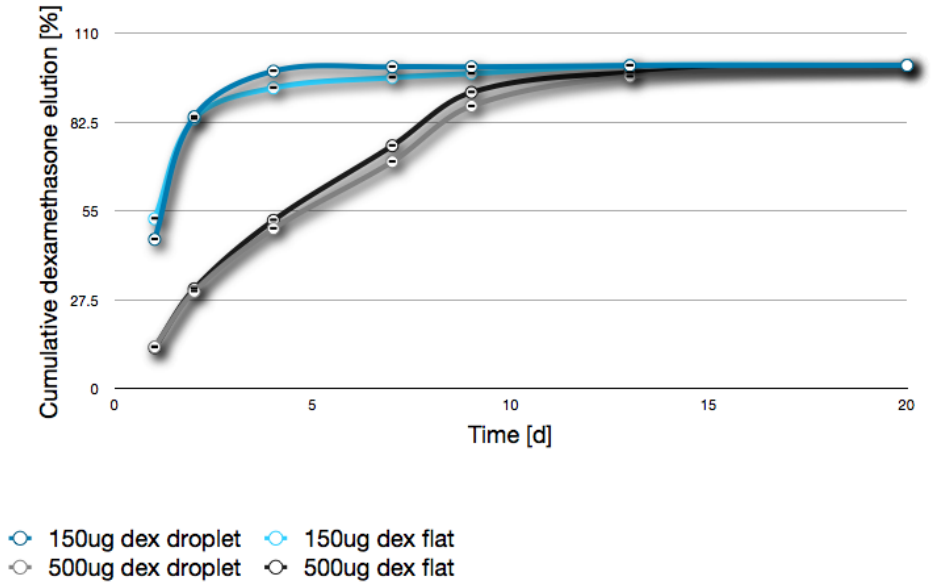

Fig. 23: Dexamethasone elution, comparing different dosages and shapes. *(n=3)*

Hydrogels carrying a higher dosage of dexamethasone released the drug at a slower rate than those that were loaded with a lower dosage. However, an increase in the surface to volume ratio of the biomaterial of 2.5fold did not influence the rate at which the drug was eluted, and this suggested that the dispersed structure of the injected gel might not influence release rate.

Interestingly, gels loaded with a higher dosage released the drug slower than the ones with less dexamethasone. This could perhaps be attributed to higher dosages resulting in larger precipitates, meaning that the water insoluble drug is entrapped more effectively within the polymer network and is therefore eluted at a slower rate – relative to the low dosage of dexamethasone.

Since the dosage as well as the way the agent is attached to the biomaterial does influence the rate of its elution, one should be able to precisely control the release of a drug into the surrounding tissue, meeting the requirements for biomaterial-based medicamentous treatment of cardiac pathologies.

2.3.2 Activity of dexamethasone eluted from PEG hydrogels

In response to stimulation of glucocorticoid receptors, the cell line MDA-kb2 expresses luciferase, which can be quantified to assay dexamethasone activity (detailed in chapter 5.4.3). Activity of released dexamethasone, entrapped in both degradable and non-degradable hydrogel as well as the drug, covalently bound to both degradable and non-degradable PEG gel was measured (Figures 24 and 25).

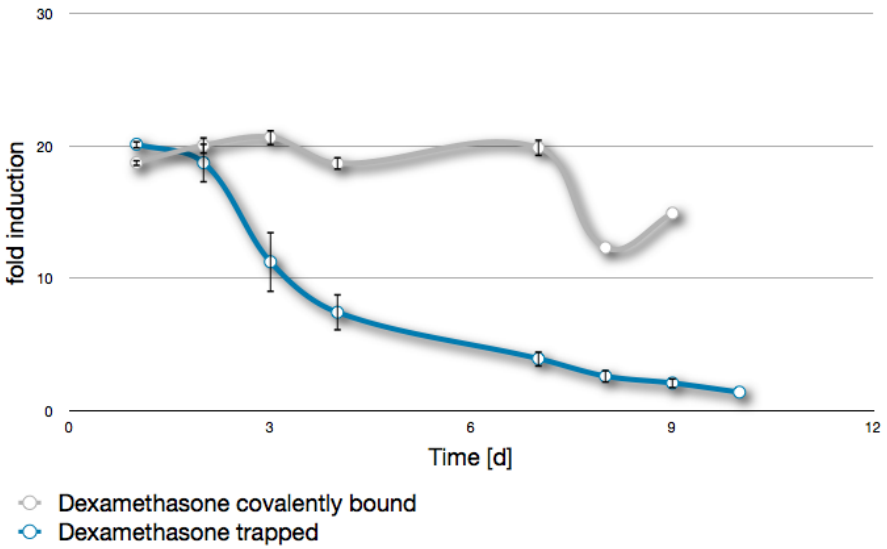

Fig. 24: Activity of dexamethasone eluted from degradable 20PEG-8Ac. (n=3)

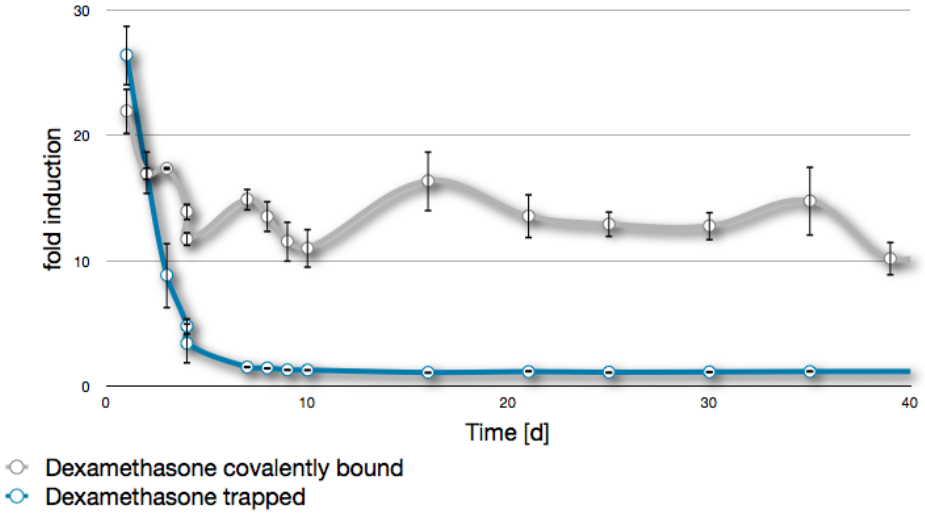

Fig. 25: Activity of dexamethasone eluted from non-degradable 20PEG-8VS. (n=3)

Activity of eluted dexamethasone was demonstrated for both degradable and non-degradable PEG hydrogels. Due to an initial burst release of the entrapped drug, the total amount of dexamethasone did drop off, as the eluate was replaced at every time point. Consequently also the activity of entrapped dexamethasone declined, while the activity of the covalently bound agent was sustained for a longer period of time (Figures 24 and 25).

2.3.3 *In vivo* evaluation of dexamethasone release from PEG hydrogels

Even though the results in this thesis demonstrate that delayed biomaterial administration is superior to immediate hydrogel injection after myocardial infarction, that concept had to be re-evaluated when it came to the combined treatment with glucocorticoids.

The influence of post-MI steroid treatment on LV remodeling and inflammation have been investigated previously, using different time points of administration [427]. Methylprednisolone was either given early (from time of MI to 24 hours post-MI) or late (two to seven days post-MI). Animals were killed at three, seven or 42 days after surgery.

Indeed the timing of treatment had an impact on the outcome: administration of methylprednisolone within the first 24 hours after infarct induction increased MMP activity, which contributed to the break down of structural proteins. However, these effects did not translate into major changes in LV structure and function. In contrast, hearts that were exposed to late methylprednisolone treatment showed significant augmentation of MMP activity, which resulted in adverse effects on global and scar LV structure as well as cardiac performance. Moreover, potentially beneficial effects of steroids, such as diminished infarct size [388, 389] as well as cardiovascular protective effects [391] can only be achieved by timely administration, before the infarct can expand and before cardiomyocytes get irreversibly damaged.

Hence, myocardial infarction was induced in rats as detailed in chapter 5.4.4. Animals were randomized to receive one of the following six treatments immediately post-MI: 150µg covalently attached dexamethasone, 150µg or 500µg dexamethasone entrapped in MMP-1 cleavable PEG hydrogel, 150µg or 500µg applied without the gel (free dexamethasone) and saline as control. Administering 150µg dexamethasone translated to 0.75mg/kg, the dosage of 500µg equaled 2.5mg/kg. For evaluation of the amount of dexamethasone that was eluted from PEG hydrogels, blood samples were taken from the tail vein, starting at two hours post-MI, followed by collections every 24h for up to ten days after infarct induction (section 5.4.4).

2.3.3.1 *In vivo* elution of dexamethasone

All rats included in this study (together with the ones belonging to the saline control group) showed an initial weight loss that persisted for three days, which can most likely be attributed to common post-operative effects, such as analgesia-related decreased food and water intake. Saline-treated rats lost significantly less body weight within the first three days post-operatively (-5.5%±1.25%) than rats treated with 500µg free dexamethasone (-16.36%±2.12%, $p \leq 0.05$) and substantially less than rats that were treated with 500µg entrapped dexamethasone (-11.5% ± 1.79%, $p<0.1$).

After three days, the weight of all animals increased (Figure 26).

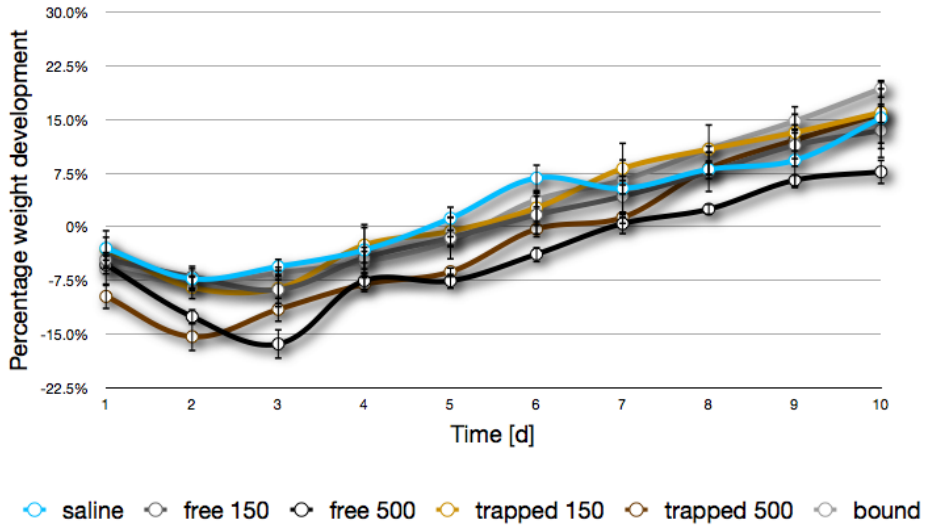

Fig. 26: Postoperative weight development of rats with MI

Interestingly, throughout the first week, rats that belonged to the saline control group gained significantly more weight (+6.8%±2.1%), relative to rats that were treated with 500µg free dexamethasone (-3.8%±1.17%, $p<0.05$) or 500µg entrapped dexamethasone (-0.3%±1.2%, $p<0.05$). As this is most likely a consequence of the catabolic effect of steroids, the weight loss was an *in vivo* confirmation of the activity of the drug throughout the first week.

Quantitative analyses of blood samples were unable to confirm this release of dexamethasone. Despite the sensitivity of the LC-MS/MS assay (chapter 5.4.5), which can easily detect concentrations down to 100ng/ml, and although slow drug release and activity had previously been proven *in vitro*, it was not possible to detect the dexamethasone in the blood.

One explanation could be a burst release, which is not uncommon *in vivo*. Studies of VEGF eluted from calcium-alginate microspheres revealed an uncontrolled elution within the first four days [428]. Those release kinetics are typically seen with hydrogel-type delivery systems, such as the release of 70-100% of growth factors initially added to fibrin glue within 24 hours [429].

The same applies to PEG hydrogels, the high water content of which is critical in maintaining the bioactivity of hydrophilic biomolecules [430]. As a result, a rapid release takes place, not only shortening the efficacy of the delivery device, but also causing a "dose-dumping" effect that is potentially detrimental for the surrounding tissue [342].

In a pharmacokinetics study of dexamethasone in a rat model of rheumatoid arthritis, healthy and arthritic animals were given either a low (0.225mg/kg) or a high (2.25mg/kg) intramuscular dose, in order to determine if the inflammation process alters distribution and clearance of the drug [431]. Dexamethasone absorption from the intramuscular site was rapid, reaching a maximum concentration after 0.5h for all doses, with hardly any difference between the plasma concentration of dexamethasone between healthy and arthritic rats. The measurements of plasma levels in the study at hand only commenced two hours after dexamethasone was administered, which is why the peak plasma concentration might have been missed. However, Earp *at al.* were able to detect dexamethasone for about 24 hours after intramuscular injection [431], while in the present study not even covalently bound dexamethasone could be quantified. This phenomenon could perhaps be explained with the covalently attached drug being eluted too slowly, which resulted in plasma concentration levels that might have been too low to be detectable. It is also possible that the pharmacokinetic methodology utilized needed optimization, as *in vitro* hydrolysis after sample collection occurs at a much faster rate in rat plasma (*in vitro* half life 1.75h) than in does in plasma of sheep or humans (*in vitro* half life ten to 12h) [432].

Further analysis of the hearts from the rats included in this study (see below) argued against further effort and expense being directed towards investigating the drug analysis methodology. Although the study was mainly designed to investigate the release rates of dexamethasone *in vivo*, it also allowed observing cardiac performance as well as scarring thickness.

2.3.3.2 Cardiac function

Cardiac function was assessed three weeks post-MI. To reduce variability and to avoid false positive results, a minimum of one eighth (12.5%) of the LV had to be infarcted for rats to be included in this study.

Fractional shortening (FS) of the saline-treated group amounted to 35.9% (±2.41%); free dexamethasone (150µg) 33.3% (±2.88%); free dexamethasone (500µg) 36.7% (±4.39%), entrapped dexamethasone (150µg) 31.2% (±1.89%), entrapped dexamethasone (500µg) 35.1% (±2.85%) and bound dexamethasone (150µg): 33.0% (±2.15%). No significant difference was found between any of the groups ($p>0.1$). Therefore, the post-MI use of corticosteroids had neither deleterious nor beneficial effects on cardiac performance.

2.3.3.3 Histological findings

To assess if dexamethasone has a thinning effect on infarct tissue, potentially contributing to the previously described complication of infarct rupture [58, 411, 412], rats were killed after three weeks and their hearts investigated histologically.

As mentioned before, a minimum of 12.5% of the LV had to be infarcted for rats to be included in this study. The overall average infarct size amounted to 24.6% (±1.97%). Average infarct size after treatment with saline was 21.8% (±2.54%), free dexamethasone (150µg): 28.0% (±5.24%), free dexamethasone (500µg): 18% (±2.31%), entrapped dexamethasone (150µg): 21.3% (±3.9%), entrapped dexamethasone (500µg): 27.3% (±10.7%) and bound dexamethasone (150µg): 26.2% (±3.22%). There was no significant difference between any of the groups ($p>0.1$).

Including all rats that were treated with dexamethasone in this study (n=16), the average scar thickness was 1.005mm (±0.03mm). As previously stated, this study was initially designed to investigate pharmacokinetics of biomaterial-based dexamethasone release, which is the reason for the small number of replicas per group (free dexamethasone (150µg): n=4, free dexamethasone (500µg): n=3, entrapped dexamethasone (150µg): n=3, entrapped dexamethasone (500µg): n=2, bound dexamethasone (150µg): n=4) and only two rats that were injected with saline as control. Being sufficient for a pharmacokinetics study, the size of the saline control group was not adequate for statistically meaningful histomorphometric analyses. Therefore, measurements of saline control hearts from previously conducted, larger studies were used as comparison, as the animals were tightly age and sex matched.

According to Holmes *et al.*, the fibrotic phase (i.e. collagen deposition) in rats is completed two weeks post-MI [58]. In accordance with that, the scar thickness of rats after three weeks should be similar to or thicker than a scar at four weeks after infarct induction.

Thus, the average scar thickness of dexamethasone-treated rats three weeks after infarct induction (1.005mm ± 0.03mm) was analyzed against the average scar thickness of saline-treated rats from previously conducted studies (1.215mm ± 0.08mm) and was found to be significantly thinner ($p<0.05$) (Figure 27).

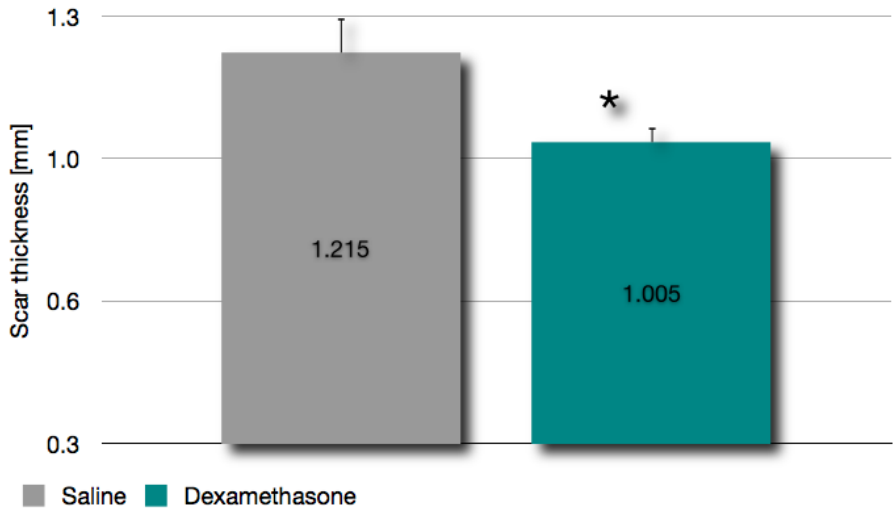

***Fig. 27: Average scar thickness of infarcted rat hearts**. Animals were treated either with saline (as control) or with dexamethasone*

2.3.4 Summary

As there was no definitive proof of an increased risk of myocardial rupture related to post-MI corticosteroid treatment in a meta-analysis involving 2646 patients, but evidence of a substantial reduction in mortality [424], the investigation of dexamethasone for treatment of acute coronary syndrome has been suggested previously [425]. Incorporating the steroid into a hydrogel would prevent possible adverse effects such as thinning of infarcted tissue, while at the same time beneficial effects such as diminished infarct size [388, 389] and reduced post-MI mortality rate [424] might be achieved.

The delivery of the agent together with a non-degradable macromer, polymerized with enzymatically degradable crosslinkers, should allow a controlled slow tissue dependent release of the appended molecules. Hence, the aim of this experiment was to incorporate dexamethasone into MMP-1s crosslinked and therefore degradable PEG hydrogels, comparing the effect of both entrapped and tethered drug on functional and histological parameters.

In the study at hand, it could be demonstrated that the attachment of a drug to an enzymatically cleavable PEG hydrogel is a feasible method, allowing the precise control of drug elution *in vitro* by using different attachment methods as well as varying dosages.

Steroids have been shown to cause a thinning of infarcted tissue, which was confirmed in the present study and which could not be prevented by the simultaneous administration with PEG hydrogels. That can, at least in part, be explained with MMP-1 sensitive PEG hydrogels being unable to improve scar thickness if injected immediately after an infarct has occurred, as shown in this thesis for the first time. Delayed injection, however, would not have been beneficial either, as reduction in infarct size and cardioprotection need to be achieved before infarct expansion can take place or cardiomyocytes suffer irreversible damage. Moreover, it has been shown previously that delayed steroid treatment had adverse effects on post-MI remodeling [427].

This randomized and blinded study was conducted to investigate whether one could take advantage of the beneficial properties of dexamethasone, whilst avoiding its adverse effects when injected together with an enzymatically degradable PEG hydrogel. The findings, however, showed that post-MI steroid administration, despite the simultaneous delivery with a hydrogel, lead to significant thinning of the infarcted wall.
Although a sustained release was proven *in vitro*, the results could not be confirmed *in vivo*, as the dexamethasone was not detectable in the blood samples. This is difficult to explain, particularly for the covalently bound agent.
As dexamethasone administration did not result in any functional improvement, but rather contributed to an increased post-MI scar thinning, no further investigations towards potential explanations were pursued. These present findings are further evidence that the use of steroids may not be advisable for post-MI treatment.

3 Determining the ability of PEG hydrogels with tethered dexamethasone to prolong transduced cardiac gene expression when delivered in conjunction with an adenovirus

3.1 Introduction

3.1.1 Adenoviral vectors for gene therapy

Gene therapy is a rapidly growing area of research that has the promise to treat many genetic and acquired diseases. The use of viruses' natural ability - to infect a host and introduce "foreign" genome into the host's cells - is a powerful tool. Thus a variety of different viruses are being explored for this purpose [433].

Despite the induction of potent host immune responses and a limited duration of transgene expression [434, 435], adenoviral vectors have received significant interest as a potential delivery vehicle [436-443]. They are medium-sized viruses (90-100nm) that mainly cause upper respiratory, eye and intestinal diseases and have a genome that consists of linear, non-segmented double-stranded DNA. After infection, adenoviral DNA does not integrate into the genome of the host cell and is therefore not replicated during cell division. The use of adenoviruses has shown some promising results for a variety of applications [444-446], the focus now being the treatment of cancer [447-458]. The frequent use of adenoviruses can be attributed to the non-pathogenicity for their host, the relatively easy production of high-concentration viral stocks, the high transduction efficiency and ability to transduce both proliferating and quiescent cells [459, 460].

An important factor that needs to be taken into account is that the transduction of cells with therapeutic genes naturally causes an immune response. Since this limits the efficacy and, most importantly, the safety of viral gene therapy [461], adequate immunosuppression has to be administered. In this context, the adenovirus is a suitable target to test, as the immune response elicited by it is particularly pronounced.

3.1.2 Modulation of immune response through combined delivery with dexamethasone

Generally, it is much more difficult to control an already established immune response as opposed to implementing prevention strategies, before it even has a chance to develop [462].

Prophylactic strategies include the design of vectors in such way that they contain only few (or ideally no) pathogenic genes [463], the use of tissue specific promoters to ensure localized "action", restricted to the target tissue [464], the regulated expression of the transgene [465, 466] or alternatively the use of drug-induced immunosuppression, the latter being a very well established strategy for organ transplantation [462].

Although being a promising approach, some possible adverse effects need to be considered: possible hindrance of transduction efficacy and vector stability, drug side effects that could aggravate underlying metabolic complications and increased susceptibility to infection by opportunistic pathogens [462, 467]. The risk of activating latent infections can be reduced though by monitoring drug levels and by aiming for a short overall duration of immunosuppression [462].

A new protocol, involving a single dose of dexamethasone, was established lately, showing diminished innate and adaptive immune responses, while at the same time avoiding adenovirus stimulated thrombocytopenia and leukocyte infiltration [468]. As dexamethasone has also already been established to attenuate foreign body reactions of the tissue around implants [417-422], it would make sense to couple gene therapy with immunosuppressive drugs, to prevent an extensive immune reaction from occurring.

3.2 Project aims

Having developed polyethylene glycol (PEG) hydrogels that can polymerize spontaneously *in vivo* to allow for controlled release of dexamethasone; it is possible that these dexamethasone-loaded gels have the potential to reduce the inflammatory and immune responses to viral vectors.

Hence, the aim of this study was to investigate the efficacy of these types of PEG hydrogels in sustaining gene expression and reducing inflammation in cardiac cells after *in vivo* transduction with adenovirus.

As an initial investigation in this area, the impact of the simultaneous delivery of dexamethasone containing PEG gel with adenovirus vector carrying the GFP gene on the longevity of cardiac GFP expression and the resulting inflammatory response was assessed.

3.3 Results and discussion

In order to assess the ability of slow release dexamethasone hydrogels to sustain green fluorescent protein (GFP) expression by adenovirus-infected cardiac cells and to reduce the inflammatory and immune response towards these cells, dexamethasone was successfully modified by acrylation, solubilized by PEGylation and covalently incorporated into PEG gels as detailed in chapter 5.5.1. A rat model that allowed for the assessment of the immune and inflammatory response to intramyocardially injected viral vectors and their transgenes was used as detailed in chapter 5.5.2.

The gels were crosslinked in situ via MMP-1s that allowed for enzymatic degradation over one to two weeks. The dexamethasone was released in its original form by hydrolysis over that period. The rats were killed after one week and assessed for GFP expression, cardiac tissue damage, macrophage and T-lymphocyte content.

3.3.1 Quantification of GFP expressing cells and tissue damage

As demonstrated in Figure 28, the total area of cells expressing GFP in the dexamethasone group was substantially higher than in the control hydrogel group (Virus/hydrogel: 60000μm^2 ± 36000μm^2, Virus/dexamethasone hydrogel 467000μm^2 ± 113000μm^2 (n=5), with a 7.7fold greater area of cells expressing GFP ($p \leq 0.05$).

There was substantial tissue damage in both groups with no significant difference between the two groups (Virus/hydrogel: 11859000μm^2 ± 401000μm^2, Virus/dexamethasone hydrogel 1650000μm^2 ± 2280000μm^2) (Figure 29).

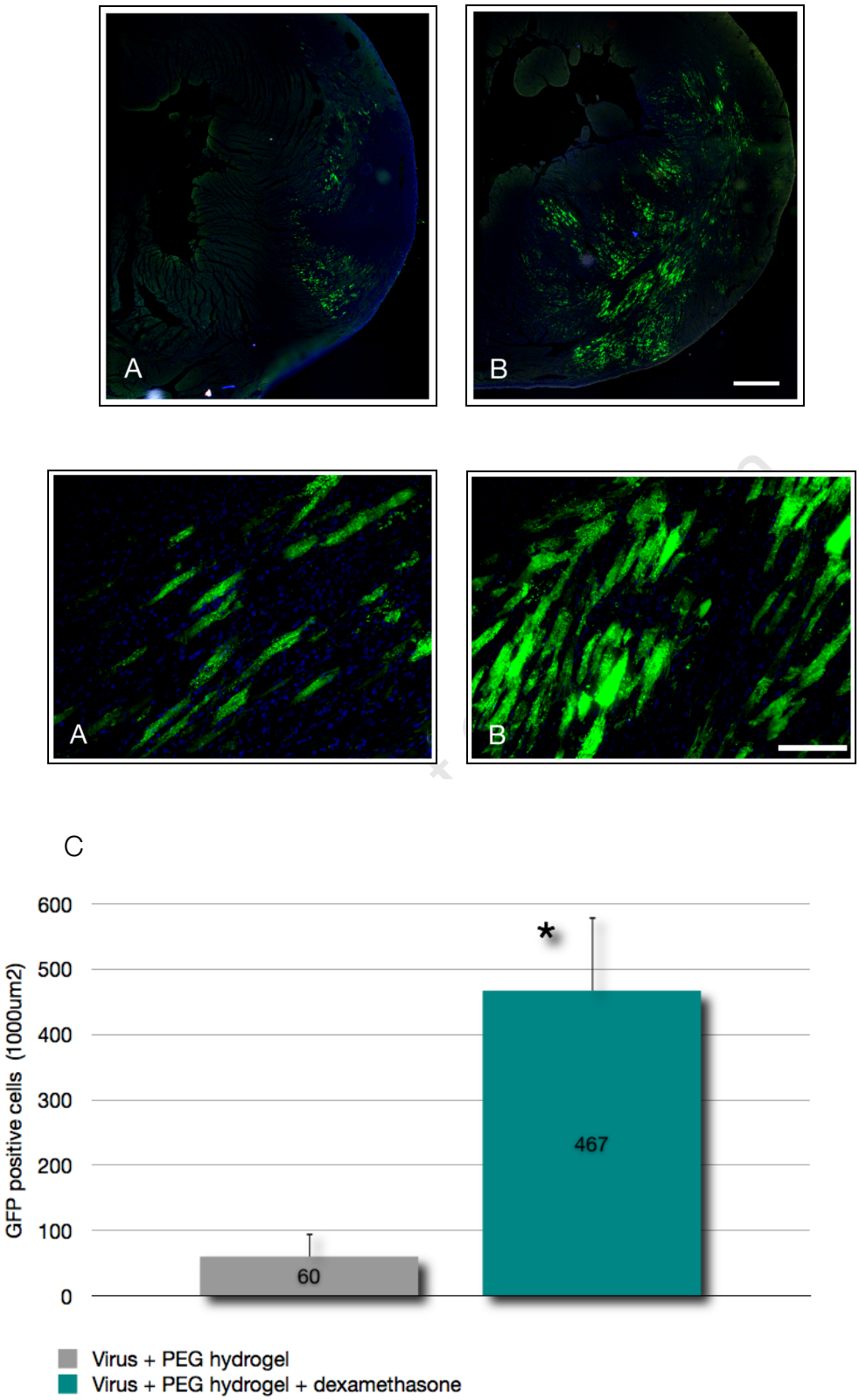

***Fig. 28: Area of cells expressing GFP**. (A) AdV + PEG hydrogel, (B) AdV + PEG hydrogel + 150µg dexamethasone. Upper row: bar represents 1mm, lower row: bar represents 100µm. Both groups were injected with a total of 100µl PEG, containing 1x10⁸ pfu AdHCN4. (C) Quantitative analysis, p≤0.05. Nuclei: blue, GFP expression: green*

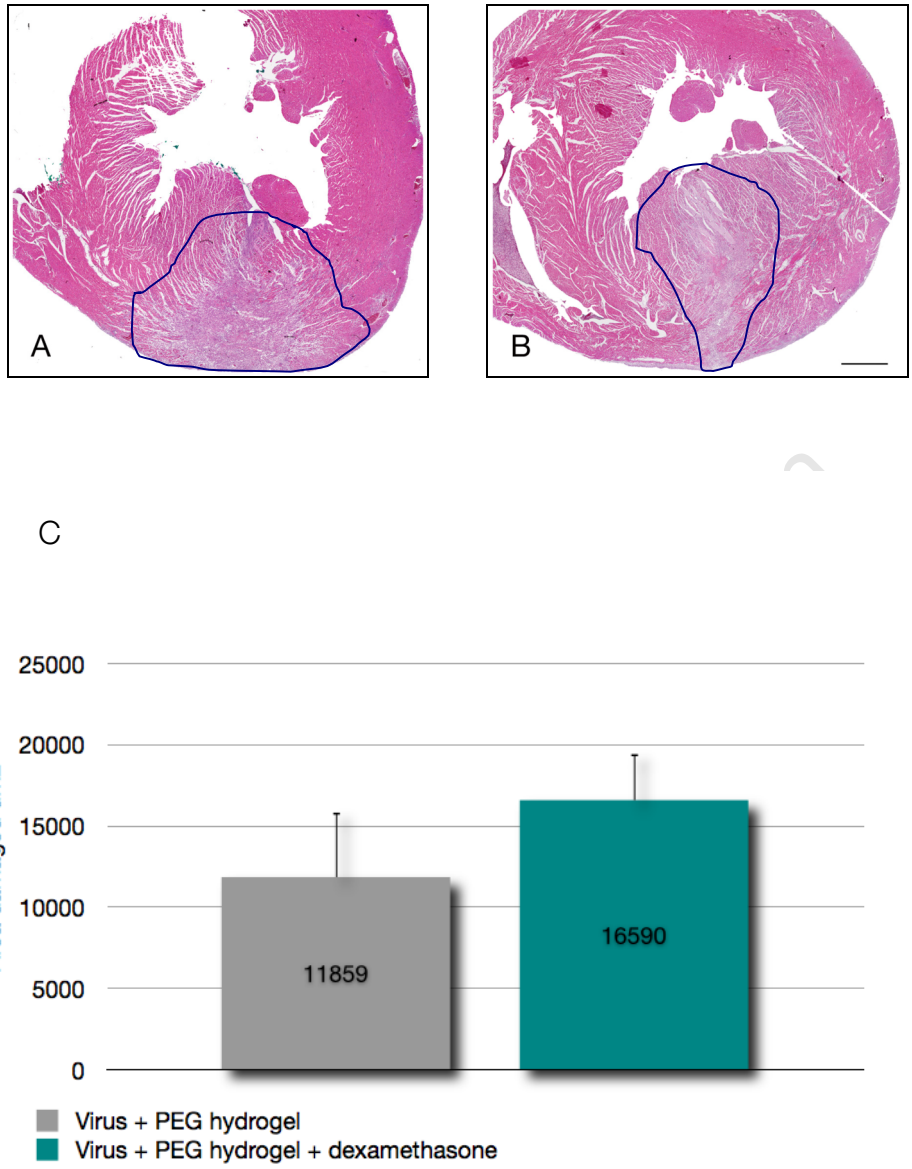

Fig. 29: Tissue damage *H&E stain of (A) AdV + PEG hydrogel, (B) AdV + PEG hydrogel + 150µg dexamethasone. Bar represents 1mm. Both groups were injected with 100µl PEG, containing 1x10⁹ pfu AdHCN4. Blue outline indicates area of tissue damage. (C) Quantitative analysis of area of tissue damage, p=0.3.*

The area of tissue damage was substantially larger than that of GFP expressing cells, indicating that 2.8% of GFP expressing cells were left at one week for the dexamethasone group whilst only 0.5% for the control group had survived. Tissue damage was spread through a larger volume of myocardial tissue.

3.3.2 Inflammatory and immune response

A similar trend was observed for the macrophage and T-lymphocyte responses (Figures 30 and 31), with both groups having similar levels of inflammation and immune responses. Image analysis results led to analogous findings (Macrophage: Virus/hydrogel: 1317000µm^2 ± 906000µm^2, Virus/dexamethasone hydrogel 1886000µm^2 ± 639000µm^2; T-lymphocyte: Virus/hydrogel: 1196000µm^2 ± 371000µm^2, Virus/dexamethasone hydrogel 1102000µm^2 ± 142000µm^2).

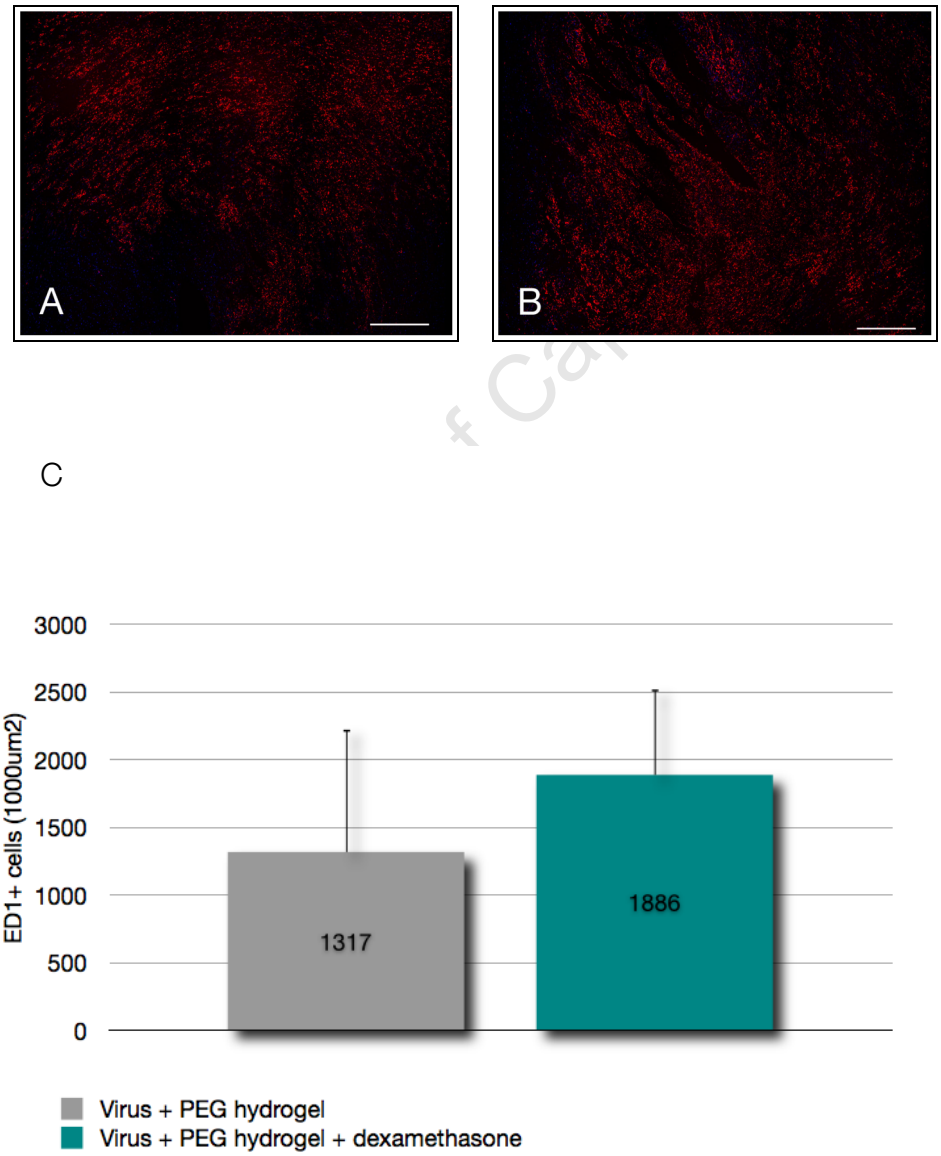

Fig. 30: Macrophage response *(A) virus + PEG hydrogel, (B) virus + PEG hydrogel + 150µg dexamethasone. (ED1 staining) Bar represents 500µm. Both groups were injection with 100µl PEG, containing 1x10⁷ pfu AdHCN4. (C) Area of macrophages relative to GFP Expression, p=0.6.*

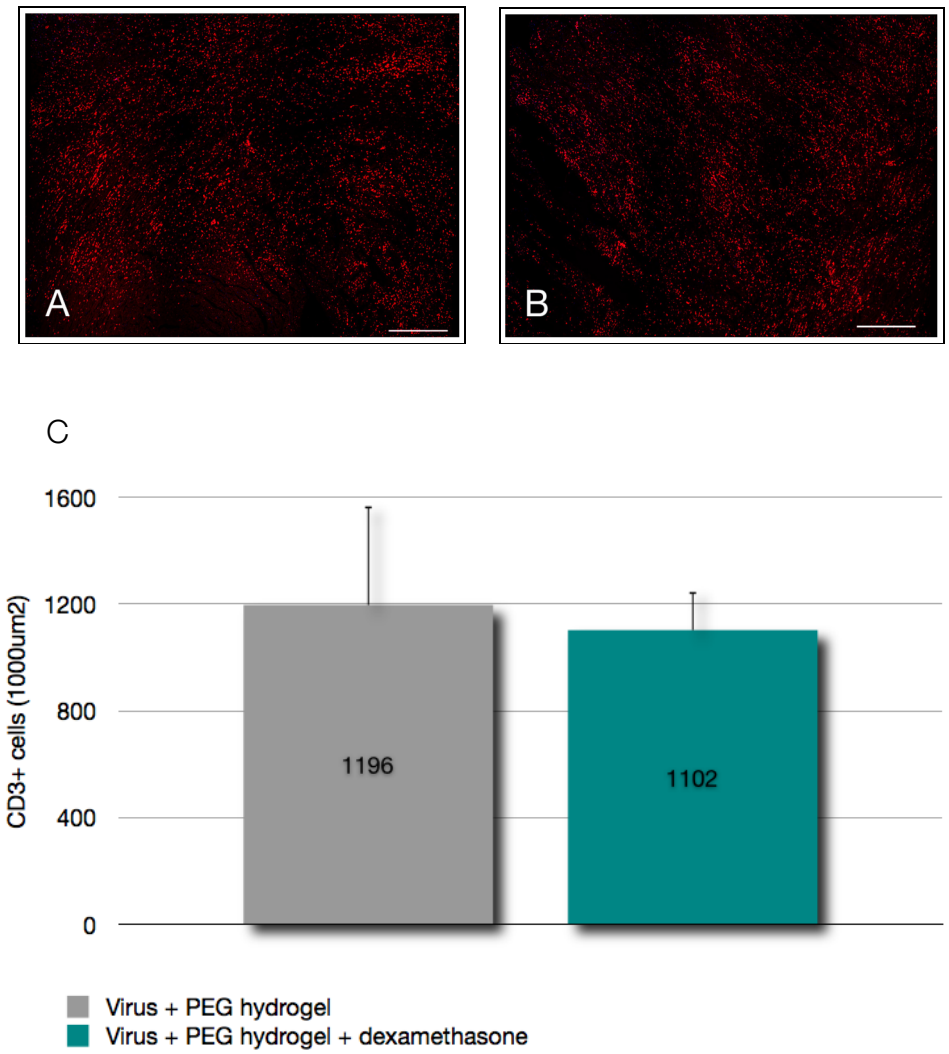

Fig. 31: T-lymphocyte response *(A) virus + PEG hydrogel, (B) virus + PEG hydrogel + 150µg dexamethasone. (CD3 staining), Bar represents 500µm. Both groups were injected with 100µl, containing 1x10⁹ pfu AdHCN4) (C) Area of T-Lymphocytes relative to area of GFP expression, p=0.7*

While the area of cells expressing GFP was substantially higher in the dexamethasone group, no decrease in tissue damage or inflammation was observed.

Although the difference was significant, data comparison between area of tissue damaged and GFP expressing area indicates that only a small number of cells were rescued. Additionally, it is possible that by looking at only one time point that there may have been an initial decrease in the inflammatory response but that this stage was missed.

There is literature showing that dexamethasone activates protective signaling pathways in cardiomyocytes [388-391, 393, 399, 401], but it is less easy to see how this might be protective for transduced cardiomyocytes that are targeted by the immune system.

3.3.3 Summary

A newly established protocol, involving pretreatment with dexamethasone, showed diminished innate and adaptive immune responses towards adenoviral vectors, without reducing their efficacy [468]. Hence, the present study was carried out to determine the efficacy of dexamethasone-releasing PEG hydrogels in prolonging GFP expression by reducing immune and inflammatory response to adenovirus.

The outcome of the present study indicates that local delivery of anti-inflammatory drugs show promise for prolonging cardiac cell expression after transduction with an adenovirus vector. This outcome was most likely achieved through reduction of the immune and inflammatory response but this could not be confirmed due to only one time point being observed. It was beyond the scope of this thesis to extend the number of time points observed. However, only a small number of cells could be rescued, which is not surprising taking into account that dexamethasone alone might not be potent enough to accomplish a meaningful reduction of immune-mediated loss of vector persistence. Hence, Wang *et al*. administered a cocktail of immunosuppressive drugs to achieve sustained AAV-mediated gene expression in a canine model [469]. In view of that, it is advantageous that the chemistry of these gels can be further refined to allow for release of other anti-inflammatory and immunosuppressant agents to enhance the positive effects demonstrated in the study at hand.

4 Conclusions

Post-infarct remodeling has been shown to cause impaired cardiac function due to complex changes in ventricular architecture, eventually leading to heart failure in many patients, who suffered a heart attack. Hence, cardiac failure has become an important therapeutic target, with the delivery of biomaterials (hydrogels) being one possible option that can result in increased wall/scar thickness, lessening of adverse LV remodeling as well as attenuated infarct expansion and improvement of functional parameters. Divergent timing regimes of previously conducted studies make it difficult to evaluate the outcome of the treatment, thus the present study is the first to directly compare immediate injection and biomaterial delivery delayed by seven days. The injection of MMP-1 degradable PEG gel into a one-week-old myocardial infarct was feasible and effective in ameliorating cardiac performance. Interestingly, although infarct patients commonly benefit from timely intervention, delayed treatment was superior to immediate one in this study. Histological analysis revealed a significantly thicker scar after delayed injection, relative to immediate treatment and to saline control group. Evidence indicates that the divergent distribution patterns and surface to volume ratio are the most likely explanation for the observed phenomenon. The findings of this experiment have practical relevance especially for those myocardial infarct patients, who could not benefit from timely treatment initiation.

In a second experiment, the value of steroid releasing PEG hydrogels for the treatment of myocardial infarction was investigated. Incorporating dexamethasone into a hydrogel would prevent possible adverse effects of the agent, such as thinning of infarcted tissue, while at the same time beneficial effects of steroids, such as diminished infarct size and reduced post-MI mortality rate might be achieved through the controlled slow tissue dependent release of the appended molecules. It could be demonstrated In the present study that the attachment of a drug to an enzymatically cleavable PEG hydrogel is a feasible method, allowing the precise control of drug elution *in vitro* by using different attachment methods as well as varying dosages. Although a sustained release was proven *in vitro*, the results could not be confirmed *in vivo*, as dexamethasone was not detectable in the blood samples.

Moreover, the present study confirmed the previously demonstrated thinning effect steroids have on infarcted tissue, which could not even be prevented by the simultaneous administration with PEG hydrogels. This can, at least in part, be explained with MMP-1 sensitive PEG hydrogels being unable to improve scar thickness if injected immediately after an infarct has occurred, as shown in this thesis for the first time. Delayed injection, however, would not have been beneficial either since reduction in infarct size and cardioprotection need to be achieved before infarct expansion can take place or cardiomyocytes suffer irreversible damage. These present findings are further evidence that the use of steroids may not be advisable for post-MI treatment.

A newly established protocol, involving pretreatment with dexamethasone, showed diminished innate and adaptive immune responses towards adenoviral vectors, without reducing their efficacy. Hence, a third set of experiments was carried out to determine the efficacy of dexamethasone-releasing PEG hydrogels in prolonging GFP expression by reducing immune and inflammatory response to adenovirus. Proof of principle for drug releasing PEG gels to aid in sustained gene expression via viral vector delivery for the treatment of pathologies of the heart could be demonstrated in the present study and might have resulted from a reduction of the immune/inflammatory response. The outcome was suggestive that prolonged duration of expression was obtained with a 7.7fold increase in GFP expression at one week for those viruses that were injected with hydrogel releasing dexamethasone relative to those injected with hydrogel alone.

In the thesis at hand, MMP-1 degradable PEG hydrogels proved to be helpful in ameliorating post-MI cardiac function, with delayed intramyocardial injection being superior to immediate treatment. Furthermore, proof of principle for biomaterial-based drug release could be demonstrated, which could aid in applications such as sustained gene expression after viral vector delivery.

5 Materials and methods

5.1 *In vitro* preparation and preliminary experiments

5.1.1 Polyethylene glycol derivatisation

As per Lutolf *et al*., 20PEG-8VS was synthesized in dry Dichloromethane (DCM) by first deprotonating 20PEG-8OH with sodium hydride (NaH) followed addition of a large excess of divinylsulphone ($C_4H_6O_2S$). The remaining NaH in the crude reaction mixture was quenched by acetic acid (CH_3COOH) prior work-up through three consecutive precipitations in ether [338]. According to Elbert *et al*., 20PEG-8Ac was synthesized in dry DCM by adding Acryloyl chloride (C_3H_3ClO) to 20PEG-8OH in presence of base (Triethylamine, TEA) in a dry environment. The crude reaction mixture was worked up by three consecutive precipitations in ether [470]. The following crosslinkers were acquired by purchase: 2kDa non-degradable dithiolated Polyethylene glycol (2nPEG-2SH), 10kDa non-degradable tetrathiolated Polyethylene glycol (10nPEG-4SH) and matrix metalloproteinase-1 substrate (MMP-1s). All polymers were stored at -20°C.

Iso-osmotic Phosphate buffered saline (iPBS), which was utilized as solvent for the polymers, was prepared as follows (Table 5):

Table 5: Content iso-osmotic PBS solution

Solution	Components	
1	2.07g 100.0ml	$NaH_2PO_4.1H_2O$ Distilled water
2	26.86g 500.0ml	$Na_2HPO_4.12H_2O$ Distilled water
3	8.766g 1000.0ml	NaCl Distilled water

95ml $NaH_2PO_4.1H_2O$ solution was mixed with 415ml $Na_2HPO_4.12H_2O$ solution, to which 508ml of solution 3 were added. This resulted in an iso-osmotic buffer with a pH of 7.6. The iPBS was autoclaved for 20min at 121°C.

5.1.2 Preliminary *in vitro* characterization of PEG hydrogels

Gels of 10% (m/v) nominal concentration were prepared by dissolving 10mg 20PEG-8Ac in 50µl iPBS and adding 50µl of a crosslinker solution. For the latter, 2-arm and 4-arm crosslinker solutions were prepared in five different ratios:

- 100% 10nPEG-4SH (10mg in 50µl iPBS)
- 75% 10nPEG-4SH (7.5mg in 37.5µl iPBS) + 25% 2nPEG-2SH (1mg in 12.5µl iPBS)
- 50% 10nPEG-4SH (5mg in 25µl iPBS) + 50% 2nPEG-2SH (2mg in 25µl iPBS)
- 25% 10nPEG-4SH (2.5mg in 12.5µl iPBS) + 75% 2nPEG-2SH (3mg in 37.5µl iPBS)
- 100% 2nPEG-2SH (4mg in 50µl iPBS)

Those hydrogels were compared to 10mg 20PEG-8VS in 50µl iPBS crosslinked with 4mg 2nPEG-2SH in 50µl iPBS and 10mg 20PEG-8VS in 25µl iPBS crosslinked with 3.45mg MMP-1s in 75µl iPBS.

For each of the seven groups, three discs with a total volume of 100µl were manufactured and then incubated in iPBS at 37°C. The gelling time was recorded and their weight was measured at set time points until the gels were degraded.

5.2 *In vivo* evaluation of degradable PEG hydrogels

5.2.1 Animals

Male outbreed Wistar rats (180-220g) were used for the *in vivo* studies. Animals were bred and housed at the *Animal Unit, Faculty of Health Sciences, University of Cape Town* for at least five to six weeks before the start of the experiments. Five to six animals were kept in each cage (*Eurostandard Type IV*, 595 x 380 x 200mm, floor area 1820cm^2) at constant room temperature (21-23°C). The rats were exposed to a 12h light/dark cycle (6am-6pm) and had free access to water and food (*Rat & Mice Feed 16%*). Wood shavings served as bedding and shredded paper was supplied for environmental enrichment.

Rats that were used for experiments testing the feasibility of cardiac delivery of viral vectors were operated on and housed in a Biosafety level 2 (BSL2) facility.

The handling and all animal experiments complied with the *Principles of Laboratory Animal Sciences* [471] as well as *The UFAW Handbook on the Care and Management of Laboratory Animals* [472] and were approved by the *Animal Research Ethics Committee, Faculty of Health Sciences, University of Cape Town*.

5.2.2 Surgical procedures

5.2.2.1 Pre-surgical preparation

Surgical procedures were carried out under aseptic conditions. The same instruments were used for five to ten animals, but were sterilized between operations in the *Hot bead sterilizer*.

Placed into the induction chamber and sedated with 5.0% Isoflurane at an oxygen output of 1.5l/min at 1bar and 21°C, the animal became unconscious within approximately two minutes. The rat was temporarily removed from the chamber for its weight to be measured and to shave off the fur from chest or dorsal skin.

5.2.2.2 Subcutaneous implantation

In preparation, discs consisting of 20PEG-8Ac crosslinked with 2nPEG-2SH, 20PEG-8VS crosslinked with MMP-1s as well as 20PEG-8VS crosslinked with 2nPEG-2SH were polymerized in between glass slides to ensure a thickness of 1.0mm and a diameter of about 0.8cm. Six gels were produced for every group, each having a total volume of 50µl.

The unconscious rat was transferred to the heated operating board and connected to the *Rodent Anesthesia Circuit Mask*, which supplied 2.0% Isoflurane at an oxygen output of 0.3l/min at 1bar and 21°C. After disinfection of the dorsal skin, up to six longitudinal incisions of 1.0cm each (up to three on either side of the spine) were made with a disposable blade. Gentle spreading of subcutaneous and connective tissue allowed the creation of subcutaneous pouches, so that one round pre-manufactured flexible PEG disc could be implanted into each pocket. A rotational algorithm was used for the implantation of the discs, so that the position of each group varied from animal to animal. The pouches were closed with 4-0 silk and the skin was thoroughly cleaned thereafter.

5.2.2.3 Myocardial infarct model

For airway protection and to provide a means of mechanical ventilation, the rat had to be intubated, which was carried out according to Theodorsson *et al*. (2005) [473]:
The animal was secured in a supine position on the *Tilting WorkStand*, the head directed towards the operator, using the *Incisor Loop* to hold the neck extended. With cotton swabs the rats tongue was rolled out and held up, while the *Rat Specula*, which was connected to an otoscope, was inserted for visualization of the vocal cords. A 16G i.v. catheter (57mm) was gently slid down the *Rat ET Tube Introducer*, between and past the vocal cords, until the hub reached the incisors. After removal of the metal guide wire, the tracheal intubation was verified with a dental mirror. Before the animal could regain consciousness, it was attached to the *Harvard Small Animal Ventilator*, supplying 2.0% Isoflurane at an oxygen output of 0.3l/min at 1bar and 21°C and at a respiratory rate of 115 breaths per minute. The correct connection to the ventilator was visually confirmed when the rhythmic movements of the rats chest were in synchrony with the ventilator.

Surgical procedures were performed according to modified protocols from Tarnavski *et al*. and Huang *et al.* [474, 475]:
Being connected to the ventilator, the animal was placed in supine position onto the heated operating board. The limbs were fixed to the platform; chest and abdomen were thoroughly cleaned. Using a disposable blade, an approximately 2cm transverse skin incision was made along the 4th intercostal space to expose the underlying subcutaneous tissue. Pectoral muscles were separated with sterilized cotton buds and gently retracted with a pair of sutures (2-0 non-absorbable polyester), which were fixed onto the platform with tape. To expose the heart, the chest cavity was opened at the 4th intercostal space by bluntly dissecting the intercostal muscles with a hemostat, taking extreme care not to damage the underlying lung. That allowed the retractor to be inserted to spread the ribs apart. Using two forceps, the pericardial sac was gently torn, providing better exposure of the heart and improving the visualization of big vessels like the LAD (left anterior descending) coronary artery, which appeared as a bright red spike. However, contrary to what is widely stated in literature, the LAD was not always clearly visible. Then, a 6-0 non-absorbable Polypropylene ligature was placed under the artery and tied with three knots 2mm distal the auricular appendix.

Discolorations of the anterior wall of the left ventricle from pink to grey and reduced contractility were hallmarks of a successful occlusion of the artery.
Once the artery was ligated, the animals were randomly assigned to receive one of the following three materials, injected either immediately after infarct induction or in a second operation seven days post-MI:

1) Injection of Alexa Fluor® labelled PEG hydrogel

Per 100µl gel, 1µl of 10mg/ml Alexa Fluor® 660 C2 maleimide in dimethyl sulfoxide (DMSO) was added to 1µl of 15.4mg/10ml dithiothreitol (DTT) in iso-osmotic phosphate-buffered saline (iPBS, pH 7.6) and reacted for 30min at 37ºC. One microliter of the above Alexa/DTT solution was added to the 20PEG-8VS solution (10mg in 25µl iPBS) and reacted for 10min at room temperature before being mixed with the MMP-1 solution (3.45mg in 75µl iPBS). 100µl of the hydrogel were aspirated into a *BD Micro-Fine + Demi* syringe and injected into the myocardium before the two components polymerized. The successful application resulted in a slight swelling of the respective area, indicating that the hydrogel did not escape into the left ventricular cavity. 100µl saline served as control.

2) Injection of lead

Alternatively, 100µl 20PEG-8VS hydrogel crosslinked with 2nPEG-2SH and labelled with lead, as described in chapter 5.3.2, were injected into the infarcted area.

3) Injection of Mercox resin

The casting material consists of two components: a resin (Mercox) and a catalyst (Benzoyl Peroxide 40%). Here, 1ml of Red Mercox resin was mixed with 20mg of catalyst just before 100µl of it were injected into the infarcted myocardium as the polymerization takes place in a relatively short period of time.

After the removal of the retractor, 4-0 silk was used to draw the rib cage together, taking care not to suture the lung. While tying a knot, slight pressure was applied on the chest to reduce the volume of free air in the cavity. The wound was stepwise closed and the skin was sutured with 4-0 silk before finally being cleaned with iodine solution. Flow of Isoflurane and oxygen was stopped and the rat was disconnected from the ventilator.

5.2.2.4 Postoperative care

As soon as spontaneous breathing was regained, 0.05mg/kg buprenorphine (*Temgesic*®) was administered intramuscularly into the hind limb. Being transferred to a single, clean cage (*Eurostandard Type III H*, 425 x 266 x 185mm - floor area 800cm^2), rats was allowed to recover, while heat was provided for about 45min by an infrared lamp in order to maintain the animals body temperature. Intubated rats were kept with the intubation tube placed in the trachea until they regained full consciousness. In 1h after surgery the animals should be completely awake and move around in the cage and were then provided with water and food ad libitum.

All rats underwent postoperative control by staff of the *Animal Unit*. Top-up doses of buprenorphine were administered twice daily for three days post-operatively.

5.2.3 Echocardiography

To evaluate cardiac function in a serial and noninvasive manner, transthoracic echocardiography was performed according to Collins *et al*. [476] on days 14 and 28 post-MI, in a blinded fashion to eliminate subjective bias. The key that identified the animals and which group they belonged to was kept by a third party and was not revealed to the examiner before all data had been recorded and analyzed.

5.2.3.1 Sedation

In order to ensure precise image acquisition during cardiac ultrasound, the animal had to be sedated. Generally, most anesthetics have a negative inotropic and chronotropic effect and consequently alter cardiac function significantly. However, the impact of various intraperitoneal and inhaled anesthetic agents on echocardiographic parameters had been compared in mice, concluding that Isoflurane resulted in the most stable fractional shortening values and the most reproducible measurements [477].

Thus, the rat was placed into the induction chamber and anaesthetized with 5% Isoflurane at an oxygen output of 1.5l/min at 1bar and 21°C for the first 2min, while for the maintenance 1.5% Isoflurane were supplied at an oxygen output of 0.3l/min at 1bar and 21°C via the *Rodent Anesthesia Circuit Mask*. The animal was placed in left lateral position onto the operating board after the fur was shaved off chest and abdomen. Ultrasound gel was used to increase probe contact during echocardiography.

To further minimize adverse effects on cardiac function the operating board was heated to avoid anesthesia-induced hypothermia and consecutive decrease of heart rate and cardiac output [478] and care was taken not to place excessive pressure on the chest with the transducer as this could result in bradycardia and hypotension; lastly a short overall time of anesthesia was aimed for.

5.2.3.2 2D and M-mode

The parasternal long axis, for which the transducer was directed towards the right shoulder of the animal, gave a first impression of LV size and function. After a 90° clockwise rotation at papillary muscle level, the parasternal short axis could be viewed and was used for 2D- and M-mode derived measurements, according to the *Recommendations for quantitation of the left ventricle by two-dimensional echocardiography* [479].

At the time of apparent maximal dilation of the left ventricle, the left ventricular end-diastolic diameter (LVEDD) was measured, whereas the left ventricular end-systolic diameter (LVESD) was obtained at the time of visible maximal left ventricular contraction. Based on those values, the fractional shortening (FS) was calculated using the following formula (Equation 2):

$$\%FS = \left(\frac{LVEDD - LVESD}{LVEDD} \right) x100$$

Eq. 2: Calculation of Fractional shortening (FS)

To reduce variability between measurements, in both 2D and M-mode imaging, left-ventricular end-diastolic diameter and left-ventricular end-systolic diameter were measured six times and their mean was calculated thereafter.

5.2.4 Termination of *in vivo* experiments

For further analysis of the *in vivo* experiments, animals had to be killed at selected time points, as specified in the relevant result section.

5.2.4.1 Preparation

For histological studies, explants were fixed in a 4% paraformaldehyde solution, which was prepared by dissolving 4.0g paraformaldehyde powder (95%) in 90ml iPBS. The mixture was heated to 60°C, cleared with five to ten drops of 10M sodium hydroxide (NaOH) and adjusted to a pH of 7.0-7.5 using hydrochloric acid (HCl). Fresh iPBS was added to obtain a total volume of 100ml.

5.2.4.2 Explantation of subcutaneously positioned PEG discs

Using Halothane, the animal was made unconscious before being killed by an intracardiac injection of *Euthapent*. PEG discs as well as surrounding subcutaneous tissue were excised and explants were fixed at room temperature in the 4% paraformaldehyde solution for a 24h period.

5.2.4.3 Harvesting the heart (myocardial infarct model)

After making the animal unconscious as described above, it was placed in supine position. Following a cutaneous incision from the abdomen towards the sternum, an intramuscular incision along the rib cage was made. By carefully lifting up the rib cage, the apex of the heart became visible through the diaphragm and was arrested with 1ml of ice-cold saturated potassium chloride (KCl) solution, injected directly into the myocardium. The organ was carefully harvested, thoroughly rinsed with 0.9% sodium chloride (NaCl) solution and fixed in the 4% paraformaldehyde solution for 24h.

5.3 Post-mortem analysis

5.3.1 Histology and image processing

5.3.1.1 Embedding of subcutaneously positioned PEG discs

After 24h fixation in 4% paraformaldehyde, the sample was kept in a 70% alcohol solution for about 1-2h. This was followed by infiltration of tissue for 48h in a mixture of 100ml *JB-4™ Solution A* and 0.9g of *JB-4™ Catalyst*. For the embedding process, 1ml of *JB-4™ Solution B* was dissolved in 25ml of fresh catalyzed *JB-4™ Solution A*, which was then added to the tissue that was placed in a mould and kept under anaerobic conditions for 2h.

Sections of the tissue, varying between 2µm and 3µm of thickness, were cut on the *Microm tissue microtome HM 360*, using an 8mm glass knife. Samples were floated on a 60°C water bath (*Tissue Floating Bath TFB 45*), which contained one drop of saturated NaOH solution, helping them to spread out evenly. The sections were then picked up on glass slides, baked on a hot plate (*Axel Johnson Lab System HP-3*) and were placed for 2-3min in running tap water prior to being stained with either Haematoxylin & Eosin (H&E) or ED1.

5.3.1.2 Embedding of hearts (myocardial infarct model)

After 24h fixation in 4% paraformaldehyde, the rat heart was cut in four equal slices using a disposable blade and was dyed with different colours to distinguish between the sections. The *Tissue-Tek® Rotary Tissue Processor* was used to process the sections overnight and included the following solutions (each for 1h): 70% alcohol, 80% alcohol, 96% alcohol, three baths of 100% alcohol, three baths of xylene and three wax baths. After processing, tissues were embedded in paraffin wax (*Histosec® Pastillen*) with the *Shandon Histocentre 2* embedder. The sections were then cut, having a slice thickness of 3µm for further staining with Haematoxylin & Eosin, Masson Trichrome or ED1 or 8µm for DAPI staining. Sections were floated on the 60°C water bath, picked up on glass slides and baked on the hot plate for 10min at 60°C. Finally, the tissues were dewaxed through three baths of xylene (10min each), agitated in three baths of absolute alcohol and hydrated for approximately 5min in running tap water.

5.3.1.3 Haematoxylin & Eosin staining

Mayer's Haematoxylin and alcoholic EosinY/Phloxine B solutions were used for routine laboratory H&E stains and were prepared as demonstrated in Tables 6 and 7:

Table 6: Protocol Mayer's Haematoxylin

	Components	Procedure
1	1g Haematoxylin 50g Aluminium potassium sulfate ($AlK(SO_4)_2$) 0.2g Sodium iodate ($NaIO_3$)	Dissolve in 1000ml distilled water using gentle heat (water bath or 37°C incubator)
2	50g Chloral hydrate ($C_2H_3Cl_3O_2$) 1g Citric acid ($C_6H_8O_7$)	Add to the mixture and dissolve well
3		Boil for 5min, cool and filter the mixture

Table 7: Protocol alcoholic EosinY/Phloxine B solution

	Components	Procedure
1	10ml 1% Phloxine B 100ml 1% Eosin Y 780ml 95% Alcohol	Mix
2	4ml Glacial acetic acid (CH_3COOH)	Add to the mixture

Sections were placed in Mayer's Haematoxylin for 5-10min and were then washed for 5-10min in running tap water to blue the nuclei of the cells. In order to stain the cytoplasm, the slides were placed for 1min in the 1% alcoholic EosinY/Phloxine B solution.

Resin-embedded sections were air-dried but not mounted, whereas samples, which were embedded in wax, were washed in running tap water, dehydrated through three baths of absolute alcohol, cleared in three baths of xylene and were mounted with *Entellan®*.

As the result, the nuclei stained blue, cytoplasm and all other tissue components appeared in varying shades of pink. In comparison to healthy myocardium, infarcted tissue was paler in color.

5.3.1.4 Modified Masson's Trichrome staining

Masson's Trichrome stain was used for a differential demonstration of muscle and collagen fibers. It typically involves three dyes, one being a nuclear stain. However, in this context a modified technique was employed, which did not include the nuclear staining.

Slides were placed for 30min in Bouin's Fluid (post fixative) in order to enhance the Masson's Trichrome stain (Table 8):

Table 8: Content Bouin's Fluid

Amount	Component
75ml	Picric acid solution (saturated aqueous)
25ml	Formaldehyde (35-40%)
5ml	Glacial acetic acid

Sections were then washed in running tap water until clear. A 0.5% Acid Fuchsin solution (Table 9) was applied to the slides for 5min, which was followed by rinsing in tap water.

Table 9: Content Acid Fuchsin

Amount	Component
0.5g	Acid Fuchsin
0.5ml	Glacial acetic acid
100.0ml	Distilled water (pH 7.4)

In order to remove excess Acid Fuchsin, the sections were treated with 1% Phosphomolybdic acid solution for 5min. The slides were washed in tap water and counterstained for 2min with 2% *Light Green SF Yellowish*. Sections were then dehydrated through three baths of absolute alcohol, cleared in three baths of xylene and mounted with *Entellan*®. Muscle tissue appeared red, collagen fibers stained green.

5.3.1.5 ED1 & Neutrophil Elastase Double Fluorescent staining

Slides were antigen retrieved with Proteinase K at 37°C for 10min (15min if the sections were embedded in resin), which was followed by washing in running tap water for 5min. After being washed with Tris-buffered saline (TBS, Table 10) for 5min, the sections were treated with 1% Bovine serum albumin (BSA) for 20min in order to prevent background staining. The 1% BSA solution was prepared by mixing 1g of BSA with 100ml of iPBS. TBS contained the following:

Table 10: Content TBS

Amount	Component
30.3g	Trizma® hydrochloride
6.95g	Tris base (Tris hydroxymethyl amino methane)
43.83g	NaCl
5.0l	Distilled water (pH 7.6-7.8)

The primary antibody was applied as a cocktail of two antibodies: monoclonal ED1 mouse anti rat CD68 (diluted 1:50 in BSA for resin-embedded sections and 1:100 for wax embedded ones) and polyclonal Neutrophil Elastase (diluted 1:200 in BSA) for 1h at room temperature. Thereafter, they were washed with TBS for 10min. Secondary antibodies were applied as a cocktail: Donkey Anti-Mouse Cy3 (diluted 1:2000 in BSA for resin-embedded slides and 1:500 in wax-embedded ones) and Alexa Fluor® 488 goat anti-rabbit IgG (diluted 1:50 in BSA) for 2h in the dark at room temperature to prevent the light from interfering with the staining. Finally, the sections were washed with TBS for 5min, coverslipped with *VECTASHIELD*® and sealed with commercially available nail polish (to prevent dehydration) before they were stored in the fridge.
The staining resulted in fluorescent red macrophages and blue nuclei.

5.3.1.6 DAPI staining

The sections were washed in TBS and were mounted with *VECTASHIELD*®, which contains DAPI, a fluorescent stain that binds strongly to DNA, thus visualizing the nuclei of cells.

Meanwhile the PEG hydrogel distribution within the myocardium was demonstrated by detecting the covalently bound Alexa fluor 660 maleimide marker using the Cy5 filter on the microscope. Nuclei appeared blue, while the PEG gel had a pink color.

5.3.1.7 Image acquisition

Images of the tissue were acquired with the *Eclipse 90i Microscope* (*X-Cite® 120 Fluorescence Illumination System*) and were captured with the *Nikon Digital Camera DXM-1200C*. That was connected to a PC with the *NIS-Elements BR 2.30 Software* to view the pictures. Slides that were used for measurements of infarct size and scar thickness were viewed on the *Eclipse E1000M Microscope* and captured with the *Nikon Digital Camera DXM-1200*, using a 0.5x magnification lens.

5.3.1.8 Measurements of infarct size and scar thickness

Both infarct size and scar thickness were calculated based on quantitative histomorphometric analyses of Masson Trichrome-stained slides. The data was derived from midline length measurements of all four sections of the heart according to Takagawa *et al.* [480].

Thus, the left ventricular myocardial midline was drawn at the centre between the epicardial and endocardial surfaces, using the *VIS - Visiopharm Integrator Systems*. The length of the midline was measured as midline circumference. The section of the midline, where the infarct took up more than 50% of the whole thickness of the myocardial wall was defined as midline infarct length. Dividing the sum of midline infarct lengths of all four sections by the sum of midline circumferences of all four sections and multiplying that by 100 determined the infarct size.

Measurements of the scar thickness were taken in 1mm intervals within the area in which the scar took up more than 50% of the thickness of the myocardial wall. The values were added and divided by the number of measurements in order to calculate the average thickness of the scar. Measurements of both the infarct size as well as the scar thickness were carried out blinded.

5.3.2 Quantification of lead

5.3.2.1 Attachment of lead to PEG hydrogels

For lead acetate loaded gels that were 10% (m/v) concentration, 40µl 10nPEG-4SH solution (250 mg/ml in Hepes) was incubated with 4.8µl lead acetate solution (40mg/ml in H_2O) for 60 minutes at 25°C. After incubation, 40µl 20PEG-8VS solution (250 mg/ml in Hepes) was added and the volume adjusted to 100µl. Gels were placed in 5ml H_2O and aliquots taken at selected times to determine binding of lead within the PEG gels.

5.3.2.2 Analysis of lead extraction from the hearts

Excised hearts were lyophilized for one day. The dried hearts were then placed in 10ml of a solution containing equal parts of nitric acid and hydrogen peroxide and shaken at 100rpm at 37°C for 24 hours in a closed 50ml Falcon tube. Subsequently the hearts were incubated at 60°C for two days until complete hydrolysis of the heart was observed and a clear pale yellow liquid obtained. Lead content of samples was assayed on an *XSeries II ICP-MS*. Samples were diluted 100 times using a "lab" solution (5% HNO_3 in which were added four internal standards - Bi, In, Re, Rh at a concentration of 10ppb). Calibration of the instrument was done with three standards made from artificial standard solutions.

5.3.3 Visualization of corrosion cast

The explanted hearts were treated with 10% KOH, then rinsed, dried, coated with gold and observed under a scanning electron microscope (SEM).

5.4 Utilization of MMP-1 degradable PEG hydrogels for controlled local drug release

5.4.1 Incorporation of dexamethasone into PEG hydrogels

Dexamethasone was dissolved in Tetrahydrofurane (THF, 5mmol in 200ml), mixed with 10mmol TEA and acryloyl chloride (C_3H_3ClO, 10mmol) was dropwise added. The solution was allowed to react overnight at room temperature before being purified by precipitation into cold deionised water.

Pegylated dexamethasone (dex_{PEG}) was manufactured by adding the acrylated dexamethasone (dex_{Ac}, 10mg in 200µl ethanol) dropwise to 2nPEG-2SH solution (45mg in 300µl iPBS), while stirring. The reaction proceeded for 24 hours at 37°C and more ethanol was added to achieve a final ethanol concentration of 80%. Unreacted dex_{Ac} was removed by two consecutive precipitations in 15ml cold ether, centrifugation and drying.

5.4.2 Dexamethasone elution

For covalently bound dexamethasone, 10mg 20PEG-8VS (non-degradable) or alternatively 10mg 20PEG-8Ac (degradable) in 50µl iPBS were crosslinked with 3.2mg 2nPEG-2SH in 25µl iPBS and 1.78mg dex_{PEG} in 25µl iPBS. PEG hydrogels with trapped dexamethasone were produced by crosslinking 10mg 20PEG-8VS or alternatively 20PEG-8Ac dissolved in 50µl iPBS with 4mg 2nPEG-2SH in 25µl iPBS and adding 0.150mg dexamethasone in 25µl iPBS. The solutions were vortex-mixed and three discs per group, each with a total volume of 100µl, were formed. Once prepolymer and crosslinker had polymerized completely, the hydrogel discs were incubated at 37°C in individual tubes, filled with 500µl iPBS.

At set time points, the eluate of each sample was removed and replaced with fresh iPBS.

UV absorbance of dexamethasone was measured on the *UV-1601PC* spectrophotometer at 241.8nm and was used to calculate the amount of dexamethasone (see Equation 3):

$$conc = \frac{absorbance}{m} \qquad m = 44.056$$

$$(m = slope\ of\ calibration\ curve)$$

$$mass_{\text{(of dex released from gel)}} = conc_{\text{(of dex in the eluate)}}\ x\ volume_{\text{(of eluate)}}$$

Eq. 3: Calculation of released dexamethasone

Chemical degradation of PEG was achieved by adding sodium hydroxide to the hydrogels.

The eluates of these four groups were also used to confirm the activity of dexamethasone as described under 5.4.3.

In a second experiment, the influence of different dexamethasone dosages as well as varying surface areas of the hydrogels on the rate of drug elution was tested. Two groups were compared: 10mg 20PEG-8VS in 50µl iPBS crosslinked with 4mg 2dPEG-2SH in 25µl iPBS and 0.5mg dexamethasone in 25µl iPBS added as well as 10mg 20PEG-8VS in 50µl iPBS crosslinked with 4mg 2dPEG-2SH in 25µl iPBS and 0.150mg dexamethasone in 25µl iPBS added.

After the solutions were vortex mixed, discs with a total volume of 100µl were formed. Three gels of each group were shaped as droplets, three were compressed in between two glass slides during polymerization to increase their surface area. The hydrogel discs were incubated at 37ºC in individual tubes, each containing 500µl iPBS. Dexamethasone elution was measured as described above.

5.4.3 Activity of dexamethasone eluted from PEG hydrogels

The human mammary gland cell line MDA-kb2, sourced from the *American Type Culture Collection (ATCC)* was used to determine the activity of dexamethasone, which was eluted from the discs into the iPBS.

MDA-kb2 expresses firefly luciferase under control of the MMTV (mouse mammary tumor virus) promoter that contains response elements for both glucocorticoid receptors (GR) and androgen receptors (AR). Luciferase was subsequently quantified with the *ONE-Glo™ Luciferase Assay System*. Using a *96-well Cell Culture Plate*, each well contained 10^4 MDA-kb2 cells and 100µl Leibovitz medium. After 4h medium was replaced by 90µl fresh medium plus 10µl of the eluate and then incubated overnight. 100µl of the reconstituted *ONE-Glo™* reagent (one bottle of *ONE-Glo™ Buffer* thoroughly mixed with one bottle of *ONE-Glo™ Substrate*) was added and the luminescence was measured using the *Veritas Microplate Luminometer*.

The dexamethasone activity was expressed as a fold increase, normalized to eluates from gels containing no dexamethasone after background correction (all reagents but no cells).

5.4.4 *In vivo* assessment

For *in vivo* assessment of dexamethasone elution from PEG hydrogels, animals were operated on as described under 5.2.2.3 and 5.2.2.4. However, immediately after infarct induction, animals were randomized to receive 100µl of one of the following solutions, to be injected into the infarcted myocardium:

4µl dexamethasone$_{150}$ solution (37.5µg dexamethasone in 1µl DMSO) in 96µl iPBS; 4µl dexamethasone$_{500}$ solution (125µg dexamethasone in 1µl DMSO) in 96µl iPBS; 10mg 20PEG-8VS in 25µl iPBS crosslinked with 3.45mg MMP-1s in 75µl iPBS and 4µl 4µl dexamethasone$_{150}$ solution; 10mg 20PEG-8VS in 25µl iPBS crosslinked with 3.45mg MMP-1s in 75µl iPBS and 4µl dexamethasone$_{500}$ solution; 10mg 20PEG-8VS in 50µl iPBS crosslinked with 3.2mg 2nPEG-2SH in 25µl iPBS and 1.78mg dex$_{PEG}$ in 25µl iPBS as well as saline as control.

To evaluate the amount of dexamethasone that was eluted from the PEG hydrogels, blood samples were taken from the tail vein, starting at 2h post-MI, followed by collections every 24h. After the samples were spun for 15min at 3200rpm and 4°C, the plasma was stored at -20°C for subsequent analyses.

Cardiac function was assessed using echocardiography before the animals were killed for histological and histomorphometric analyses of the explanted hearts as described under 5.2.3 and 5.3.1.

5.4.5 Dexamethasone quantification

Blood samples were analyzed using a liquid chromatographic tandem mass spectrometric (LC-MS/MS) assay.

The samples were processed with a protein precipitation extraction method, using 50µl plasma and 150µl acetonitrile. The internal standard used, was 4-androstene-3,17-dione, and was spiked into the precipitation solvent at a concentration of 200ng/ml. The plasma samples with the precipitation solvent were vortex mixed for 1min, ultra-sonicated for 5min, and centrifuged at 13000 rpm for 5min. A 100µl of the supernatant was transferred to a 96 well plate and 10µl was injected onto the HPLC column. Gradient chromatography was performed on a Gemini-NX analytical column, using acetonitrile and 0.1% formic acid as mobile phase, and was delivered at a flow rate of 500µl/min.

An AB Sciex API 3200 mass spectrometer was operated at unit resolution in the multiple reaction monitoring (MRM) mode, monitoring the transition of the protonated molecular ions at m/z 393.3 to the product ions at m/z 355.3 for dexamethasone, and also monitoring the protonated molecular ions at m/z 287.3 to the product ions at m/z 97.1 for the internal standard. The accuracies (%Nom) for the dexamethasone calibration standards were between 95.6% and 102.7%. The precision (%CV) for the dexamethasone calibration standards was between 0.3% and 14.5% for the entire calibration range. The calibration range used for sample analysis was between 78.0ng/ml and 1250ng/ml.

5.5 Determining the ability of PEG hydrogels with tethered dexamethasone to prolong cardiac gene expression when delivered in conjunction with adenovirus

5.5.1 *In vitro* preparation

To test whether PEG hydrogels can be used to advance viral vector delivery, Adv-AcGFP-HCN4t-M2-final, provided by Medtronic, Inc., was incorporated into a 10% 20PEG-8VS hydrogel, crosslinked with MMP-1s (total volume of 100µl), to be injected intramyocardially with and without dexamethasone. The dexamethasone content was 150µg and was the acrylated form that covalently attached to the hydrogel via a hydrolytically degradable linkage.

5.5.2 *In vivo* procedure

Ten rats were operated on as described in chapter 5.2.2.3 and 5.2.2.4, however no myocardial infarction was induced. After pericardiotomy the rats were randomized to receive $1.5x10^9$pfu of either Adv preparation, hence there were five replicates per group. The experiment was terminated after one week as described in chapter 5.2.4

5.5.3 Analysis

Image analysis was carried out on stitched images derived from the Nikon 90i using the analysis software Visiopharm.

For analysis of GFP, the entire cross section was captured where GFP expression was observed. Similarly for tissue damage assessment from H&E sections.

For macrophages and T-lymphocytes, the intensity of the fluorescent label did not allow for the use of low magnification objectives and thus the microscope was unable to stitch entire cross sections. Therefore a blinded observer captured 3.2mm^2 (3x3 fields) representative regions. The software identified all fluorescent cells accurately and precisely.

5.6 Statistical analyses

Animal studies were randomized and blinded. Comparison between the groups was made by means of 1-way ANOVA (STATISTICA), followed by Fisher's PLSD test. Statistical significance was defined at $p \leq 0.05$. All date are expressed as means ± SEM.

5.7 Reagents and equipment

Table 11: Reagents

Product	Producer	Product No.
Acetonitrile LiChrosolv®	Merck kGaA Darmstadt, Germany	100029
Acid Fuchsin	Merck KGaA Darmstadt, Germany	105231
Acryloyl chloride (C_3H_3ClO)	Merck KGaA Darmstadt, Germany	800826
Alexa Fluor® 660 C_2-maleimide	Invitrogen Molecular Probes® Eugene, Oregon, USA	A-20343
Alexa Fluor® 488 goat anti-rabbit IgG	Invitrogen Molecular Probes® Eugene, Oregon, USA	A-11034
Aluminum potassium sulfate ($AlK(SO_4)_2$)	Saarchem Merck Chemicals (Pty) Ltd Gauteng, South Africa	SAAR1118000EM
4-Androstene-3,17-dione	Sigma-Aldrich® Chemie GmbH Steinheim, Germany	A9630
Bovine serum albumin (BSA), IgG-Free, Protease-Free	Jackson ImmunoResearch Laboratories, Inc. West Grove, PA, USA	001-000-162
Chloral hydrate ($C_2H_3Cl_3O_2$)	Saarchem Merck Chemicals (Pty) Ltd Gauteng, South Africa	SAAR1591500EM
Citric acid ($C_6H_8O_7$)	Saarchem Merck Chemicals (Pty) Ltd Gauteng, South Africa	SAAR1605020EM
Dexamethasone	Sigma-Aldrich® Chemie GmbH Steinheim, Germany	D1756
Dichloromethane (DCM)	Sigma-Aldrich® Chemie GmbH Steinheim, Germany	270997
Diethyl ether	Sigma-Aldrich® Chemie GmbH Steinheim, Germany	32208

Product	Producer	Product No.
Dimethyl sulfoxide (DMSO)	Sigma-Aldrich® Chemie GmbH Steinheim, Germany	D2650
Dithiothreitol (DTT)	Sigma-Aldrich® Chemie GmbH Steinheim, Germany	D9779
Divinyl sulfone ($C_4H_6O_2S$)	Sigma-Aldrich® Chemie GmbH Steinheim, Germany	V3700
Donkey Anti-Mouse IgG (H+L), Cy3	Jackson ImmunoResearch Laboratories, Inc. West Grove, PA, USA	715-166-151
ED1 mouse anti rat CD68 Monoclonal Antibody	AbD serotec Oxford, UK	MCA341R
Entellan®	Merck KGaA Darmstadt, Germany	107961
Eosin Y	BDH Ltd. Poole, UK	341972Q
Euthapent	Kyron Laboratories Johannesburg, South Africa	-
Ethyl Alcohol (C_2H_5OH)	Illovo Sugar Ltd. Durban, South Africa	500
Formaldehyde (35-40%)	Radchem, Brackendowns, South Africa	F1666X
Formic acid	Sigma-Aldrich® Chemie GmbH Steinheim, Germany	F0507
Glacial acetic acid (CH_3COOH)	Radchem Brackendowns, South Africa	A1034X
Haematoxylin	Saarchem Merck Chemicals (Pty) Ltd Gauteng, South Africa	SAAR2822000CB
Halothane	Safeline Pharmaceuticals (Pty) Ltd. Johannesburg, South Africa	-
Histosec® Pastillen	Merck KGaA Darmstadt, Germany	111609

Product	Producer	Product No.
Hepes Buffer 100mM	Sigma-Aldrich® Chemie GmbH Steinheim, Germany	H-4034
Hydrochloric acid (HCl)	BDH Poole, England	103076P
Hydrogen peroxide (H_2O_2)	Sigma-Aldrich® Chemie GmbH Steinheim, Germany	216763
Isofor (Isoflurane) 250ml	Safeline Pharmaceuticals (Pty) Ltd. Johannesburg, South Africa	_
JB-4 Embedding solution A	Polysciences, Inc. Warrington, PA, USA	0226A
JB-4 Embedding solution B	Polysciences, Inc. Warrington, PA, USA	0226B
JB-4 Catalyst	Polysciences, Inc. Warrington, PA, USA	02618
Lead II acetate trihydrate	Sigma-Aldrich® Chemie GmbH Steinheim, Germany	316512
Leibovitz medium	Sigma-Aldrich® Chemie GmbH Steinheim, Germany	L4386
Light Green SF Yellowish	Sigma-Aldrich® Chemie GmbH Steinheim, Germany	L1886
Liquid nitrogen	Air Liquide South Africa	_
Marking Dye for Tissue	Polysciences, Inc. Warrington, PA, USA	24109 Red 24110 Green 24111 Blue 24112 Yellow
MDA-kb2	American Type Culture Collection Manassas, VA, USA	CRL-2713
Medical Oxygen	Afrox Cape Town, South Africa	-
MMP-1s (Peptide sequence GCREGPQGIWGQERCG)	GenScript USA, Inc. Piscataway, NJ, USA	60151-1

Product	Producer	Product No.
Neutrophil Elastase antibody	abcam Cambridge, MA, USA	ab21595
Nitric acid (HNO_3) (AR 67%)	Sigam-Aldrich ® Chemie GmbH Steinheim, Germany	38270
OCT Medium	Medite Burgdorf, Germany	–
ONE-Glo Luciferase Assay System	Promega Madison, WI, USA	E6110
Paraformaldehyde, powder, 95%	Sigam-Aldrich ® Chemie GmbH Steinheim, Germany	158127
Phloxine B	Merck KGaA Darmstadt, Germany	115926
Phosphomolybdic acid hydrate	Sigma-Aldrich® Chemie GmbH Steinheim, Germany	P7390
Picric acid solution (saturated aqueous)	Sigma-Aldrich® Chemie GmbH Steinheim, Germany	80456
Polyethylene glycol 20PEG-8OH	The Shearwater Group Inc. Dallas, TX, USA	0J000P08
Polyethylene glycol 2nPEG-2SH	Creative PEGWorks Winston Salem, NC, USA	PSB-613
Polyethylene glycol 10nPEG-4SH	Creative PEGWorks Winston Salem, NC, USA	PSB-441
Potassium chloride (KCl)	Saarchem Merck Chemicals (Pty) Ltd Gauteng, South Africa	SAAR5042020EM
Potassium hydroxide (KOH)	Sigma-Aldrich® Chemie GmbH Steinheim, Germany	P5958
Povidone Iodine Solution (10%)	Dismed Pharma (Pty) Ltd. Gauteng, South Africa	–
Proteinase K	Dako Denmark A/S Glostrup, Denmark	S3020
Sodium chloride (NaCl)	Sigma-Aldrich® Chemie GmbH Steinheim, Germany	S7653

Product	Producer	Product No.
Sodium chloride 0.9% 1000ml	Adcock Ingram Critical Care Johannesburg, South Africa	AFB 1324
Sodium hydride (NaH)	Sigma-Aldrich® Chemie GmbH Steinheim, Germany	71620
Sodium hydroxide (NaOH)	Sigma-Aldrich® Chemie GmbH Steinheim, Germany	S8045
Sodium iodate ($NaIO_3$)	Merck KGaA Darmstadt, Germany	106525
Sodium phosphate dibasic dodecahydrate ($Na_2HPO_4.12H_2O$)	Sigma-Aldrich® Chemie GmbH Steinheim, Germany	71649
Sodium phosphate monobasic monohydrate ($NaH_2PO_4.1H_2O$)	Sigma-Aldrich® Chemie GmbH Steinheim, Germany	S9638
Temgesic® (Buprenorphine)	Schering-Plough Woodmead, South Africa	-
Tetrahydrofurane (THF)	Sigma-Aldrich® Chemie GmbH Steinheim, Germany	178810
Triethylamine (TEA)	Sigma-Aldrich® Chemie GmbH Steinheim, Germany	471283
Tris base (Tris hydroxymethyl amino methane)	Merck KGaA Darmstadt, Germany	1.08382.0500
Trizma® hydrochloride	Sigma-Aldrich® Chemie GmbH Steinheim, Germany	T5941
VECTASHIELD® Mounting Medium with DAPI	Vector Laboratories, Inc. Burlingame, CA, USA	H-1200
Xylene	Saarchem Merck Chemicals (Pty) Ltd Gauteng, South Africa	SAAR7221120LC

Table 12: Equipment

Product	Producer	Product No.
Accu-Edge® Disposable Microtome Blades	Sakura Finetek USA, Inc. Torrance, CA, USA	4689
ACUSON Sequoia 512	Siemens AG Erlangen, Germany	_
Alcohol Prep Pads Kendall WEBCOL	Tyco Healthcare (Pty) Ltd. Gauteng, South Africa	16818
Alm Retractor – 4cm Spread 5.5mm Teeth	Fine Science Tools Inc. Heidelberg, Germany	17008-07
API 3200™	AB Sciex Johannesburg, South Africa	_
Axel Johnson Lab System HP-3	Kunz Instruments AB Nynäshamn, Sweden	205100
Baby-Mixter Haemostat – Curved 14cm	Fine Science Tools Inc. Heidelberg, Germany	13013-14
BD Micro-Fine + Demi	BD Becton Dickinson Franklin Lakes, NJ, USA	320829
Cages	Tecniplast Buguggiate, Italy	Type III H: 1291H Type IV: 1354G
Carbon Steel Blades Size 23	Surgical Blades CE South Africa	0197
Castroviejo Needle Holder – w/Lock Tungsten Carbide 14cm	Fine Science Tools Inc. Heidelberg, Germany	12565-14
Catheter, 16G (57mm) Introcan	B. Braun Melsungen AG Melsungen, Germany	4252160B
CO_2 absorber Omnicon f/air	A.M. Bickford, Inc. Wales Center, NY, USA	80120
Cotton Swabs	Hallowell EMC Pittsfield, MA, USA	210A3832A
Cryostat Microtome	Microm Heidelberg Walldorf, Germany	_

Product	Producer	Product No.
Deltaphase® Operating Board and 2 pads	Braintree Scientific, Inc. Braintree, MA, USA	39OP
Eclipse 90i Microscope	Nikon Corporation Tokyo, Japan	_
Eclipse E1000M Microscope	Nikon Corporation Tokyo, Japan	_
Embedding Mould 16x8mm	Taab, Ltd. Aldermaston, UK	E080
Embedding Stubs	Taab, Ltd. Aldermaston, UK	E081
Eppendorf tubes	Eppendorf AG Hamburg, Germany	_
Falcon tubes (50ml)	BD Biosciences Franklin Lakes, NJ, USA	_
Gauze Swabs	GMS Cape Town, South Africa	AM7508
Gemini NX 5u, C18, 110A, 50 x 2mm	Phenomenex Torrance, CA, USA	_
Glass knife 406mm x 25mm x 8mm	Agar Scientific Ltd. Stansted, UK	G3516
Gloves, sterile	sempermed Vienna, Austria	8260 54620
Graefe Forceps - 0.8mm Tips Straight	Fine Science Tools Inc. Heidelberg, Germany	11050-10
Graefe Forceps - 0.8mm Tips Slight Curve	Fine Science Tools Inc. Heidelberg, Germany	11051-10
Harvard Small Animal Ventilator Model 683	Harvard Apparatus Holliston, MA, USA	550000
Hot bead sterilizer Steri 250	Simon Keller AG Burgdorf, Switzerland	31100
Incisor Loop	Hallowell EMC Pittsfield, MA, USA	210A3490A

Product	Producer	Product No.
Incubator	Heraeus Hanau, Germany	_
Induction chamber	Stoelting Co. Wood Dale, IL, USA	50216
Infraphil R95E Infrared lamp	Royal Philips Electronics Amsterdam, The Netherlands	_
Injekt® 10ml	B. Braun Melsungen AG Melsungen, Germany	4606108V
Metzenbaum Scissors – Curved 14.5cm	Fine Science Tools Inc. Heidelberg, Germany	14017-14
Microm Tissue Microtome HM 360	Thermo Scientific Walldorf, Germany	Serial number 6832
Microscope cover glasses 22x40mm	Marienfeld GmbH & Co.KG Lauda-Königshofen, Germany	01 011 22
Microscope glass slides 76x26x1mm	Marienfeld GmbH & Co.KG Lauda-Königshofen, Germany	08 100 00 and 10 016 12
Mirror for Intubation Verification	Hallowell EMC Pittsfield, MA, USA	200A3683
Nikon Digital Camera DXM-1200 and -1200C	Nikon Corporation Tokyo, Japan	_
NIS-Elements BR 2.30	Nikon Instruments Inc. Melville, NY, USA	_
Omnican® 100	B. Braun Melsungen AG Melsungen, Germany	9151141S
Otoscope, Welch Allyn Li-Ion with operation Head	Hallowell EMC Pittsfield, MA, USA	000A3756
Pipettes	Gilson, Inc. Middleton, WI, USA	_
Rat and Mice Feed 16%	Afresh Vention (Pty) Ltd Durbanville, South Africa	_
Rat ET Tube Introducer	Hallowell EMC Pittsfield, MA, USA	210A3492

Product	Producer	Product No.
Rat Specula	Hallowell EMC Pittsfield, MA, USA	200A3588
Rodent Anesthesia Circuit Mask	Harvard Apparatus Holliston, MA, USA	723026
Scale	Sartorius GmbH Göttingen, Germany	PT1200
SEM JSM-5200	Jeol Ltd. Tokyo, Japan	_
Shandon Histocentre 2	Shandon Southern Products Ltd. Astmoore, England	Serial number 64000011
Simpleware	Simpleware Ltd. Exeter, UK	_
Spring Scissors 8mm	Fine Science Tools Inc. Heidelberg, Germany	15025-10
Student Adson Forceps	Fine Science Tools Inc. Heidelberg, Germany	91106-12
Student Adson Tissue Forceps – 1x2 Teeth	Fine Science Tools Inc. Heidelberg, Germany	91127-12
Terumo needle 23G x 1¼”	Terumo Medical Corporation Tokyo, Japan	_
Tilting WorkStand, Rodent	Hallowell EMC Pittsfield, MA, USA	000A3467
Tissue Floating Bath TFB 45	MEDITE® GmbH Burgdorf, Germany	_
Tissue-Tek® Rotary Tissue Processor	Sakura Finetek Tokyo, Japan	4634
Transducer 15L8	Siemens AG Erlangen, Germany	_
Ultrasonic	Integral Systems	_
UV-1601PC	Shimadzu Kyoto, Japan	_

Product	Producer	Product No.
Vaporizer Modell 100	SurgiVet Wankesha, WI, USA	V720100
Veritas Microplate Luminometer	Turner Biosystems	_
VIS - Visiopharm Integrator System Version 2.12.3.0	Visiopharm Hørsholm, Denmark	_
Vortex Genie® 2	Scientific Industries, Inc. Bohemia, NY, USA	SI-0256
X-Cite® 120 Fluorescence Illumination System	EXFO Life Sciences Division Ontario, Canada	Serial number X120-01517
XSeries II ICP-MS	Thermo Fisher Scientific	_
2-0 Ethibond Excel Polyester Suture	Johnson & Johnson (Pty) Ltd Midrand, South Africa	X937
4-0 Mersilk Non-absorbable silk	Johnson & Johnson (Ptd) Ltd Brussels, Belgium	W505
6-0 Ethicon Prolene™ Polypropylene Sutures	Ethicon Inc. Somerville, NJ, USA	M8706
96-well Cell Culture Plate	Nunc A/S Roskilde, Denmark	165306

6 References

1. Lloyd-Jones, D., et al., *Heart disease and stroke statistics--2010 update: a report from the American Heart Association.* Circulation. **121**(7): p. e46-e215.
2. Hsiao, C.J., et al., *National Ambulatory Medical Care Survey: 2007 summary.* Natl Health Stat Report, (27): p. 1-32.
3. Niska, R., F. Bhuiya, and J. Xu, *National Hospital Ambulatory Medical Care Survey: 2007 emergency department summary.* Natl Health Stat Report, (26): p. 1-31.
4. Thom, T., *Hurst's the Heart*. 10 ed. 2001, New York.
5. Roger, V.L., et al., *Heart disease and stroke statistics--2011 update: a report from the American Heart Association.* Circulation. **123**(4): p. e18-e209.
6. Lloyd-Jones, D., et al., *Heart disease and stroke statistics--2009 update: a report from the American Heart Association Statistics Committee and Stroke Statistics Subcommittee.* Circulation, 2009. **119**(3): p. e21-181.
7. WHO, *Cardiovascular diseases (CVDs), Fact sheet No 317.* 2011.
8. WHO, *The Global Burden of Disease: 2004 Update.* 2008.
9. Lenfant, C., *Can we prevent cardiovascular diseases in low- and middle-income countries?* Bull World Health Organ, 2001. **79**(10): p. 980-2; discussion 983-7.
10. WHO, *The Atlas of Heart Disease and Stroke.* 2004.
11. Yusuf, S., et al., *Effect of potentially modifiable risk factors associated with myocardial infarction in 52 countries (the INTERHEART study): case-control study.* Lancet, 2004. **364**(9438): p. 937-52.
12. Wild, S., et al., *Global prevalence of diabetes: estimates for the year 2000 and projections for 2030.* Diabetes Care, 2004. **27**(5): p. 1047-53.
13. *Trends in cholesterol screening and awareness of high blood cholesterol--United States, 1991-2003.* MMWR Morb Mortal Wkly Rep, 2005. **54**(35): p. 865-70.
14. AHA, *Statistical Fact Sheet, 2009 Update* 2009.
15. Goldenberg, I., et al., *Current smoking, smoking cessation, and the risk of sudden cardiac death in patients with coronary artery disease.* Arch Intern Med, 2003. **163**(19): p. 2301-5.
16. Pate, R.R., et al., *Physical activity and public health. A recommendation from the Centers for Disease Control and Prevention and the American College of Sports Medicine.* JAMA, 1995. **273**(5): p. 402-7.
17. Shaw, K., et al., *Exercise for overweight or obesity.* Cochrane Database Syst Rev, 2006(4): p. CD003817.
18. Daniels, S.R., et al., *American Heart Association Childhood Obesity Research Summit: executive summary.* Circulation, 2009. **119**(15): p. 2114-23.

19. Lloyd-Jones, D.M., et al., *Parental cardiovascular disease as a risk factor for cardiovascular disease in middle-aged adults: a prospective study of parents and offspring.* JAMA, 2004. **291**(18): p. 2204-11.
20. Murabito, J.M., et al., *Sibling cardiovascular disease as a risk factor for cardiovascular disease in middle-aged adults.* JAMA, 2005. **294**(24): p. 3117-23.
21. Lee, D.S., et al., *Association of parental heart failure with risk of heart failure in offspring.* N Engl J Med, 2006. **355**(2): p. 138-47.
22. Friedlander, Y., et al., *Sudden death and myocardial infarction in first degree relatives as predictors of primary cardiac arrest.* Atherosclerosis, 2002. **162**(1): p. 211-6.
23. Parikh, N.I., et al., *Parental occurrence of premature cardiovascular disease predicts increased coronary artery and abdominal aortic calcification in the Framingham Offspring and Third Generation cohorts.* Circulation, 2007. **116**(13): p. 1473-81.
24. Nasir, K., et al., *Family history of premature coronary heart disease and coronary artery calcification: Multi-Ethnic Study of Atherosclerosis (MESA).* Circulation, 2007. **116**(6): p. 619-26.
25. Lusis, A.J., *Atherosclerosis.* Nature, 2000. **407**(6801): p. 233-41.
26. Ross, R. and J.A. Glomset, *Atherosclerosis and the arterial smooth muscle cell: Proliferation of smooth muscle is a key event in the genesis of the lesions of atherosclerosis.* Science, 1973. **180**(93): p. 1332-9.
27. Ross, R. and J.A. Glomset, *The pathogenesis of atherosclerosis (second of two parts).* N Engl J Med, 1976. **295**(8): p. 420-5.
28. Ross, R. and J.A. Glomset, *The pathogenesis of atherosclerosis (first of two parts).* N Engl J Med, 1976. **295**(7): p. 369-77.
29. Mitchell, R.S.K., V.; Abbas, A. K., Fausto, N., *Robbins Basic Pathology: With STUDENT CONSULT Online Access.* 8th edition ed. 2007.
30. Ross, R., *The pathogenesis of atherosclerosis: a perspective for the 1990s.* Nature, 1993. **362**(6423): p. 801-9.
31. Faggiotto, A. and R. Ross, *Studies of hypercholesterolemia in the nonhuman primate. II. Fatty streak conversion to fibrous plaque.* Arteriosclerosis, 1984. **4**(4): p. 341-56.
32. Faggiotto, A., R. Ross, and L. Harker, *Studies of hypercholesterolemia in the nonhuman primate. I. Changes that lead to fatty streak formation.* Arteriosclerosis, 1984. **4**(4): p. 323-40.
33. Masuda, J. and R. Ross, *Atherogenesis during low level hypercholesterolemia in the nonhuman primate. II. Fatty streak conversion to fibrous plaque.* Arteriosclerosis, 1990. **10**(2): p. 178-87.
34. Masuda, J. and R. Ross, *Atherogenesis during low level hypercholesterolemia in the nonhuman primate. I. Fatty streak formation.* Arteriosclerosis, 1990. **10**(2): p. 164-77.
35. Rosenfeld, M.E., et al., *Fatty streak expansion and maturation in Watanabe Heritable Hyperlipemic and comparably hypercholesterolemic fat-fed rabbits.* Arteriosclerosis, 1987. **7**(1): p. 24-34.
36. Rosenfeld, M.E., et al., *Fatty streak initiation in Watanabe Heritable Hyperlipemic and comparably hypercholesterolemic fat-fed rabbits.* Arteriosclerosis, 1987. **7**(1): p. 9-23.
37. Glagov, S., et al., *Compensatory enlargement of human atherosclerotic coronary arteries.* N Engl J Med, 1987. **316**(22): p. 1371-5.

38. Libby, P., *Cytokines and growth regulatory molecules*, in *Atheroscerosis and coronary artery disease*, V. Fuster, Editor. 1996, Philadelphia: Lippincott-Raven. p. 585-94.
39. Raines, E.W., *The role of macrophages* in *Atherosclerosis and coronary artery disease*, V. Fuster, Editor. 1996, Philadelphia: Lippincott-Raven. p. 539-55.
40. Falk, E., *Pathogenesis of plaque disruption*, in *Atherosclerosis and coronary artery disease*, V. Fuster, Editor. 1996, Philadelphia: Lippincott-Raven. p. 492-510.
41. Ross, R., *Atherosclerosis--an inflammatory disease.* N Engl J Med, 1999. **340**(2): p. 115-26.
42. Tobin, K.J., *Stable angina pectoris: what does the current clinical evidence tell us?* J Am Osteopath Assoc. **110**(7): p. 364-70.
43. Hombach, V., et al., *Pathophysiology of unstable angina pectoris--correlations with coronary angioscopic imaging.* Eur Heart J, 1988. **9 Suppl N**: p. 40-5.
44. Patel, D.J., et al., *Pathophysiology of transient myocardial ischemia in acute coronary syndromes. Characterization by continuous ST-segment monitoring.* Circulation, 1997. **95**(5): p. 1185-92.
45. Kumar, A. and C.P. Cannon, *Acute coronary syndromes: diagnosis and management, part I.* Mayo Clin Proc, 2009. **84**(10): p. 917-38.
46. Fenton, D., *Myocardial infarction*. 2010, eMedicine (retrieved Mar 26, 2011).
47. Canto, J.G., et al., *Prevalence, clinical characteristics, and mortality among patients with myocardial infarction presenting without chest pain.* JAMA, 2000. **283**(24): p. 3223-9.
48. Alexander, K.P., et al., *Acute coronary care in the elderly, part II: ST-segment-elevation myocardial infarction: a scientific statement for healthcare professionals from the American Heart Association Council on Clinical Cardiology: in collaboration with the Society of Geriatric Cardiology.* Circulation, 2007. **115**(19): p. 2570-89.
49. Boland, L.L., et al., *Occurrence of unrecognized myocardial infarction in subjects aged 45 to 65 years (the ARIC study).* Am J Cardiol, 2002. **90**(9): p. 927-31.
50. Grech, E.D. and D.R. Ramsdale, *Acute coronary syndrome: unstable angina and non-ST segment elevation myocardial infarction.* BMJ, 2003. **326**(7401): p. 1259-61.
51. *2005 American Heart Association Guidelines for Cardiopulmonary Resuscitation and Emergency Cardiovascular Care.* Circulation, 2005. **112**(24 Suppl): p. IV1-203.
52. Braunwald, E., et al., *ACC/AHA 2002 guideline update for the management of patients with unstable angina and non-ST-segment elevation myocardial infarction--summary article: a report of the American College of Cardiology/American Heart Association task force on practice guidelines (Committee on the Management of Patients With Unstable Angina).* J Am Coll Cardiol, 2002. **40**(7): p. 1366-74.
53. Anderson, J.L., et al., *ACC/AHA 2007 guidelines for the management of patients with unstable angina/non-ST-Elevation myocardial infarction: a report of the American College of Cardiology/American Heart Association Task Force on Practice Guidelines (Writing Committee to Revise the 2002 Guidelines for the Management of Patients With Unstable Angina/Non-ST-*

Elevation Myocardial Infarction) developed in collaboration with the American College of Emergency Physicians, the Society for Cardiovascular Angiography and Interventions, and the Society of Thoracic Surgeons endorsed by the American Association of Cardiovascular and Pulmonary Rehabilitation and the Society for Academic Emergency Medicine. J Am Coll Cardiol, 2007. **50**(7): p. e1-e157.

54. Alpert, J.S., et al., *Myocardial infarction redefined--a consensus document of The Joint European Society of Cardiology/American College of Cardiology Committee for the redefinition of myocardial infarction.* J Am Coll Cardiol, 2000. **36**(3): p. 959-69.
55. Shih, H., et al., *The aging heart and post-infarction left ventricular remodeling.* J Am Coll Cardiol, 2010. **57**(1): p. 9-17.
56. Gaballa, M.A. and S. Goldman, *Ventricular remodeling in heart failure.* J Card Fail, 2002. **8**(6 Suppl): p. S476-85.
57. Yousef, Z.R., S.R. Redwood, and M.S. Marber, *Postinfarction left ventricular remodelling: where are the theories and trials leading us?* Heart, 2000. **83**(1): p. 76-80.
58. Holmes, J.W., T.K. Borg, and J.W. Covell, *Structure and mechanics of healing myocardial infarcts.* Annu Rev Biomed Eng, 2005. **7**: p. 223-53.
59. Neely, J.R. and L.W. Grotyohann, *Role of glycolytic products in damage to ischemic myocardium. Dissociation of adenosine triphosphate levels and recovery of function of reperfused ischemic hearts.* Circ Res, 1984. **55**(6): p. 816-24.
60. Graham, R.M., et al., *A unique pathway of cardiac myocyte death caused by hypoxia-acidosis.* J Exp Biol, 2004. **207**(Pt 18): p. 3189-200.
61. Vaughan-Jones, R.D., K.W. Spitzer, and P. Swietach, *Spatial aspects of intracellular pH regulation in heart muscle.* Prog Biophys Mol Biol, 2006. **90**(1-3): p. 207-24.
62. Bountra, C., K. Kaila, and R.D. Vaughan-Jones, *Effect of repetitive activity upon intracellular pH, sodium and contraction in sheep cardiac Purkinje fibres.* J Physiol, 1988. **398**: p. 341-60.
63. Elliott, A.C., G.L. Smith, and D.G. Allen, *The metabolic consequences of an increase in the frequency of stimulation in isolated ferret hearts.* J Physiol, 1994. **474**(1): p. 147-59.
64. Garlick, P.B., G.K. Radda, and P.J. Seeley, *Studies of acidosis in the ischaemic heart by phosphorus nuclear magnetic resonance.* Biochem J, 1979. **184**(3): p. 547-54.
65. Katz, A.M. and H.H. Hecht, *Editorial: the early "pump" failure of the ischemic heart.* Am J Med, 1969. **47**(4): p. 497-502.
66. Orchard, C.H. and H.E. Cingolani, *Acidosis and arrhythmias in cardiac muscle.* Cardiovasc Res, 1994. **28**(9): p. 1312-9.
67. Handy, J.M. and N. Soni, *Physiological effects of hyperchloraemia and acidosis.* Br J Anaesth, 2008. **101**(2): p. 141-50.
68. Sato, S., et al., *Connective tissue changes in early ischemia of porcine myocardium: an ultrastructural study.* J Mol Cell Cardiol, 1983. **15**(4): p. 261-75.
69. Caulfield, J.B., S.B. Tao, and M. Nachtigal, *Ventricular collagen matrix and alterations.* Adv Myocardiol, 1985. **5**: p. 257-69.

70. Herzog, E., et al., *Early Activation of Metalloproteinases after Experimental Myocardial Infarction Occurs in Infarct and Non-infarct Zones* Cardiovascular Pathology, 1998. **7**(6): p. 307-312.
71. Tyberg, J.V., et al., *An analysis of segmental ischemic dysfunction utilizing the pressure-length loop.* Circulation, 1974. **49**(4): p. 748-54.
72. Forrester, J.S., et al., *Early increase in left ventricular compliance after myocardial infarction.* J Clin Invest, 1972. **51**(3): p. 598-603.
73. Diamond, G. and J.S. Forrester, *Effect of coronary artery disease and acute myocardial infarction on left ventricular compliance in man.* Circulation, 1972. **45**(1): p. 11-9.
74. Zhao, M.J., et al., *Profound structural alterations of the extracellular collagen matrix in postischemic dysfunctional ("stunned") but viable myocardium.* J Am Coll Cardiol, 1987. **10**(6): p. 1322-34.
75. Whittaker, P., et al., *Stunned myocardium and myocardial collagen damage: differential effects of single and repeated occlusions.* Am Heart J, 1991. **121**(2 Pt 1): p. 434-41.
76. Allaart, C.P., P. Sipkema, and N. Westerhof, *Effect of perfusion pressure on diastolic stress-strain relations of isolated rat papillary muscle.* Am J Physiol, 1995. **268**(3 Pt 2): p. H945-54.
77. Opie, L.H., et al., *Controversies in ventricular remodelling.* Lancet, 2006. **367**(9507): p. 356-67.
78. Anversa, P., et al., *Left ventricular failure induced by myocardial infarction. I. Myocyte hypertrophy.* Am J Physiol, 1985. **248**(6 Pt 2): p. H876-82.
79. Pfeffer, M.A. and E. Braunwald, *Ventricular remodeling after myocardial infarction. Experimental observations and clinical implications.* Circulation, 1990. **81**(4): p. 1161-72.
80. McKay, R.G., et al., *Left ventricular remodeling after myocardial infarction: a corollary to infarct expansion.* Circulation, 1986. **74**(4): p. 693-702.
81. Fishbein, M.C., D. Maclean, and P.R. Maroko, *The histopathologic evolution of myocardial infarction.* Chest, 1978. **73**(6): p. 843-9.
82. Cleutjens, J.P., et al., *Regulation of collagen degradation in the rat myocardium after infarction.* J Mol Cell Cardiol, 1995. **27**(6): p. 1281-92.
83. Carlyle, W.C., et al., *Delayed reperfusion alters matrix metalloproteinase activity and fibronectin mRNA expression in the infarct zone of the ligated rat heart.* J Mol Cell Cardiol, 1997. **29**(9): p. 2451-63.
84. Tyagi, S.C., et al., *Matrix metalloproteinase activity expression in infarcted, noninfarcted and dilated cardiomyopathic human hearts.* Mol Cell Biochem, 1996. **155**(1): p. 13-21.
85. Danielsen, C.C., H. Wiggers, and H.R. Andersen, *Increased amounts of collagenase and gelatinase in porcine myocardium following ischemia and reperfusion.* J Mol Cell Cardiol, 1998. **30**(7): p. 1431-42.
86. Tyagi, S.C., et al., *Post-transcriptional regulation of extracellular matrix metalloproteinase in human heart end-stage failure secondary to ischemic cardiomyopathy.* J Mol Cell Cardiol, 1996. **28**(7): p. 1415-28.
87. Whittaker, P., D.R. Boughner, and R.A. Kloner, *Role of collagen in acute myocardial infarct expansion.* Circulation, 1991. **84**(5): p. 2123-34.
88. Kim, H.E., et al., *Disruption of the myocardial extracellular matrix leads to cardiac dysfunction.* J Clin Invest, 2000. **106**(7): p. 857-66.

89. Spinale, F.G., *Myocardial matrix remodeling and the matrix metalloproteinases: influence on cardiac form and function.* Physiol Rev, 2007. **87**(4): p. 1285-342.
90. Gunja-Smith, Z., et al., *Remodeling of human myocardial collagen in idiopathic dilated cardiomyopathy. Role of metalloproteinases and pyridinoline cross-links.* Am J Pathol, 1996. **148**(5): p. 1639-48.
91. Woodiwiss, A.J., et al., *Reduction in myocardial collagen cross-linking parallels left ventricular dilatation in rat models of systolic chamber dysfunction.* Circulation, 2001. **103**(1): p. 155-60.
92. Olivetti, G., et al., *Side-to-side slippage of myocytes participates in ventricular wall remodeling acutely after myocardial infarction in rats.* Circ Res, 1990. **67**(1): p. 23-34.
93. Salem, B.I., et al., *The potential impact of the thrombolytic era on cardiac rupture complicating acute myocardial infarction.* Angiology, 1994. **45**(11): p. 931-6.
94. Batts, K.P., D.M. Ackermann, and W.D. Edwards, *Postinfarction rupture of the left ventricular free wall: clinicopathologic correlates in 100 consecutive autopsy cases.* Hum Pathol, 1990. **21**(5): p. 530-5.
95. Shapira, I., et al., *Cardiac rupture in patients with acute myocardial infarction.* Chest, 1987. **92**(2): p. 219-23.
96. Raitt, M.H., et al., *Subacute ventricular free wall rupture complicating myocardial infarction.* Am Heart J, 1993. **126**(4): p. 946-55.
97. Birnbaum, Y., et al., *Ventricular free wall rupture following acute myocardial infarction.* Coron Artery Dis, 2003. **14**(6): p. 463-70.
98. Wehrens, X.H. and P.A. Doevendans, *Cardiac rupture complicating myocardial infarction.* Int J Cardiol, 2004. **95**(2-3): p. 285-92.
99. Becker, R.C., et al., *A composite view of cardiac rupture in the United States National Registry of Myocardial Infarction.* J Am Coll Cardiol, 1996. **27**(6): p. 1321-6.
100. Becker, R.C., et al., *Cardiac rupture associated with thrombolytic therapy: impact of time to treatment in the Late Assessment of Thrombolytic Efficacy (LATE) study.* J Am Coll Cardiol, 1995. **25**(5): p. 1063-8.
101. Kleiman, N.S., et al., *Mechanisms of early death despite thrombolytic therapy: experience from the Thrombolysis in Myocardial Infarction Phase II (TIMI II) study.* J Am Coll Cardiol, 1992. **19**(6): p. 1129-35.
102. Peuhkurinen, K.J., et al., *Thrombolytic therapy with streptokinase stimulates collagen breakdown.* Circulation, 1991. **83**(6): p. 1969-75.
103. Yasuno, M., et al., *Angiographic and pathologic evidence of hemorrhage into the myocardium after coronary reperfusion.* Angiology, 1984. **35**(12): p. 797-801.
104. Honan, M.B., et al., *Cardiac rupture, mortality and the timing of thrombolytic therapy: a meta-analysis.* J Am Coll Cardiol, 1990. **16**(2): p. 359-67.
105. Frantz, S., J. Bauersachs, and G. Ertl, *Post-infarct remodelling: contribution of wound healing and inflammation.* Cardiovasc Res, 2009. **81**(3): p. 474-81.
106. Knuefermann, P., J. Vallejo, and D.L. Mann, *The role of innate immune responses in the heart in health and disease.* Trends Cardiovasc Med, 2004. **14**(1): p. 1-7.
107. Gallucci, S., M. Lolkema, and P. Matzinger, *Natural adjuvants: endogenous activators of dendritic cells.* Nat Med, 1999. **5**(11): p. 1249-55.

108. Frangogiannis, N.G., *The mechanistic basis of infarct healing.* Antioxid Redox Signal, 2006. **8**(11-12): p. 1907-39.
109. Linde, A., et al., *Innate immunity and inflammation--New frontiers in comparative cardiovascular pathology.* Cardiovasc Res, 2007. **73**(1): p. 26-36.
110. Palojoki, E., et al., *Cardiomyocyte apoptosis and ventricular remodeling after myocardial infarction in rats.* Am J Physiol Heart Circ Physiol, 2001. **280**(6): p. H2726-31.
111. Jones, W.K., et al., *NF-kappaB as an integrator of diverse signaling pathways: the heart of myocardial signaling?* Cardiovasc Toxicol, 2003. **3**(3): p. 229-54.
112. Knowlton, A.A., et al., *Rapid expression of fibronectin in the rabbit heart after myocardial infarction with and without reperfusion.* J Clin Invest, 1992. **89**(4): p. 1060-8.
113. Ulrich, M.M., et al., *Increased expression of fibronectin isoforms after myocardial infarction in rats.* J Mol Cell Cardiol, 1997. **29**(9): p. 2533-43.
114. Morishita, N., et al., *Sequential changes in laminin and type IV collagen in the infarct zone--immunohistochemical study in rat myocardial infarction.* Jpn Circ J, 1996. **60**(2): p. 108-14.
115. Theroux, P., et al., *Regional myocardial function and dimensions early and late after myocardial infarction in the unanesthetized dog.* Circ Res, 1977. **40**(2): p. 158-65.
116. Sun, Y., et al., *Infarct scar as living tissue.* Basic Res Cardiol, 2002. **97**(5): p. 343-7.
117. Jugdutt, B.I. and R.W. Amy, *Healing after myocardial infarction in the dog: changes in infarct hydroxyproline and topography.* J Am Coll Cardiol, 1986. **7**(1): p. 91-102.
118. Reimer, K.A. and R.B. Jennings, *The changing anatomic reference base of evolving myocardial infarction. Underestimation of myocardial collateral blood flow and overestimation of experimental anatomic infarct size due to tissue edema, hemorrhage and acute inflammation.* Circulation, 1979. **60**(4): p. 866-76.
119. Choong, C.Y., et al., *Relationship of functional recovery to scar contraction after myocardial infarction in the canine left ventricle.* Am Heart J, 1989. **117**(4): p. 819-29.
120. Gibbons, E.F., et al., *The natural history of regional dysfunction in a canine preparation of chronic infarction.* Circulation, 1985. **71**(2): p. 394-402.
121. Kittleson, M.D., G.G. Knowlen, and L.E. Johnson, *Early and late global and regional left ventricular function after experimental transmural myocardial infarction: relationships of regional wall motion, wall thickening, and global performance.* Am Heart J, 1987. **114**(1 Pt 1): p. 70-8.
122. Pfeffer, M.A., et al., *Myocardial infarct size and ventricular function in rats.* Circ Res, 1979. **44**(4): p. 503-12.
123. Pfeffer, J.M., et al., *Progressive ventricular remodeling in rat with myocardial infarction.* Am J Physiol, 1991. **260**(5 Pt 2): p. H1406-14.
124. Jessup, M. and S. Brozena, *Heart failure.* N Engl J Med, 2003. **348**(20): p. 2007-18.
125. Mitchell, G.F., et al., *Left ventricular remodeling in the year after first anterior myocardial infarction: a quantitative analysis of contractile segment lengths and ventricular shape.* J Am Coll Cardiol, 1992. **19**(6): p. 1136-44.

126. Nelson, D.M., et al., *Intra-myocardial biomaterial injection therapy in the treatment of heart failure: Materials, outcomes and challenges.* Acta Biomater. **7**(1): p. 1-15.
127. Dipla, K., et al., *Myocyte recovery after mechanical circulatory support in humans with end-stage heart failure.* Circulation, 1998. **97**(23): p. 2316-22.
128. Bristow, M.R., et al., *Myocardial alpha- and beta-adrenergic receptors in heart failure: is cardiac-derived norepinephrine the regulatory signal?* Eur Heart J, 1988. **9 Suppl H**: p. 35-40.
129. Bristow, M.R., et al., *Beta 1- and beta 2-adrenergic receptor-mediated adenylate cyclase stimulation in nonfailing and failing human ventricular myocardium.* Mol Pharmacol, 1989. **35**(3): p. 295-303.
130. Brodde, O.E., et al., *Myocardial beta-adrenoceptor changes in heart failure: concomitant reduction in beta 1- and beta 2-adrenoceptor function related to the degree of heart failure in patients with mitral valve disease.* J Am Coll Cardiol, 1989. **14**(2): p. 323-31.
131. Ginsburg, R., et al., *Study of the normal and failing isolated human heart: decreased response of failing heart to isoproterenol.* Am Heart J, 1983. **106**(3): p. 535-40.
132. *Criteria Commitee of the New York Heart Association: Diseases of the Heart and Blood Vessels: Nomenclature and Criteria for Diagnosis*. 6th ed. 1964, Boston: Little Brown and Company.
133. Axford J, *Medicine*. 2nd ed. 2004: Blackwell Publishing.
134. Neubauer, S., *The failing heart--an engine out of fuel.* N Engl J Med, 2007. **356**(11): p. 1140-51.
135. Hunt, S.A., et al., *ACC/AHA 2005 Guideline Update for the Diagnosis and Management of Chronic Heart Failure in the Adult: a report of the American College of Cardiology/American Heart Association Task Force on Practice Guidelines (Writing Committee to Update the 2001 Guidelines for the Evaluation and Management of Heart Failure): developed in collaboration with the American College of Chest Physicians and the International Society for Heart and Lung Transplantation: endorsed by the Heart Rhythm Society.* Circulation, 2005. **112**(12): p. e154-235.
136. Boersma, E., et al., *Early thrombolytic treatment in acute myocardial infarction: reappraisal of the golden hour.* Lancet, 1996. **348**(9030): p. 771-5.
137. Weaver, W.D., et al., *Prehospital-initiated vs hospital-initiated thrombolytic therapy. The Myocardial Infarction Triage and Intervention Trial.* JAMA, 1993. **270**(10): p. 1211-6.
138. *Indications for fibrinolytic therapy in suspected acute myocardial infarction: collaborative overview of early mortality and major morbidity results from all randomised trials of more than 1000 patients. Fibrinolytic Therapy Trialists' (FTT) Collaborative Group.* Lancet, 1994. **343**(8893): p. 311-22.
139. Larsen, M.P., et al., *Predicting survival from out-of-hospital cardiac arrest: a graphic model.* Ann Emerg Med, 1993. **22**(11): p. 1652-8.
140. Valenzuela, T.D., et al., *Estimating effectiveness of cardiac arrest interventions: a logistic regression survival model.* Circulation, 1997. **96**(10): p. 3308-13.
141. Swor, R.A., et al., *Bystander CPR, ventricular fibrillation, and survival in witnessed, unmonitored out-of-hospital cardiac arrest.* Ann Emerg Med, 1995. **25**(6): p. 780-4.

142. Holmberg, M., S. Holmberg, and J. Herlitz, *Incidence, duration and survival of ventricular fibrillation in out-of-hospital cardiac arrest patients in sweden.* Resuscitation, 2000. **44**(1): p. 7-17.
143. Dracup, K., et al., *Acute coronary syndrome: what do patients know?* Arch Intern Med, 2008. **168**(10): p. 1049-54.
144. Baigent, C., et al., *Aspirin in the primary and secondary prevention of vascular disease: collaborative meta-analysis of individual participant data from randomised trials.* Lancet, 2009. **373**(9678): p. 1849-60.
145. *Randomised trial of intravenous streptokinase, oral aspirin, both, or neither among 17,187 cases of suspected acute myocardial infarction: ISIS-2. ISIS-2 (Second International Study of Infarct Survival) Collaborative Group.* Lancet, 1988. **2**(8607): p. 349-60.
146. Anderson, J.L., L.A. Karagounis, and R.M. Califf, *Metaanalysis of five reported studies on the relation of early coronary patency grades with mortality and outcomes after acute myocardial infarction.* Am J Cardiol, 1996. **78**(1): p. 1-8.
147. *An international randomized trial comparing four thrombolytic strategies for acute myocardial infarction. The GUSTO investigators.* N Engl J Med, 1993. **329**(10): p. 673-82.
148. Keeley, E.C., J.A. Boura, and C.L. Grines, *Primary angioplasty versus intravenous thrombolytic therapy for acute myocardial infarction: a quantitative review of 23 randomised trials.* Lancet, 2003. **361**(9351): p. 13-20.
149. Fox, K.A., et al., *Decline in rates of death and heart failure in acute coronary syndromes, 1999-2006.* JAMA, 2007. **297**(17): p. 1892-900.
150. *Effects of tissue plasminogen activator and a comparison of early invasive and conservative strategies in unstable angina and non-Q-wave myocardial infarction. Results of the TIMI IIIB Trial. Thrombolysis in Myocardial Ischemia.* Circulation, 1994. **89**(4): p. 1545-56.
151. Jeremias, A., et al., *The impact of revascularization on mortality in patients with nonacute coronary artery disease.* Am J Med, 2009. **122**(2): p. 152-61.
152. Antman, E.M., et al., *ACC/AHA guidelines for the management of patients with ST-elevation myocardial infarction: a report of the American College of Cardiology/American Heart Association Task Force on Practice Guidelines (Committee to Revise the 1999 Guidelines for the Management of Patients with Acute Myocardial Infarction).* Circulation, 2004. **110**(9): p. e82-292.
153. Antman, E.M., et al., *2007 focused update of the ACC/AHA 2004 guidelines for the management of patients with ST-elevation myocardial infarction: a report of the American College of Cardiology/American Heart Association Task Force on Practice Guidelines.* J Am Coll Cardiol, 2008. **51**(2): p. 210-47.
154. Aikawa, Y., et al., *Regional wall stress predicts ventricular remodeling after anteroseptal myocardial infarction in the Healing and Early Afterload Reducing Trial (HEART): an echocardiography-based structural analysis.* Am Heart J, 2001. **141**(2): p. 234-42.
155. Pfeffer, M.A., et al., *Effect of captopril on progressive ventricular dilatation after anterior myocardial infarction.* N Engl J Med, 1988. **319**(2): p. 80-6.
156. Pfeffer, M.A., et al., *Effect of captopril on mortality and morbidity in patients with left ventricular dysfunction after myocardial infarction. Results of the*

survival and ventricular enlargement trial. The SAVE Investigators. N Engl J Med, 1992. **327**(10): p. 669-77.
157. Pfeffer, J.M., *Progressive ventricular dilation in experimental myocardial infarction and its attenuation by angiotensin-converting enzyme inhibition.* Am J Cardiol, 1991. **68**(14): p. 17D-25D.
158. Tsoporis, J.N., et al., *S100B expression modulates left ventricular remodeling after myocardial infarction in mice.* Circulation, 2005. **111**(5): p. 598-606.
159. Peters, R.J., et al., *Effects of aspirin dose when used alone or in combination with clopidogrel in patients with acute coronary syndromes: observations from the Clopidogrel in Unstable angina to prevent Recurrent Events (CURE) study.* Circulation, 2003. **108**(14): p. 1682-7.
160. Sacks, F.M., et al., *The effect of pravastatin on coronary events after myocardial infarction in patients with average cholesterol levels. Cholesterol and Recurrent Events Trial investigators.* N Engl J Med, 1996. **335**(14): p. 1001-9.
161. Sacks, F.M., et al., *Relationship between plasma LDL concentrations during treatment with pravastatin and recurrent coronary events in the Cholesterol and Recurrent Events trial.* Circulation, 1998. **97**(15): p. 1446-52.
162. Keating, G.M. and G.L. Plosker, *Eplerenone : a review of its use in left ventricular systolic dysfunction and heart failure after acute myocardial infarction.* Drugs, 2004. **64**(23): p. 2689-707.
163. St John Sutton, M., et al., *Cardiovascular death and left ventricular remodeling two years after myocardial infarction: baseline predictors and impact of long-term use of captopril: information from the Survival and Ventricular Enlargement (SAVE) trial.* Circulation, 1997. **96**(10): p. 3294-9.
164. Gheorghiade, M. and R.O. Bonow, *Chronic heart failure in the United States: a manifestation of coronary artery disease.* Circulation, 1998. **97**(3): p. 282-9.
165. Flather, M.D., et al., *Long-term ACE-inhibitor therapy in patients with heart failure or left-ventricular dysfunction: a systematic overview of data from individual patients. ACE-Inhibitor Myocardial Infarction Collaborative Group.* Lancet, 2000. **355**(9215): p. 1575-81.
166. van Zwieten, P.A., *Current and newer approaches in the drug treatment of congestive heart failure.* Cardiovasc Drugs Ther, 1997. **10**(6): p. 693-702.
167. Nelson, G.S., et al., *Left ventricular or biventricular pacing improves cardiac function at diminished energy cost in patients with dilated cardiomyopathy and left bundle-branch block.* Circulation, 2000. **102**(25): p. 3053-9.
168. Yu, C.M., et al., *Predictors of left ventricular reverse remodeling after cardiac resynchronization therapy for heart failure secondary to idiopathic dilated or ischemic cardiomyopathy.* Am J Cardiol, 2003. **91**(6): p. 684-8.
169. Starling, R.C., et al., *Sustained benefits of the CorCap Cardiac Support Device on left ventricular remodeling: three year follow-up results from the Acorn clinical trial.* Ann Thorac Surg, 2007. **84**(4): p. 1236-42.
170. Klodell, C.T., Jr., et al., *Worldwide surgical experience with the Paracor HeartNet cardiac restraint device.* J Thorac Cardiovasc Surg, 2008. **135**(1): p. 188-95.
171. Sartipy, U., A. Albage, and D. Lindblom, *The Dor procedure for left ventricular reconstruction. Ten-year clinical experience.* Eur J Cardiothorac Surg, 2005. **27**(6): p. 1005-10.

172. Batista, R., *Partial left ventriculectomy--the Batista procedure.* Eur J Cardiothorac Surg, 1999. **15 Suppl 1**: p. S12-9; discussion S39-43.
173. Levy, D., et al., *Long-term trends in the incidence of and survival with heart failure.* N Engl J Med, 2002. **347**(18): p. 1397-402.
174. Taylor, D.O., et al., *Registry of the International Society for Heart and Lung Transplantation: twenty-third official adult heart transplantation report--2006.* J Heart Lung Transplant, 2006. **25**(8): p. 869-79.
175. Goldstein, D.J., M.C. Oz, and E.A. Rose, *Implantable left ventricular assist devices.* N Engl J Med, 1998. **339**(21): p. 1522-33.
176. Terracciano, C.M., et al., *Clinical recovery from end-stage heart failure using left-ventricular assist device and pharmacological therapy correlates with increased sarcoplasmic reticulum calcium content but not with regression of cellular hypertrophy.* Circulation, 2004. **109**(19): p. 2263-5.
177. Murry, C.E. and R.T. Lee, *Development biology. Turnover after the fallout.* Science, 2009. **324**(5923): p. 47-8.
178. Bergmann, O., et al., *Evidence for cardiomyocyte renewal in humans.* Science, 2009. **324**(5923): p. 98-102.
179. Ertl, G. and S. Frantz, *Healing after myocardial infarction.* Cardiovasc Res, 2005. **66**(1): p. 22-32.
180. Poss, K.D., L.G. Wilson, and M.T. Keating, *Heart regeneration in zebrafish.* Science, 2002. **298**(5601): p. 2188-90.
181. Anversa, P., et al., *Life and death of cardiac stem cells: a paradigm shift in cardiac biology.* Circulation, 2006. **113**(11): p. 1451-63.
182. Kocher, A.A., et al., *Stem cells and cardiac regeneration.* Transpl Int, 2007. **20**(9): p. 731-46.
183. Segers, V.F. and R.T. Lee, *Stem-cell therapy for cardiac disease.* Nature, 2008. **451**(7181): p. 937-42.
184. Collins, S.D., R. Baffour, and R. Waksman, *Cell therapy in myocardial infarction.* Cardiovasc Revasc Med, 2007. **8**(1): p. 43-51.
185. Rubart, M. and L.J. Field, *Cardiac regeneration: repopulating the heart.* Annu Rev Physiol, 2006. **68**: p. 29-49.
186. Menasche, P., *Skeletal myoblasts as a therapeutic agent.* Prog Cardiovasc Dis, 2007. **50**(1): p. 7-17.
187. Murry, C.E., et al., *Skeletal myoblast transplantation for repair of myocardial necrosis.* J Clin Invest, 1996. **98**(11): p. 2512-23.
188. Chiu, R.C., A. Zibaitis, and R.L. Kao, *Cellular cardiomyoplasty: myocardial regeneration with satellite cell implantation.* Ann Thorac Surg, 1995. **60**(1): p. 12-8.
189. Bonaros, N., et al., *Combined transplantation of skeletal myoblasts and angiopoietic progenitor cells reduces infarct size and apoptosis and improves cardiac function in chronic ischemic heart failure.* J Thorac Cardiovasc Surg, 2006. **132**(6): p. 1321-8.
190. Abraham, M.R., et al., *Antiarrhythmic engineering of skeletal myoblasts for cardiac transplantation.* Circ Res, 2005. **97**(2): p. 159-67.
191. Laflamme, M.A. and C.E. Murry, *Regenerating the heart.* Nat Biotechnol, 2005. **23**(7): p. 845-56.
192. Taylor, D.A., et al., *Regenerating functional myocardium: improved performance after skeletal myoblast transplantation.* Nat Med, 1998. **4**(8): p. 929-33.

193. Cleland, J.G., et al., *Clinical trials update from the American Heart Association 2006: OAT, SALT 1 and 2, MAGIC, ABCD, PABA-CHF, IMPROVE-CHF, and percutaneous mitral annuloplasty.* Eur J Heart Fail, 2007. **9**(1): p. 92-7.
194. Orlic, D., et al., *Bone marrow cells regenerate infarcted myocardium.* Nature, 2001. **410**(6829): p. 701-5.
195. Orlic, D., et al., *Mobilized bone marrow cells repair the infarcted heart, improving function and survival.* Proc Natl Acad Sci U S A, 2001. **98**(18): p. 10344-9.
196. Jackson, K.A., et al., *Regeneration of ischemic cardiac muscle and vascular endothelium by adult stem cells.* J Clin Invest, 2001. **107**(11): p. 1395-402.
197. Murry, C.E., et al., *Haematopoietic stem cells do not transdifferentiate into cardiac myocytes in myocardial infarcts.* Nature, 2004. **428**(6983): p. 664-8.
198. Balsam, L.B., et al., *Haematopoietic stem cells adopt mature haematopoietic fates in ischaemic myocardium.* Nature, 2004. **428**(6983): p. 668-73.
199. Nygren, J.M., et al., *Bone marrow-derived hematopoietic cells generate cardiomyocytes at a low frequency through cell fusion, but not transdifferentiation.* Nat Med, 2004. **10**(5): p. 494-501.
200. Toma, C., et al., *Human mesenchymal stem cells differentiate to a cardiomyocyte phenotype in the adult murine heart.* Circulation, 2002. **105**(1): p. 93-8.
201. Amado, L.C., et al., *Cardiac repair with intramyocardial injection of allogeneic mesenchymal stem cells after myocardial infarction.* Proc Natl Acad Sci U S A, 2005. **102**(32): p. 11474-9.
202. Gnecchi, M., et al., *Evidence supporting paracrine hypothesis for Akt-modified mesenchymal stem cell-mediated cardiac protection and functional improvement.* FASEB J, 2006. **20**(6): p. 661-9.
203. Lunde, K., et al., *Intracoronary injection of mononuclear bone marrow cells in acute myocardial infarction.* N Engl J Med, 2006. **355**(12): p. 1199-209.
204. Assmus, B., et al., *Transcoronary transplantation of progenitor cells after myocardial infarction.* N Engl J Med, 2006. **355**(12): p. 1222-32.
205. Kocher, A.A., et al., *Neovascularization of ischemic myocardium by human bone-marrow-derived angioblasts prevents cardiomyocyte apoptosis, reduces remodeling and improves cardiac function.* Nat Med, 2001. **7**(4): p. 430-6.
206. Abdel-Latif, A., et al., *Adult bone marrow-derived cells for cardiac repair: a systematic review and meta-analysis.* Arch Intern Med, 2007. **167**(10): p. 989-97.
207. Schachinger, V., et al., *Intracoronary bone marrow-derived progenitor cells in acute myocardial infarction.* N Engl J Med, 2006. **355**(12): p. 1210-21.
208. Oh, H., et al., *Cardiac progenitor cells from adult myocardium: homing, differentiation, and fusion after infarction.* Proc Natl Acad Sci U S A, 2003. **100**(21): p. 12313-8.
209. Beltrami, A.P., et al., *Adult cardiac stem cells are multipotent and support myocardial regeneration.* Cell, 2003. **114**(6): p. 763-76.
210. Dawn, B., et al., *Cardiac stem cells delivered intravascularly traverse the vessel barrier, regenerate infarcted myocardium, and improve cardiac function.* Proc Natl Acad Sci U S A, 2005. **102**(10): p. 3766-71.

211. Linke, A., et al., *Stem cells in the dog heart are self-renewing, clonogenic, and multipotent and regenerate infarcted myocardium, improving cardiac function.* Proc Natl Acad Sci U S A, 2005. **102**(25): p. 8966-71.
212. Kehat, I., et al., *Human embryonic stem cells can differentiate into myocytes with structural and functional properties of cardiomyocytes.* J Clin Invest, 2001. **108**(3): p. 407-14.
213. Kehat, I., et al., *Electromechanical integration of cardiomyocytes derived from human embryonic stem cells.* Nat Biotechnol, 2004. **22**(10): p. 1282-9.
214. Hodgson, D.M., et al., *Stable benefit of embryonic stem cell therapy in myocardial infarction.* Am J Physiol Heart Circ Physiol, 2004. **287**(2): p. H471-9.
215. Laflamme, M.A., et al., *Formation of human myocardium in the rat heart from human embryonic stem cells.* Am J Pathol, 2005. **167**(3): p. 663-71.
216. Nussbaum, J., et al., *Transplantation of undifferentiated murine embryonic stem cells in the heart: teratoma formation and immune response.* FASEB J, 2007. **21**(7): p. 1345-57.
217. Nishikawa, S., R.A. Goldstein, and C.R. Nierras, *The promise of human induced pluripotent stem cells for research and therapy.* Nat Rev Mol Cell Biol, 2008. **9**(9): p. 725-9.
218. Nelson, T.J., et al., *Repair of acute myocardial infarction by human stemness factors induced pluripotent stem cells.* Circulation, 2009. **120**(5): p. 408-16.
219. Muller-Ehmsen, J., et al., *Survival and development of neonatal rat cardiomyocytes transplanted into adult myocardium.* J Mol Cell Cardiol, 2002. **34**(2): p. 107-16.
220. Muller-Ehmsen, J., et al., *Effective engraftment but poor mid-term persistence of mononuclear and mesenchymal bone marrow cells in acute and chronic rat myocardial infarction.* J Mol Cell Cardiol, 2006. **41**(5): p. 876-84.
221. Teng, C.J., et al., *Massive mechanical loss of microspheres with direct intramyocardial injection in the beating heart: implications for cellular cardiomyoplasty.* J Thorac Cardiovasc Surg, 2006. **132**(3): p. 628-32.
222. Aicher, A., et al., *Assessment of the tissue distribution of transplanted human endothelial progenitor cells by radioactive labeling.* Circulation, 2003. **107**(16): p. 2134-9.
223. Zhang, H., et al., *Injection of bone marrow mesenchymal stem cells in the borderline area of infarcted myocardium: heart status and cell distribution.* J Thorac Cardiovasc Surg, 2007. **134**(5): p. 1234-40.
224. Hale, S.L., et al., *Mesenchymal stem cell administration at coronary artery reperfusion in the rat by two delivery routes: a quantitative assessment.* Life Sci, 2008. **83**(13-14): p. 511-5.
225. Al Kindi, A., et al., *Cellular cardiomyoplasty: routes of cell delivery and retention.* Front Biosci, 2008. **13**: p. 2421-34.
226. Miyahara, Y., et al., *Monolayered mesenchymal stem cells repair scarred myocardium after myocardial infarction.* Nat Med, 2006. **12**(4): p. 459-65.
227. Dai, W., et al., *Delivering stem cells to the heart in a collagen matrix reduces relocation of cells to other organs as assessed by nanoparticle technology.* Regen Med, 2009. **4**(3): p. 387-95.

228. Cortes-Morichetti, M., et al., *Association between a cell-seeded collagen matrix and cellular cardiomyoplasty for myocardial support and regeneration.* Tissue Eng, 2007. **13**(11): p. 2681-7.
229. Laflamme, M.A., et al., *Cardiomyocytes derived from human embryonic stem cells in pro-survival factors enhance function of infarcted rat hearts.* Nat Biotechnol, 2007. **25**(9): p. 1015-24.
230. Kofidis, T., et al., *Novel injectable bioartificial tissue facilitates targeted, less invasive, large-scale tissue restoration on the beating heart after myocardial injury.* Circulation, 2005. **112**(9 Suppl): p. I173-7.
231. Kofidis, T., et al., *Injectable bioartificial myocardial tissue for large-scale intramural cell transfer and functional recovery of injured heart muscle.* J Thorac Cardiovasc Surg, 2004. **128**(4): p. 571-8.
232. Lu, W.N., et al., *Functional improvement of infarcted heart by co-injection of embryonic stem cells with temperature-responsive chitosan hydrogel.* Tissue Eng Part A, 2009. **15**(6): p. 1437-47.
233. Chekanov, V., et al., *Transplantation of autologous endothelial cells induces angiogenesis.* Pacing Clin Electrophysiol, 2003. **26**(1 Pt 2): p. 496-9.
234. Christman, K.L., et al., *Fibrin glue alone and skeletal myoblasts in a fibrin scaffold preserve cardiac function after myocardial infarction.* Tissue Eng, 2004. **10**(3-4): p. 403-9.
235. Christman, K.L., et al., *Injectable fibrin scaffold improves cell transplant survival, reduces infarct expansion, and induces neovasculature formation in ischemic myocardium.* J Am Coll Cardiol, 2004. **44**(3): p. 654-60.
236. Wang, T., et al., *Bone marrow stem cells implantation with alpha-cyclodextrin/MPEG-PCL-MPEG hydrogel improves cardiac function after myocardial infarction.* Acta Biomater, 2009. **5**(8): p. 2939-44.
237. Wall, S.T., et al., *Theoretical impact of the injection of material into the myocardium: a finite element model simulation.* Circulation, 2006. **114**(24): p. 2627-35.
238. Jawad, H., et al., *Myocardial tissue engineering: a review.* J Tissue Eng Regen Med, 2007. **1**(5): p. 327-42.
239. Davis, M.E., et al., *Custom design of the cardiac microenvironment with biomaterials.* Circ Res, 2005. **97**(1): p. 8-15.
240. Christman, K.L. and R.J. Lee, *Biomaterials for the treatment of myocardial infarction.* J Am Coll Cardiol, 2006. **48**(5): p. 907-13.
241. Landa, N., et al., *Effect of injectable alginate implant on cardiac remodeling and function after recent and old infarcts in rat.* Circulation, 2008. **117**(11): p. 1388-96.
242. Dai, W., et al., *Thickening of the infarcted wall by collagen injection improves left ventricular function in rats: a novel approach to preserve cardiac function after myocardial infarction.* J Am Coll Cardiol, 2005. **46**(4): p. 714-9.
243. Fujimoto, K.L., et al., *Synthesis, characterization and therapeutic efficacy of a biodegradable, thermoresponsive hydrogel designed for application in chronic infarcted myocardium.* Biomaterials, 2009. **30**(26): p. 4357-68.
244. Dobner, S., et al., *A synthetic non-degradable polyethylene glycol hydrogel retards adverse post-infarct left ventricular remodeling.* J Card Fail, 2009. **15**(7): p. 629-36.
245. Leor, J., et al., *Intracoronary injection of in situ forming alginate hydrogel reverses left ventricular remodeling after myocardial infarction in Swine.* J Am Coll Cardiol, 2009. **54**(11): p. 1014-23.

246. Mukherjee, R., et al., *Targeted myocardial microinjections of a biocomposite material reduces infarct expansion in pigs.* Ann Thorac Surg, 2008. **86**(4): p. 1268-76.
247. Wang, T., et al., *Novel thermosensitive hydrogel injection inhibits post-infarct ventricle remodelling.* Eur J Heart Fail, 2009. **11**(1): p. 14-9.
248. Hoffman, A.S., *Hydrogels for biomedical applications.* Adv Drug Deliv Rev, 2002. **54**(1): p. 3-12.
249. Zisch, A.H., M.P. Lutolf, and J.A. Hubbell, *Biopolymeric delivery matrices for angiogenic growth factors.* Cardiovasc Pathol, 2003. **12**(6): p. 295-310.
250. Nuttelman, C.R., M.C. Tripodi, and K.S. Anseth, *Synthetic hydrogel niches that promote hMSC viability.* Matrix Biol, 2005. **24**(3): p. 208-18.
251. Lee, K.Y. and D.J. Mooney, *Hydrogels for tissue engineering.* Chem Rev, 2001. **101**(7): p. 1869-79.
252. Kim, B.S. and D.J. Mooney, *Development of biocompatible synthetic extracellular matrices for tissue engineering.* Trends Biotechnol, 1998. **16**(5): p. 224-30.
253. Corkhill, P.H., C.J. Hamilton, and B.J. Tighe, *Synthetic hydrogels. VI. Hydrogel composites as wound dressings and implant materials.* Biomaterials, 1989. **10**(1): p. 3-10.
254. Drury, J.L. and D.J. Mooney, *Hydrogels for tissue engineering: scaffold design variables and applications.* Biomaterials, 2003. **24**(24): p. 4337-51.
255. Lutolf, M.P. and J.A. Hubbell, *Synthetic biomaterials as instructive extracellular microenvironments for morphogenesis in tissue engineering.* Nat Biotechnol, 2005. **23**(1): p. 47-55.
256. Bennett, S.L., et al., *Next-generation hydrogel films as tissue sealants and adhesion barriers.* J Card Surg, 2003. **18**(6): p. 494-9.
257. Hubbell, J.A., *Synthetic biodegradable polymers for tissue engineering and drug delivery.* Current Opinion in Solid State & Materials Science, 1998. **3**: p. 246-51.
258. Kashyap, N., N. Kumar, and M.N. Kumar, *Hydrogels for pharmaceutical and biomedical applications.* Crit Rev Ther Drug Carrier Syst, 2005. **22**(2): p. 107-49.
259. Zheng Shu, X., et al., *In situ crosslinkable hyaluronan hydrogels for tissue engineering.* Biomaterials, 2004. **25**(7-8): p. 1339-48.
260. Wang, D.A., et al., *Synthesis and characterization of a novel degradable phosphate-containing hydrogel.* Biomaterials, 2003. **24**(22): p. 3969-80.
261. Li, J., X. Ni, and K.W. Leong, *Injectable drug-delivery systems based on supramolecular hydrogels formed by poly(ethylene oxide)s and alpha-cyclodextrin.* J Biomed Mater Res A, 2003. **65**(2): p. 196-202.
262. Wu, D.Q., et al., *Fabrication of supramolecular hydrogels for drug delivery and stem cell encapsulation.* Langmuir, 2008. **24**(18): p. 10306-12.
263. Lee, B.H. and B. Vernon, *In situ-gelling, erodible N-isopropylacrylamide copolymers.* Macromol Biosci, 2005. **5**(7): p. 629-35.
264. Jeong, B., S.W. Kim, and Y.H. Bae, *Thermosensitive sol-gel reversible hydrogels.* Adv Drug Deliv Rev, 2002. **54**(1): p. 37-51.
265. Shireman, P.K. and H.P. Greisler, *Fibrin sealant in vascular surgery: a review.* J Long Term Eff Med Implants, 1998. **8**(2): p. 117-32.
266. Jackson, M.R., *Fibrin sealants in surgical practice: An overview.* Am J Surg, 2001. **182**(2 Suppl): p. 1S-7S.

267. Sierra, D.H., *Fibrin sealant adhesive systems: a review of their chemistry, material properties and clinical applications.* J Biomater Appl, 1993. **7**(4): p. 309-52.
268. Fasol, R., et al., *Experimental use of a modified fibrin glue to induce site-directed angiogenesis from the aorta to the heart.* J Thorac Cardiovasc Surg, 1994. **107**(6): p. 1432-9.
269. Bach, A.D., et al., *Fibrin glue as matrix for cultured autologous urothelial cells in urethral reconstruction.* Tissue Eng, 2001. **7**(1): p. 45-53.
270. Andree, C., et al., *Plasmid gene delivery to human keratinocytes through a fibrin-mediated transfection system.* Tissue Eng, 2001. **7**(6): p. 757-66.
271. Chekanov, V.S., et al., *Biologic glue increases capillary ingrowth after cardiomyoplasty in an ischemic cardiomyopathy model.* ASAIO J, 1996. **42**(5): p. M480-7.
272. Christman, K.L., et al., *Enhanced neovasculature formation in ischemic myocardium following delivery of pleiotrophin plasmid in a biopolymer.* Biomaterials, 2005. **26**(10): p. 1139-44.
273. Yu, J., et al., *Restoration of left ventricular geometry and improvement of left ventricular function in a rodent model of chronic ischemic cardiomyopathy.* J Thorac Cardiovasc Surg, 2009. **137**(1): p. 180-7.
274. Huang, N.F., et al., *Injectable biopolymers enhance angiogenesis after myocardial infarction.* Tissue Eng, 2005. **11**(11-12): p. 1860-6.
275. Lee, C.H., A. Singla, and Y. Lee, *Biomedical applications of collagen.* Int J Pharm, 2001. **221**(1-2): p. 1-22.
276. Kaufmann, P.M., et al., *Highly porous polymer matrices as a three-dimensional culture system for hepatocytes.* Cell Transplant, 1997. **6**(5): p. 463-8.
277. Auger, F.A., et al., *Tissue-engineered human skin substitutes developed from collagen-populated hydrated gels: clinical and fundamental applications.* Med Biol Eng Comput, 1998. **36**(6): p. 801-12.
278. Seliktar, D., et al., *Dynamic mechanical conditioning of collagen-gel blood vessel constructs induces remodeling in vitro.* Ann Biomed Eng, 2000. **28**(4): p. 351-62.
279. Peppas, N.A., *Hydrogelsin Biology and Medicine: From Molecular Principles to Bionanotchnology* Advanced Materials, 2006. **18**: p. 1345-60.
280. Pulapura, S. and J. Kohn, *Trends in the development of bioresorbable polymers for medical applications.* J Biomater Appl, 1992. **6**(3): p. 216-50.
281. Shao, Z.Q., et al., *Effects of intramyocardial administration of slow-release basic fibroblast growth factor on angiogenesis and ventricular remodeling in a rat infarct model.* Circ J, 2006. **70**(4): p. 471-7.
282. Singelyn, J.M. and K.L. Christman, *Injectable materials for the treatment of myocardial infarction and heart failure: the promise of decellularized matrices.* J Cardiovasc Transl Res. **3**(5): p. 478-86.
283. Draget, K.I., G. Skjak-Braek, and O. Smidsrod, *Alginate based new materials.* Int J Biol Macromol, 1997. **21**(1-2): p. 47-55.
284. Augst, A.D., H.J. Kong, and D.J. Mooney, *Alginate hydrogels as biomaterials.* Macromol Biosci, 2006. **6**(8): p. 623-33.
285. Simmons, C.A., et al., *Dual growth factor delivery and controlled scaffold degradation enhance in vivo bone formation by transplanted bone marrow stromal cells.* Bone, 2004. **35**(2): p. 562-9.

286. Lee, K.W., et al., *Sustained release of vascular endothelial growth factor from calcium-induced alginate hydrogels reinforced by heparin and chitosan.* Transplant Proc, 2004. **36**(8): p. 2464-5.
287. Peters, M.C., et al., *Release from alginate enhances the biological activity of vascular endothelial growth factor.* J Biomater Sci Polym Ed, 1998. **9**(12): p. 1267-78.
288. Tonnesen, H.H. and J. Karlsen, *Alginate in drug delivery systems.* Drug Dev Ind Pharm, 2002. **28**(6): p. 621-30.
289. Alsberg, E., et al., *Cell-interactive alginate hydrogels for bone tissue engineering.* J Dent Res, 2001. **80**(11): p. 2025-9.
290. Rowley, J.A., G. Madlambayan, and D.J. Mooney, *Alginate hydrogels as synthetic extracellular matrix materials.* Biomaterials, 1999. **20**(1): p. 45-53.
291. Leor, J., et al., *Bioengineered cardiac grafts: A new approach to repair the infarcted myocardium?* Circulation, 2000. **102**(19 Suppl 3): p. III56-61.
292. Hao, X., et al., *Angiogenic effects of sequential release of VEGF-A165 and PDGF-BB with alginate hydrogels after myocardial infarction.* Cardiovasc Res, 2007. **75**(1): p. 178-85.
293. Ruvinov, E., J. Leor, and S. Cohen, *The promotion of myocardial repair by the sequential delivery of IGF-1 and HGF from an injectable alginate biomaterial in a model of acute myocardial infarction.* Biomaterials. **32**(2): p. 565-78.
294. Smidsrod, O. and G. Skjak-Braek, *Alginate as immobilization matrix for cells.* Trends Biotechnol, 1990. **8**(3): p. 71-8.
295. Otterlei, M., et al., *Induction of cytokine production from human monocytes stimulated with alginate.* J Immunother (1991), 1991. **10**(4): p. 286-91.
296. Entwistle, J., C.L. Hall, and E.A. Turley, *HA receptors: regulators of signalling to the cytoskeleton.* J Cell Biochem, 1996. **61**(4): p. 569-77.
297. Dowthwaite, G.P., J.C. Edwards, and A.A. Pitsillides, *An essential role for the interaction between hyaluronan and hyaluronan binding proteins during joint development.* J Histochem Cytochem, 1998. **46**(5): p. 641-51.
298. Cheung, W.F., T.F. Cruz, and E.A. Turley, *Receptor for hyaluronan-mediated motility (RHAMM), a hyaladherin that regulates cell responses to growth factors.* Biochem Soc Trans, 1999. **27**(2): p. 135-42.
299. Choi, Y.S., et al., *Studies on gelatin-containing artificial skin: II. Preparation and characterization of cross-linked gelatin-hyaluronate sponge.* J Biomed Mater Res, 1999. **48**(5): p. 631-9.
300. Kirker, K.R., et al., *Glycosaminoglycan hydrogel films as bio-interactive dressings for wound healing.* Biomaterials, 2002. **23**(17): p. 3661-71.
301. Duranti, F., et al., *Injectable hyaluronic acid gel for soft tissue augmentation. A clinical and histological study.* Dermatol Surg, 1998. **24**(12): p. 1317-25.
302. Miller, D., P. O'Connor, and J. Williams, *Use of Na-hyaluronate during intraocular lens implantation in rabbits.* Ophthalmic Surg, 1977. **8**(6): p. 58-61.
303. Karlsson, J., L.S. Sjogren, and L.S. Lohmander, *Comparison of two hyaluronan drugs and placebo in patients with knee osteoarthritis. A controlled, randomized, double-blind, parallel-design multicentre study.* Rheumatology (Oxford), 2002. **41**(11): p. 1240-8.
304. Luo, Y., K.R. Kirker, and G.D. Prestwich, *Cross-linked hyaluronic acid hydrogel films: new biomaterials for drug delivery.* J Control Release, 2000. **69**(1): p. 169-84.

305. Pouyani, T. and G.D. Prestwich, *Functionalized derivatives of hyaluronic acid oligosaccharides: drug carriers and novel biomaterials.* Bioconjug Chem, 1994. **5**(4): p. 339-47.
306. Vercruysse, K.P. and G.D. Prestwich, *Hyaluronate derivatives in drug delivery.* Crit Rev Ther Drug Carrier Syst, 1998. **15**(5): p. 513-55.
307. Liu, L.S., et al., *An osteoconductive collagen/hyaluronate matrix for bone regeneration.* Biomaterials, 1999. **20**(12): p. 1097-108.
308. Ifkovits, J.L., et al., *Injectable hydrogel properties influence infarct expansion and extent of postinfarction left ventricular remodeling in an ovine model.* Proc Natl Acad Sci U S A. **107**(25): p. 11507-12.
309. Segers, V.F. and R.T. Lee, *Local delivery of proteins and the use of self-assembling peptides.* Drug Discov Today, 2007. **12**(13-14): p. 561-8.
310. Zhang, S., *Fabrication of novel biomaterials through molecular self-assembly.* Nat Biotechnol, 2003. **21**(10): p. 1171-8.
311. Zhang, S., F. Gelain, and X. Zhao, *Designer self-assembling peptide nanofiber scaffolds for 3D tissue cell cultures.* Semin Cancer Biol, 2005. **15**(5): p. 413-20.
312. Zhao, X. and S. Zhang, *Molecular designer self-assembling peptides.* Chem Soc Rev, 2006. **35**(11): p. 1105-10.
313. Holmes, T.C., *Novel peptide-based biomaterial scaffolds for tissue engineering.* Trends Biotechnol, 2002. **20**(1): p. 16-21.
314. Lin, Y.D., et al., *Intramyocardial peptide nanofiber injection improves postinfarction ventricular remodeling and efficacy of bone marrow cell therapy in pigs.* Circulation. **122**(11 Suppl): p. S132-41.
315. Davis, M.E., et al., *Injectable self-assembling peptide nanofibers create intramyocardial microenvironments for endothelial cells.* Circulation, 2005. **111**(4): p. 442-50.
316. Davis, M.E., et al., *Local myocardial insulin-like growth factor 1 (IGF-1) delivery with biotinylated peptide nanofibers improves cell therapy for myocardial infarction.* Proc Natl Acad Sci U S A, 2006. **103**(21): p. 8155-60.
317. Hsieh, P.C., et al., *Local controlled intramyocardial delivery of platelet-derived growth factor improves postinfarction ventricular function without pulmonary toxicity.* Circulation, 2006. **114**(7): p. 637-44.
318. Hsieh, P.C., et al., *Controlled delivery of PDGF-BB for myocardial protection using injectable self-assembling peptide nanofibers.* J Clin Invest, 2006. **116**(1): p. 237-48.
319. Segers, V.F., et al., *Local delivery of protease-resistant stromal cell derived factor-1 for stem cell recruitment after myocardial infarction.* Circulation, 2007. **116**(15): p. 1683-92.
320. Guan, J., et al., *Protein-reactive, thermoresponsive copolymers with high flexibility and biodegradability.* Biomacromolecules, 2008. **9**(4): p. 1283-92.
321. Ma, Z., et al., *Thermally responsive injectable hydrogel incorporating methacrylate-polylactide for hydrolytic lability.* Biomacromolecules. **11**(7): p. 1873-81.
322. Kim, S. and K.E. Healy, *Synthesis and characterization of injectable poly(N-isopropylacrylamide-co-acrylic acid) hydrogels with proteolytically degradable cross-links.* Biomacromolecules, 2003. **4**(5): p. 1214-23.
323. Wu, D.Q., et al., *Toward the development of partially biodegradable and injectable thermoresponsive hydrogels for potential biomedical applications.* ACS Appl Mater Interfaces, 2009. **1**(2): p. 319-27.

324. Ron, E.S. and L.E. Bromberg, *Temperature-responsive gels and thermogelling polymer matrices for protein and peptide delivery.* Adv Drug Deliv Rev, 1998. **31**(3): p. 197-221.
325. Peppas, N.A., et al., *Poly(ethylene glycol)-containing hydrogels in drug delivery.* J Control Release, 1999. **62**(1-2): p. 81-7.
326. Di Palma, J.A., et al., *A randomized, multicenter comparison of polyethylene glycol laxative and tegaserod in treatment of patients with chronic constipation.* Am J Gastroenterol, 2007. **102**(9): p. 1964-71.
327. Krause, T.L. and G.D. Bittner, *Rapid morphological fusion of severed myelinated axons by polyethylene glycol.* Proc Natl Acad Sci U S A, 1990. **87**(4): p. 1471-5.
328. Corpet, D.E., et al., *Consistent and fast inhibition of colon carcinogenesis by polyethylene glycol in mice and rats given various carcinogens.* Cancer Res, 2000. **60**(12): p. 3160-4.
329. Mellott, M.B., K. Searcy, and M.V. Pishko, *Release of protein from highly cross-linked hydrogels of poly(ethylene glycol) diacrylate fabricated by UV polymerization.* Biomaterials, 2001. **22**(9): p. 929-41.
330. Borgens, R.B. and D. Bohnert, *Rapid recovery from spinal cord injury after subcutaneously administered polyethylene glycol.* J Neurosci Res, 2001. **66**(6): p. 1179-86.
331. West JL, H.J., *Polymeric Biomaterials with Degredation Sites for Proteases Involved in Cell Migration.* Macromolecules, 1999. **32**: p. 241-4.
332. Ekblom, P. and R. Timpl, *Cell-to-cell contact and extracellular matrix. A multifaceted approach emerging.* Curr Opin Cell Biol, 1996. **8**(5): p. 599-601.
333. Chapman, H.A., *Plasminogen activators, integrins, and the coordinated regulation of cell adhesion and migration.* Curr Opin Cell Biol, 1997. **9**(5): p. 714-24.
334. Rabbani, S.A., *Metalloproteases and urokinase in angiogenesis and tumor progression.* In Vivo, 1998. **12**(1): p. 135-42.
335. Basbaum, C.B. and Z. Werb, *Focalized proteolysis: spatial and temporal regulation of extracellular matrix degradation at the cell surface.* Curr Opin Cell Biol, 1996. **8**(5): p. 731-8.
336. Hiraoka, N., et al., *Matrix metalloproteinases regulate neovascularization by acting as pericellular fibrinolysins.* Cell, 1998. **95**(3): p. 365-77.
337. Patterson, J. and J.A. Hubbell, *Enhanced proteolytic degradation of molecularly engineered PEG hydrogels in response to MMP-1 and MMP-2.* Biomaterials. **31**(30): p. 7836-45.
338. Lutolf, M.P., et al., *Synthetic matrix metalloproteinase-sensitive hydrogels for the conduction of tissue regeneration: engineering cell-invasion characteristics.* Proc Natl Acad Sci U S A, 2003. **100**(9): p. 5413-8.
339. Halstenberg, S., et al., *Biologically engineered protein-graft-poly(ethylene glycol) hydrogels: a cell adhesive and plasmin-degradable biosynthetic material for tissue repair.* Biomacromolecules, 2002. **3**(4): p. 710-23.
340. Gobin, A.S. and J.L. West, *Cell migration through defined, synthetic ECM analogs.* FASEB J, 2002. **16**(7): p. 751-3.
341. Mann, B.K., et al., *Smooth muscle cell growth in photopolymerized hydrogels with cell adhesive and proteolytically degradable domains: synthetic ECM analogs for tissue engineering.* Biomaterials, 2001. **22**(22): p. 3045-51.

342. Lin, C.C. and K.S. Anseth, *PEG hydrogels for the controlled release of biomolecules in regenerative medicine.* Pharm Res, 2009. **26**(3): p. 631-43.
343. Veronese, F.M. and G. Pasut, *PEGylation, successful approach to drug delivery.* Drug Discov Today, 2005. **10**(21): p. 1451-8.
344. Sawhney, A.S., et al., *Optimization of photopolymerized bioerodible hydrogel properties for adhesion prevention.* J Biomed Mater Res, 1994. **28**(7): p. 831-8.
345. Hill-West, J.L., et al., *Efficacy of a resorbable hydrogel barrier, oxidized regenerated cellulose, and hyaluronic acid in the prevention of ovarian adhesions in a rabbit model.* Fertil Steril, 1994. **62**(3): p. 630-4.
346. Hill-West, J.L., et al., *Prevention of postoperative adhesions in the rat by in situ photopolymerization of bioresorbable hydrogel barriers.* Obstet Gynecol, 1994. **83**(1): p. 59-64.
347. West, J.L. and J.A. Hubbell, *Separation of the arterial wall from blood contact using hydrogel barriers reduces intimal thickening after balloon injury in the rat: the roles of medial and luminal factors in arterial healing.* Proc Natl Acad Sci U S A, 1996. **93**(23): p. 13188-93.
348. Chowdhury, S.M. and J.A. Hubbell, *Adhesion prevention with ancrod released via a tissue-adherent hydrogel.* J Surg Res, 1996. **61**(1): p. 58-64.
349. Hill-West, J.L., R.C. Dunn, and J.A. Hubbell, *Local release of fibrinolytic agents for adhesion prevention.* J Surg Res, 1995. **59**(6): p. 759-63.
350. Burdick, J.A. and K.S. Anseth, *Photoencapsulation of osteoblasts in injectable RGD-modified PEG hydrogels for bone tissue engineering.* Biomaterials, 2002. **23**(22): p. 4315-23.
351. Kao, W.J. and D. Lee, *In vivo modulation of host response and macrophage behavior by polymer networks grafted with fibronectin-derived biomimetic oligopeptides: the role of RGD and PHSRN domains.* Biomaterials, 2001. **22**(21): p. 2901-9.
352. Hu, W.J., et al., *Molecular basis of biomaterial-mediated foreign body reactions.* Blood, 2001. **98**(4): p. 1231-8.
353. Anderson, J.M., A. Rodriguez, and D.T. Chang, *Foreign body reaction to biomaterials.* Semin Immunol, 2008. **20**(2): p. 86-100.
354. Tang, L., et al., *Molecular determinants of acute inflammatory responses to biomaterials.* J Clin Invest, 1996. **97**(5): p. 1329-34.
355. Bridges, A.W., et al., *Reduced acute inflammatory responses to microgel conformal coatings.* Biomaterials, 2008. **29**(35): p. 4605-15.
356. Ratner, B.D. and S.J. Bryant, *Biomaterials: where we have been and where we are going.* Annu Rev Biomed Eng, 2004. **6**: p. 41-75.
357. Pankowsky, D.A., et al., *Morphologic characteristics of adsorbed human plasma proteins on vascular grafts and biomaterials.* J Vasc Surg, 1990. **11**(4): p. 599-606.
358. Andrade, J.D. and V. Hlady, *Plasma protein adsorption: the big twelve.* Ann N Y Acad Sci, 1987. **516**: p. 158-72.
359. Jauregui, H.O., *Cell adhesion to biomaterials. The role of several extracellular matrix components in the attachment of non-transformed fibroblasts and parenchymal cells.* ASAIO Trans, 1987. **33**(2): p. 66-74.
360. Salthouse, T.N., *Some aspects of macrophage behavior at the implant interface.* J Biomed Mater Res, 1984. **18**(4): p. 395-401.
361. Anderson, J.M., *Inflammatory response to implants.* ASAIO Trans, 1988. **34**(2): p. 101-7.

362. Quinn, C.P., et al., *Photo-crosslinked copolymers of 2-hydroxyethyl methacrylate, poly(ethylene glycol) tetra-acrylate and ethylene dimethacrylate for improving biocompatibility of biosensors.* Biomaterials, 1995. **16**(5): p. 389-96.
363. Zhang, F., et al., *Surface modification of stainless steel by grafting of poly(ethylene glycol) for reduction in protein adsorption.* Biomaterials, 2001. **22**(12): p. 1541-8.
364. Collier, T.O., et al., *Inhibition of macrophage development and foreign body giant cell formation by hydrophilic interpenetrating polymer network.* J Biomed Mater Res A, 2004. **69**(4): p. 644-50.
365. Lee, J.H., et al., *Surface properties of copolymers of alkyl methacrylates with methoxy (polyethylene oxide) methacrylates and their application as protein-resistant coatings.* Biomaterials, 1990. **11**(7): p. 455-64.
366. Shen, M., et al., *PEO-like plasma polymerized tetraglyme surface interactions with leukocytes and proteins: in vitro and in vivo studies.* J Biomater Sci Polym Ed, 2002. **13**(4): p. 367-90.
367. Wagner, V.E. and J.D. Bryers, *Monocyte/macrophage interactions with base and linear- and star-like PEG-modified PEG-poly(acrylic acid) co-polymers.* J Biomed Mater Res A, 2003. **66**(1): p. 62-78.
368. Tan, J. and J.L. Brash, *Nonfouling biomaterials based on polyethylene oxide-containing amphiphilic triblock copolymers as surface modifying additives: solid state structure of PEO-copolymer/polyurethane blends.* J Biomed Mater Res A, 2008. **85**(4): p. 862-72.
369. Lee, H.J., et al., *Platelet and bacterial repellence on sulfonated poly(ethylene glycol)-acrylate copolymer surfaces.* Colloids Surf B Biointerfaces, 2000. **18**(3-4): p. 355-370.
370. Merrill, E.W., et al., *Platelet-compatible hydrophilic segmented polyurethanes from polyethylene glycols and cyclohexane diisocyanate.* Trans Am Soc Artif Intern Organs, 1982. **28**: p. 482-7.
371. Sanborn, T.J., P.B. Messersmith, and A.E. Barron, *In situ crosslinking of a biomimetic peptide-PEG hydrogel via thermally triggered activation of factor XIII.* Biomaterials, 2002. **23**(13): p. 2703-10.
372. Burdick, J.A., *Biomaterials for Tissue Engineering Applications*. 2011: Springer.
373. Neuburger, *Critical Experimental Test of the Flory-Rehner Theory of Swelling* Macromolecules, 1988. **21**: p. 3060-70.
374. Hamed GR, *Materials and Compounds*, Gupta Verlag. p. 11-34.
375. Mark, J.E., *Physical Properties of Polymers Handbook*. 2nd ed. 2007: Springer
376. Santoro, M.M. and G. Gaudino, *Cellular and molecular facets of keratinocyte reepithelization during wound healing.* Exp Cell Res, 2005. **304**(1): p. 274-86.
377. [cited 05.08.2011]; Available from: http://www.udel.edu/biology/Wags/histopage/vascularmodelingpage/corrosioncasts/corrosioncastingpage.html.
378. Kr zel, A., et al., *Coordination of heavy metals by dithiothreitol, a commonly used thiol group protectant.* J Inorg Biochem, 2001. **84**(1-2): p. 77-88.
379. Sabatine, M.S., et al., *Complementary roles for biomarkers of biomechanical strain ST2 and N-terminal prohormone B-type natriuretic peptide in patients*

with ST-elevation myocardial infarction. Circulation, 2008. **117**(15): p. 1936-44.
380. Zhang, Y., et al., *Timing of bone marrow cell therapy is more important than repeated injections after myocardial infarction.* Cardiovasc Pathol. **20**(4): p. 204-12.
381. Yellon, D.M. and D.J. Hausenloy, *Myocardial reperfusion injury.* N Engl J Med, 2007. **357**(11): p. 1121-35.
382. van der Worp, H.B., et al., *Can animal models of disease reliably inform human studies?* PLoS Med. **7**(3): p. e1000245.
383. Gould, K.E., et al., *Heart failure and greater infarct expansion in middle-aged mice: a relevant model for postinfarction failure.* Am J Physiol Heart Circ Physiol, 2002. **282**(2): p. H615-21.
384. Patten, R.D. and M.R. Hall-Porter, *Small animal models of heart failure: development of novel therapies, past and present.* Circ Heart Fail, 2009. **2**(2): p. 138-44.
385. Barnes, P.J., *Inhaled glucocorticoids for asthma.* N Engl J Med, 1995. **332**(13): p. 868-75.
386. McGregor, A.M., *Immunoendocrine interactions and autoimmunity.* N Engl J Med, 1990. **322**(24): p. 1739-41.
387. Kirwan, J.R., *The effect of glucocorticoids on joint destruction in rheumatoid arthritis. The Arthritis and Rheumatism Council Low-Dose Glucocorticoid Study Group.* N Engl J Med, 1995. **333**(3): p. 142-6.
388. Libby, P., et al., *Reduction of experimental myocardial infarct size by corticosteroid administration.* J Clin Invest, 1973. **52**(3): p. 599-607.
389. Johnson, A.S., et al., *Effect of cortisone on the size of experimentally produced myocardial infarcts.* Circulation, 1953. **7**(2): p. 224-8.
390. Thiemermann, C., *Corticosteroids and cardioprotection.* Nat Med, 2002. **8**(5): p. 453-5.
391. Hafezi-Moghadam, A., et al., *Acute cardiovascular protective effects of corticosteroids are mediated by non-transcriptional activation of endothelial nitric oxide synthase.* Nat Med, 2002. **8**(5): p. 473-9.
392. Chen, L.L., et al., *Inhibition of MAPK signaling by eNOS gene transfer improves ventricular remodeling after myocardial infarction through reduction of inflammation.* Mol Biol Rep. **37**(7): p. 3067-72.
393. Fan, W.J., et al., *Dexamethasone-induced cardioprotection: a role for the phosphatase MKP-1?* Life Sci, 2009. **84**(23-24): p. 838-46.
394. Zhang, M., et al., *TNF-alpha as a potential mediator of cardiac dysfunction due to intracellular Ca2+-overload.* Biochem Biophys Res Commun, 2005. **327**(1): p. 57-63.
395. Rhen, T. and J.A. Cidlowski, *Antiinflammatory action of glucocorticoids--new mechanisms for old drugs.* N Engl J Med, 2005. **353**(16): p. 1711-23.
396. Barnes, P.J., *How corticosteroids control inflammation: Quintiles Prize Lecture 2005.* Br J Pharmacol, 2006. **148**(3): p. 245-54.
397. La, M., et al., *Annexin 1 peptides protect against experimental myocardial ischemia-reperfusion: analysis of their mechanism of action.* FASEB J, 2001. **15**(12): p. 2247-56.
398. Zingarelli, B., et al., *Sesquiterpene lactone parthenolide, an inhibitor of IkappaB kinase complex and nuclear factor-kappaB, exerts beneficial effects in myocardial reperfusion injury.* Shock, 2002. **17**(2): p. 127-34.

399. Bernauer, W., *Inhibiting effect of dexamethasone on evolving myocardial necrosis in coronary-ligated rats, with and without reperfusion.* Pharmacology, 1985. **31**(6): p. 328-36.
400. Valen, G., et al., *Glucocorticoid pretreatment protects cardiac function and induces cardiac heat shock protein 72.* Am J Physiol Heart Circ Physiol, 2000. **279**(2): p. H836-43.
401. Spath, J.A. and A.M. Lefer, *Effects of dexamethasone on myocardial cells in the early phase of acute myocardial infarction.* Am Heart J, 1975. **90**(1): p. 50-5.
402. Gerisch, R.A. and L. Compeau, *Treatment of acute myocardial infarction in man with cortisone.* Am J Cardiol, 1958. **1**(4): p. 535-6.
403. Dall, J.L. and A.A. Peel, *A Trial of Hydrocartisone in Acute Myocardial Infarction.* Lancet, 1963. **2**(7317): p. 1097-8.
404. Barzilai, D., et al., *Use of hydrocortisone in the treatment of acute myocardial infarction. Summary of a clinical trial in 446 patients.* Chest, 1972. **61**(5): p. 488-91.
405. Metz, C.A., D.F. Stubbs, and M.S. Hearron, *Significance of infarct site and methylprednisolone on survival following acute myocardial infarction.* J Int Med Res, 1986. **14 Suppl 1**: p. 11-4.
406. Burton, G.W., M.C. Holderness, and H.T. John, *Hydrocortisone in Severe Myocardial Infarction. Trial Conducted by the Scientific Subcommittee of the Scottish Society of Physicians.* Lancet, 1964. **2**(7363): p. 785-6.
407. Bush, C.A., W. Renner, and H. Boudoulas, *Corticosteroids in acute myocardial infarction.* Angiology, 1980. **31**(10): p. 710-4.
408. Peters, R.W., et al., *Effect of therapy with methylprednisolone on the size of myocardial infarcts in man.* Chest, 1978. **73**(4): p. 483-8.
409. Opdyke, D.F., et al., *Failure to reduce the size of experimentally produced myocardial infarcts by cortisone treatment.* Circulation, 1953. **8**(4): p. 544-8.
410. Hepper, N.G., et al., *The effect of cortisone on experimentally produced myocardial infarcts.* Circulation, 1955. **11**(5): p. 742-8.
411. Hammerman, H., et al., *Drug-induced expansion of infarct: morphologic and functional correlations.* Circulation, 1984. **69**(3): p. 611-7.
412. Mannisi, J.A., et al., *Steroid administration after myocardial infarction promotes early infarct expansion. A study in the rat.* J Clin Invest, 1987. **79**(5): p. 1431-9.
413. Sholter, D.E. and P.W. Armstrong, *Adverse effects of corticosteroids on the cardiovascular system.* Can J Cardiol, 2000. **16**(4): p. 505-11.
414. Richardson, T.P., et al., *Polymeric system for dual growth factor delivery.* Nat Biotechnol, 2001. **19**(11): p. 1029-34.
415. Chen, R.R., et al., *Spatio-temporal VEGF and PDGF delivery patterns blood vessel formation and maturation.* Pharm Res, 2007. **24**(2): p. 258-64.
416. Wang, T., et al., *The inhibition of postinfarct ventricle remodeling without polycythaemia following local sustained intramyocardial delivery of erythropoietin within a supramolecular hydrogel.* Biomaterials, 2009. **30**(25): p. 4161-7.
417. Zhong, Y. and R.V. Bellamkonda, *Dexamethasone-coated neural probes elicit attenuated inflammatory response and neuronal loss compared to uncoated neural probes.* Brain Res, 2007. **1148**: p. 15-27.

418. Sung, J., et al., *Sequential delivery of dexamethasone and VEGF to control local tissue response for carbon nanotube fluorescence based micro-capillary implantable sensors.* Biomaterials, 2009. **30**(4): p. 622-31.
419. Kim, D.H. and D.C. Martin, *Sustained release of dexamethasone from hydrophilic matrices using PLGA nanoparticles for neural drug delivery.* Biomaterials, 2006. **27**(15): p. 3031-7.
420. Hickey, T., et al., *In vivo evaluation of a dexamethasone/PLGA microsphere system designed to suppress the inflammatory tissue response to implantable medical devices.* J Biomed Mater Res, 2002. **61**(2): p. 180-7.
421. Norton, L.W., et al., *Vascular endothelial growth factor and dexamethasone release from nonfouling sensor coatings affect the foreign body response.* J Biomed Mater Res A, 2007. **81**(4): p. 858-69.
422. Bunger, C.M., et al., *Deletion of the tissue response against alginate-pll capsules by temporary release of co-encapsulated steroids.* Biomaterials, 2005. **26**(15): p. 2353-60.
423. Galeska, I., et al., *Controlled release of dexamethasone from PLGA microspheres embedded within polyacid-containing PVA hydrogels.* AAPS J, 2005. **7**(1): p. E231-40.
424. Giugliano, G.R., et al., *Meta-analysis of corticosteroid treatment in acute myocardial infarction.* Am J Cardiol, 2003. **91**(9): p. 1055-9.
425. Alisky, J.M., *Dexamethasone could improve myocardial infarction outcomes and provide new therapeutic options for non-interventional patients.* Med Hypotheses, 2006. **67**(1): p. 53-6.
426. Apicella, *Poly(ethylene oxide)-based delivery systems*, in *Polymeric Drugs and Drug Administration* Ottenbrite, Editor. 1994, American Chemical Society: Washington DC. p. 111-125.
427. Garcia, R.A., K.V. Go, and F.J. Villarreal, *Effects of timed administration of doxycycline or methylprednisolone on post-myocardial infarction inflammation and left ventricular remodeling in the rat heart.* Mol Cell Biochem, 2007. **300**(1-2): p. 159-69.
428. Elcin, Y.M., V. Dixit, and G. Gitnick, *Extensive in vivo angiogenesis following controlled release of human vascular endothelial cell growth factor: implications for tissue engineering and wound healing.* Artif Organs, 2001. **25**(7): p. 558-65.
429. Shireman, P.K., et al., *Modulation of vascular cell growth kinetics by local cytokine delivery from fibrin glue suspensions.* J Vasc Surg, 1999. **29**(5): p. 852-61; discussion 862.
430. Lin, C.C. and A.T. Metters, *Hydrogels in controlled release formulations: network design and mathematical modeling.* Adv Drug Deliv Rev, 2006. **58**(12-13): p. 1379-408.
431. Earp, J.C., et al., *Pharmacokinetics of dexamethasone in a rat model of rheumatoid arthritis.* Biopharm Drug Dispos, 2008. **29**(6): p. 366-72.
432. Samtani, M.N. and W.J. Jusko, *Stability of dexamethasone sodium phosphate in rat plasma.* Int J Pharm, 2005. **301**(1-2): p. 262-6.
433. Kay, M.A., J.C. Glorioso, and L. Naldini, *Viral vectors for gene therapy: the art of turning infectious agents into vehicles of therapeutics.* Nat Med, 2001. **7**(1): p. 33-40.
434. Newman, K.D., et al., *Adenovirus-mediated gene transfer into normal rabbit arteries results in prolonged vascular cell activation, inflammation, and neointimal hyperplasia.* J Clin Invest, 1995. **96**(6): p. 2955-65.

435. Chu, D., et al., *Direct comparison of efficiency and stability of gene transfer into the mammalian heart using adeno-associated virus versus adenovirus vectors.* J Thorac Cardiovasc Surg, 2003. **126**(3): p. 671-9.
436. Bramson, J.L., F.L. Graham, and J. Gauldie, *The use of adenoviral vectors for gene therapy and gene transfer in vivo.* Curr Opin Biotechnol, 1995. **6**(5): p. 590-5.
437. Hitt, M.M. and F.L. Graham, *Adenovirus vectors for human gene therapy.* Adv Virus Res, 2000. **55**: p. 479-505.
438. St George, J.A., *Gene therapy progress and prospects: adenoviral vectors.* Gene Ther, 2003. **10**(14): p. 1135-41.
439. Benihoud, K., P. Yeh, and M. Perricaudet, *Adenovirus vectors for gene delivery.* Curr Opin Biotechnol, 1999. **10**(5): p. 440-7.
440. Brody, S.L. and R.G. Crystal, *Adenovirus-mediated in vivo gene transfer.* Ann N Y Acad Sci, 1994. **716**: p. 90-101; discussion 101-3.
441. Kovesdi, I., et al., *Adenoviral vectors for gene transfer.* Curr Opin Biotechnol, 1997. **8**(5): p. 583-9.
442. Hitt, M.M., C.L. Addison, and F.L. Graham, *Human adenovirus vectors for gene transfer into mammalian cells.* Adv Pharmacol, 1997. **40**: p. 137-206.
443. Parks, R., C. Evelegh, and F. Graham, *Use of helper-dependent adenoviral vectors of alternative serotypes permits repeat vector administration.* Gene Ther, 1999. **6**(9): p. 1565-73.
444. Rosengart, T.K., et al., *Angiogenesis gene therapy: phase I assessment of direct intramyocardial administration of an adenovirus vector expressing VEGF121 cDNA to individuals with clinically significant severe coronary artery disease.* Circulation, 1999. **100**(5): p. 468-74.
445. Gruchala, M., et al., *Gene transfer into rabbit arteries with adeno-associated virus and adenovirus vectors.* J Gene Med, 2004. **6**(5): p. 545-54.
446. Alton, E. and C. Kitson, *Gene therapy for cystic fibrosis.* Expert Opin Investig Drugs, 2000. **9**(7): p. 1523-35.
447. Alemany, R., C. Balague, and D.T. Curiel, *Replicative adenoviruses for cancer therapy.* Nat Biotechnol, 2000. **18**(7): p. 723-7.
448. Curiel, D.T., *The development of conditionally replicative adenoviruses for cancer therapy.* Clin Cancer Res, 2000. **6**(9): p. 3395-9.
449. Liu, Y., et al., *Intratumoral coinjection of two adenoviral vectors expressing functional interleukin-18 and inducible protein-10, respectively, synergizes to facilitate regression of established tumors.* Cancer Gene Ther, 2002. **9**(6): p. 533-42.
450. Ambar, B.B., et al., *Treatment of experimental glioma by administration of adenoviral vectors expressing Fas ligand.* Hum Gene Ther, 1999. **10**(10): p. 1641-8.
451. Emtage, P.C., et al., *Enhanced interleukin-2 gene transfer immunotherapy of breast cancer by coexpression of B7-1 and B7-2.* J Interferon Cytokine Res, 1998. **18**(11): p. 927-37.
452. Trudel, S., et al., *Adenovector engineered interleukin-2 expressing autologous plasma cell vaccination after high-dose chemotherapy for multiple myeloma--a phase 1 study.* Leukemia, 2001. **15**(5): p. 846-54.
453. Wen, X.Y., et al., *Tricistronic viral vectors co-expressing interleukin-12 (1L-12) and CD80 (B7-1) for the immunotherapy of cancer: preclinical studies in myeloma.* Cancer Gene Ther, 2001. **8**(5): p. 361-70.

454. Cao, L., et al., *Cytokine gene transfer in cancer therapy.* Stem Cells, 1998. **16 Suppl 1**: p. 251-60.
455. Feldman, A.L. and S.K. Libutti, *Progress in antiangiogenic gene therapy of cancer.* Cancer, 2000. **89**(6): p. 1181-94.
456. Roth, J.A. and R.J. Cristiano, *Gene therapy for cancer: what have we done and where are we going?* J Natl Cancer Inst, 1997. **89**(1): p. 21-39.
457. Hermiston, T., *Gene delivery from replication-selective viruses: arming guided missiles in the war against cancer.* J Clin Invest, 2000. **105**(9): p. 1169-72.
458. Heise, C. and D.H. Kirn, *Replication-selective adenoviruses as oncolytic agents.* J Clin Invest, 2000. **105**(7): p. 847-51.
459. Yla-Herttuala, S. and K. Alitalo, *Gene transfer as a tool to induce therapeutic vascular growth.* Nat Med, 2003. **9**(6): p. 694-701.
460. Bangari, D.S. and S.K. Mittal, *Current strategies and future directions for eluding adenoviral vector immunity.* Curr Gene Ther, 2006. **6**(2): p. 215-26.
461. Raper, S.E., et al., *Fatal systemic inflammatory response syndrome in a ornithine transcarbamylase deficient patient following adenoviral gene transfer.* Mol Genet Metab, 2003. **80**(1-2): p. 148-58.
462. Arruda, V.R., P. Favaro, and J.D. Finn, *Strategies to modulate immune responses: a new frontier for gene therapy.* Mol Ther, 2009. **17**(9): p. 1492-503.
463. Thomas, C.E., A. Ehrhardt, and M.A. Kay, *Progress and problems with the use of viral vectors for gene therapy.* Nat Rev Genet, 2003. **4**(5): p. 346-58.
464. Wolff, L.J., J.A. Wolff, and M.G. Sebestyen, *Effect of tissue-specific promoters and microRNA recognition elements on stability of transgene expression after hydrodynamic naked plasmid DNA delivery.* Hum Gene Ther, 2009. **20**(4): p. 374-88.
465. Ye, X., et al., *Regulated delivery of therapeutic proteins after in vivo somatic cell gene transfer.* Science, 1999. **283**(5398): p. 88-91.
466. Yang, W., et al., *Regulation of gene expression by synthetic dimerizers with novel specificity.* Bioorg Med Chem Lett, 2003. **13**(19): p. 3181-4.
467. Fishman, J.A., *Infection in solid-organ transplant recipients.* N Engl J Med, 2007. **357**(25): p. 2601-14.
468. Seregin, S.S., et al., *Transient pretreatment with glucocorticoid ablates innate toxicity of systemically delivered adenoviral vectors without reducing efficacy.* Mol Ther, 2009. **17**(4): p. 685-96.
469. Wang, Z., et al., *Sustained AAV-mediated dystrophin expression in a canine model of Duchenne muscular dystrophy with a brief course of immunosuppression.* Mol Ther, 2007. **15**(6): p. 1160-6.
470. Elbert, D.L., et al., *Protein delivery from materials formed by self-selective conjugate addition reactions.* J Control Release, 2001. **76**(1-2): p. 11-25.
471. Zutphen LFM, Baumans V, and B. AC, *Principles of Laboratory Animal Science, Revised Edition*. 2003: Elsevier Science B.V.

.

472. Poole T and E. P, *The UFAW Handbook on the Care and Management of Laboratory Animals, Seventh Edition, Volume 1 Terrestrial Vertebrates*. 2000: Blackwell Science Ltd.
473. Theodorsson, A., L. Holm, and E. Theodorsson, *Modern anesthesia and peroperative monitoring methods reduce per- and postoperative mortality*

during transient occlusion of the middle cerebral artery in rats. Brain Res Brain Res Protoc, 2005. **14**(3): p. 181-90.
474. Tarnavski, O., et al., *Mouse cardiac surgery: comprehensive techniques for the generation of mouse models of human diseases and their application for genomic studies.* Physiol Genomics, 2004. **16**(3): p. 349-60.
475. Huang, N.F., et al., *A rodent model of myocardial infarction for testing the efficacy of cells and polymers for myocardial reconstruction.* Nat Protoc, 2006. **1**(3): p. 1596-609.
476. Collins, K.A., C.E. Korcarz, and R.M. Lang, *Use of echocardiography for the phenotypic assessment of genetically altered mice.* Physiol Genomics, 2003. **13**(3): p. 227-39.
477. Roth, D.M., et al., *Impact of anesthesia on cardiac function during echocardiography in mice.* Am J Physiol Heart Circ Physiol, 2002. **282**(6): p. H2134-40.
478. Sabharwal, R., et al., *Effect of hypothermia on baroreflex control of heart rate and renal sympathetic nerve activity in anaesthetized rats.* J Physiol, 2004. **557**(Pt 1): p. 247-59.
479. Schiller, N.B., et al., *Recommendations for quantitation of the left ventricle by two-dimensional echocardiography. American Society of Echocardiography Committee on Standards, Subcommittee on Quantitation of Two-Dimensional Echocardiograms.* J Am Soc Echocardiogr, 1989. **2**(5): p. 358-67.
480. Takagawa, J., et al., *Myocardial infarct size measurement in the mouse chronic infarction model: comparison of area- and length-based approaches.* J Appl Physiol, 2007. **102**(6): p. 2104-11.